Seismic design and performance of high cut slopes
July 2018
(replacing the version released in February 2017)

P Brabhaharan, D Mason and E Gkeli
Opus International Consultants Ltd

NZ Transport Agency research report 613
Contracted research organisation – Opus International Consultants Ltd

ISBN 978-1-98-851217-4 (electronic)
ISSN 1173-3764 (electronic)

NZ Transport Agency
Private Bag 6995, Wellington 6141, New Zealand
Telephone 64 4 894 5400; facsimile 64 4 894 6100
research@nzta.govt.nz
www.nzta.govt.nz

Brabhaharan, P, D Mason and E Gkeli (2017) Seismic design and performance of high cut slopes. *NZ Transport Agency research report 613*. 149pp.

Opus International Consultants Ltd was contracted by the NZ Transport Agency in 2014 to carry out this research.

Keywords: cuttings, design, earthquake, guidelines, landslides, seismic, slopes, topographic amplification

An important note for the reader

The NZ Transport Agency is a Crown entity established under the Land Transport Management Act 2003. The objective of the Agency is to undertake its functions in a way that contributes to an efficient, effective and safe land transport system in the public interest. Each year, the NZ Transport Agency funds innovative and relevant research that contributes to this objective.

The views expressed in research reports are the outcomes of the independent research, and should not be regarded as being the opinion or responsibility of the NZ Transport Agency. The material contained in the reports should not be construed in any way as policy adopted by the NZ Transport Agency or indeed any agency of the NZ Government. The reports may, however, be used by NZ Government agencies as a reference in the development of policy.

While research reports are believed to be correct at the time of their preparation, the NZ Transport Agency and agents involved in their preparation and publication do not accept any liability for use of the research. People using the research, whether directly or indirectly, should apply and rely on their own skill and judgement. They should not rely on the contents of the research reports in isolation from other sources of advice and information. If necessary, they should seek appropriate legal or other expert advice.

Changes made to version of report published in February 2017

Pages 32–33, section 3.4.2.4 – text revised

Pages 33–34, section 3.4.2.5 – text revised

Acknowledgements

- This research has been carried out by P Brabhaharan, Doug Mason, Eleni Gkeli and Andy Tai of Opus International Consultants, assisted by other staff, and Graham Hancox of GNS Science. The contribution of Graham Hancox forms appendix A of this report.
- The contribution of the peer reviewers, Prof George Bouckovalas, and Dr Trevor Matuschka is gratefully acknowledged, for:
  - the valuable discussions with the project team in person and through teleconferences on various aspects of this research, and in particular the topographic amplification, numerical analyses and the development of the design guidance
  - the valuable review of the report and provision of comments.
- The contribution of Prof Nick Sitar from the University of California, Berkeley, USA is gratefully acknowledged. He is thanked for the valuable discussions with researchers through teleconferences and during the 6th International Conference in Earthquake Geotechnical Engineering in Christchurch in November 2015.

Abbreviations and acronyms

DEM	digital elevation model
EC8	Eurocode 8
EIL	earthquake induced landslides
GPa	Giga pascal (standard unit for stress)
HW	highly weathered
M	magnitude
M_L	local magnitude
M_s	moment magnitude
M_w	surface wave magnitude
MHA	maximum horizontal acceleration
MM	modified Mercalli
MPa	Mega Pascal (standard unit for stress)
P	primary (compressional) wave
PGA	peak ground acceleration
PGAh	peak ground acceleration (horizontal)
PGAv	peak ground acceleration (vertical)
PGD	peak ground displacement
PGV	peak groud velocity
SH	secondary wave (shear wave or transverse wave) polarised in the horizontal plane
SV	secondary wave (shear wave or transverse wave) polarised in the vertical plane

Contents

Executive summary **7**
Abstract **8**
1 Introduction **9**
2 Objectives of the research **10**
3 Literature review **11**
3.1 Earthquake effects on slopes in New Zealand 11
3.2 Earthquake effects on slopes worldwide 11
3.3 Research into topographic effects 22
3.3.1 Early studies 22
3.3.2 Recent studies 22
3.3.3 Summary of findings of previous research 27
3.4 Current design methods and standards 29
3.4.1 Scope 29
3.4.2 New Zealand 29
3.4.3 Europe 34
3.4.4 USA – California 37
3.4.5 Discussion 37
4 Characterisation of New Zealand's topography and seismicity **39**
5 Observations from past earthquakes **44**
5.1 In New Zealand 44
5.2 Worldwide 44
5.2.1 Types of common slope failures in large earthquakes 46
5.2.2 Topographic and geological characteristics 48
5.2.3 Seismicity effects and seismotectonic regime 48
5.2.4 Antecedent conditions 49
5.2.5 Post-earthquake triggers 49
5.2.6 Effectiveness of slope stabilisation measures 49
5.2.7 Cut slope design records 49
6 Numerical analysis of topographic effects **50**
6.1 Purpose and scope 50
6.2 Numerical modelling 50
6.2.1 Software 50
6.2.2 Boundary conditions 50
6.2.3 Application of seismic motions 50
6.2.4 Geometry of the models 50
6.2.5 Material parameters 52
6.3 Seismic input motions 53
6.3.1 Simple harmonics 53
6.3.2 Time histories 53
6.4 Results of the analysis 53
6.4.1 Derivation of results 53
6.4.2 Terrace and ridge underlain by bedrock, with harmonics inputs 53

6.4.3 Ridge terrain underlain by bedrock, with time history inputs 56
6.4.4 Terrace and ridge bedrock with soil overburden, harmonic inputs 57
6.4.5 Terrace and ridge bedrock overlain by weathered rock and harmonic inputs 59
6.4.6 Ridge bedrock with lower slope cutting and harmonic inputs 60
6.4.7 Influence of normalised height and width on amplification factor 62
6.4.8 Parasitic vertical accelerations generated in ridge terrain 63
6.5 Discussion of analysis results 64
6.5.1 Terrace topography 64
6.5.2 Ridge terrain 64
7 Development of guidelines for design of high cut slopes 67
7.1 Purpose 67
7.2 Introduction of resilience principles 67
7.3 Importance of cut slopes 68
7.3.1 Purpose 68
7.3.2 Importance level 68
7.3.3 Resilience importance category 69
7.4 Design approach 70
7.4.1 Outline of design approach 70
7.4.2 Selection of design approach 71
7.4.3 Description of design approach 71
7.5 Selection of ground motions for design 72
7.5.1 Peak ground accelerations for design 72
7.5.2 Topographic amplification 74
7.5.3 Presence of soil overburden 75
7.5.4 Design ground accelerations for slope design 75
7.5.5 Time history records for design 76
7.6 Earthquake design of cut slopes 76
7.6.1 Design for resilience 76
7.6.2 Design for safety 77
7.6.3 Deformation or displacement-based design 77
7.7 Comparison with current design standards 78
8 Conclusions 79
8.1 Past earthquakes 79
8.2 New Zealand topography and seismicity 79
8.3 Research into topographic effects 80
8.4 Existing design guidance 80
8.5 Development of design guidelines 81
9 Recommendations 82
9.1 Earthquake design and implementation of design guidance 82
9.2 Further research and development 82
10 References 84
Appendix A: Performance of slopes in past New Zealand earthquakes: Literature review and lessons learned from historical earthquakes 94

Executive summary

Transportation routes are critical lifelines for the community, particularly in the event of natural hazards. New Zealand has a rugged terrain and high seismicity over much of the country, which means that high cut slopes are required to form transportation routes, and the performance of these slopes in earthquakes is critical to ensure a resilient transportation system.

Currently there is very little guidance available for the earthquake design of high cut slopes either in New Zealand or internationally. Recent awareness of the potential for topographical amplification of earthquake shaking, and the observation of the large landslides that have affected transportation routes in earthquake events has raised the awareness of the need for research and development of guidelines for the seismic design of high cut slopes.

The New Zealand Transport Agency engaged Opus International Consultants to carry out this research and development of guidance. The research team from Opus was supplemented by Graham Hancox from GNS Science who reviewed landsliding in past New Zealand earthquakes. The scope of the research included review of current design practice in New Zealand and overseas; review of the performance of high cut slopes in recent worldwide earthquakes; review of relevant recent research from New Zealand and overseas; consideration of the influences of the distinctive aspects of New Zealand' seismicity and topography; and development of criteria and guidelines for the earthquake design of high cut slopes in New Zealand. The outcomes of this research is presented in this report.

A comprehensive review of landslides in past New Zealand and worldwide earthquakes showed that steep slopes have failed in large earthquakes, and the initiation of failures in the upper part of slopes indicate that topographical amplification of shaking may be contributing to such failures. Observations also show that landslides are concentrated in hanging wall areas relative to fault rupture, particularly in earthquakes associated with a thrust component of fault rupture.

Research into topographical amplification over the past 15 years has shown that topographical amplification at the crest of ridge and terrace slopes is likely, and the magnitude of the amplification is dependent on the frequency of the earthquake motions relative to the shape of the topography. Actual observed amplifications have tended to be larger than those derived from numerical analyses.

Limited numerical analyses carried out as part of this research have shown that topographical amplifications are likely based on New Zealand topography and seismicity, and are consistent with the previous overseas studies. The research also shows that the presence of weathered rock overburden overlying unweathered rock (or the presence of soil overburden), can give rise to larger amplifications of ground shaking. This may explain the difference between the actual observations and numerical studies by overseas researchers. The analyses show that amplification is also likely at the top of cut slopes, even when the cut slopes do not extend to the ridge/terrace crest. Amplifications are much smaller or absent at the middle and lower reaches of slopes and at the toe.

Guidelines have been developed for the seismic design of high cut slopes along transportation routes in New Zealand. The guidance has been based on a novel resilience-based design approach. This provides for assessment of a resilience importance category based on the importance level of the route and the resilience expectations for the route. Four design approaches have been developed for use depending on the importance and complexity of the cut slopes, and a method of selection of a suitable design approach is proposed.

The design guidance also proposes selection of earthquake motions based on a consistent approach that is common to the transportation route regardless of the type of road form and structures. Modification of

the motions to allow for topographical effects is proposed as an interim measure based on the research evidence to date. Derivation of pseudo static design accelerations for different scale and location of failure mechanisms on the slope are also proposed.

Guidance is also provided on the mechanisms to be considered in the design of steep high cut slopes in rock, soil and failures along the interface between soil and rock. Also guidance is provided on displacement-based design and its limitations and caution in using this for rock slopes that exhibit a more brittle behaviour.

A resilience-based design approach is proposed, to achieve an economical design, consistent with the resilience expectations for the transportation route. This would allow acceptance of small failures in earthquakes that do not affect the carriageway or can be quickly cleared and reinstated economically to restore access, while avoiding large failures that impair access and which would take a long time (and cost) to reinstate and recover from.

Abstract

A review of the performance of slopes in historical earthquakes, a review of relevant literature describing recent research, consideration of New Zealand's distinctive topography and seismicity, and limited numerical analyses have been carried out. Steep slopes have failed in past earthquakes, with the initiation of failures in the upper part of slopes indicating the contribution of topographical amplification of earthquake motions. Landslides have been concentrated in hanging wall areas relative to fault rupture, particularly in thrust fault rupture earthquakes.

Past research and numerical analyses show that topographical amplification at the crest of a ridge and terrace slopes is likely, with the magnitude of the amplification being dependent on the frequency of the earthquake motions relative to the shape of the topography. The presence of weathered rock (or soil) overlying unweathered rock was shown to rise to larger amplifications of ground shaking. Amplification was also found to be likely at the top of cut slopes, even when the cut slopes do not extend to the ridge/terrace crest.

Guidelines have been developed for the seismic design of high cut slopes along transportation routes. A resilience-based design approach is proposed, to achieve an economical design, consistent with the resilience expectations for the transportation route.

1 Introduction

Opus International Consultants (Opus) was engaged by the New Zealand Transport Agency to carry out research into the design and performance of high cut slopes in New Zealand.

The purpose of this research was to review existing research outcomes and develop design criteria and guidelines to enable assessment of the seismic performance and seismic design of high cut slopes to achieve an acceptable level of resilience for our transportation infrastructure.

The guidelines have taken into consideration observations from New Zealand and worldwide earthquakes, international and local research, experience in the design of cut slopes and prevailing worldwide design standards, as well as New Zealand's topographical, cut slope configurations, and seismological and geological context.

Some limited targeted numerical modelling has been carried out as part of this research to test the topographical effects and variation of seismic shaking over the height of the slope, using specific New Zealand-centric parametric analyses.

It is recognised that this is an area of recent research and development, and there is more research yet required to develop a good understanding of the issues. However, it is proposed that this limited research and development of guidelines will help bring up-to-date research and current knowledge to the design of major transportation infrastructure involving high cut slopes, currently happening or planned for the near future in New Zealand.

Guidelines for design of high cut slopes have been prepared to aid design for transportation projects in New Zealand. The guidance provides for different design approaches depending on the importance of the transportation corridor, resilience requirements for the route and the scale of the cut slopes and complexity. The guidance includes assessment of suitable topographical amplification factors for typical hilly terrain where highway cut slopes are commonly formed in New Zealand, and factoring of the peak ground acceleration for derivation of equivalent pseudo-static loads for use in design.

This report documents and summarises the results of the literature review, derivation of key lessons, numerical analyses and the draft guidelines developed.

2 Objectives of the research

The objectives of the research were to:

- Collate existing international literature on the seismic performance of slopes, design standards, and research on topographical amplification and variation of seismic shaking over the height of high slopes.
- Review and critically assess current design practice and standards in New Zealand and overseas, for cut slopes, particularly high cut slopes where there is any differentiation.
- Review reports and experience on the performance of slopes (including high cut slopes) in different geological conditions in New Zealand and overseas.
- Review relevant recent research outputs from New Zealand and overseas, including the behaviour of slopes subject to earthquake shaking and the variation of earthquake shaking over the slope topography, and relevant design approaches.
- Characterise distinctive aspects of New Zealand's seismicity and topography, and understand their influence on the behaviour of cut slopes in earthquakes.
- Formulate clear design criteria and guidelines for the earthquake design of high cut slopes in New Zealand, with a view to achieving resilient and cost-effective cut slopes, including taking into account the variation of peak ground acceleration over the height of the slope.
- Present the research outcomes including the design guidelines in the research report so that they can be cited in the NZ Transport Agency's (2014) *Bridge manual*, 3rd edition (referred to in this report as the *Bridge manual*).
- Provide clear recommendations on implementation of the proposed design guidelines including dissemination of the new design principles within the New Zealand engineering community and incorporation of those into the *Bridge manual*.
- Advise on any additional work required to further improve design practice and achieve safe, resilient and cost-effective design of high slopes.

The following additional issues were considered, depending on the information available from the literature:

- Consider the observed effects of earthquakes on slopes in the vicinity of fault rupture, such as influences due to geographical differences between hanging wall and foot wall areas, and near-field effects. Understand their influences for the design of high cut slopes.
- Identify the likely mechanisms of failure of slopes in earthquakes, for the common geological situations in which high cut slopes are formed for highways and their implications for design.
- Test the influences of distinctive aspects of New Zealand's seismicity and topography upon the earthquake ground shaking of high cut slopes with state of the art parametric numerical analysis.
- Incorporate international advice from peer review to get the benefit from the extensive research that has happened in this area in the recent past, and the thinking behind overseas design standards (Europe and USA in particular).

3 Literature review

3.1 Earthquake effects on slopes in New Zealand

An extensive literature review of earthquake-induced slope failure in past New Zealand earthquakes was carried out as part of this research. The results from this review on earthquake-induced landslides in New Zealand earthquakes) is presented in appendix A of this report.

3.2 Earthquake effects on slopes worldwide

A literature review of the effects of large earthquakes on slopes, and in particular, the performance of cut slopes, in past worldwide earthquakes has been carried out. The literature search covered research and practice related to the seismic performance and design of slopes, with emphasis on the following:

- Reconnaissance reports of earthquake damage to slopes and case histories of slope performance from around the world. The focus of this research was to gather data regarding the types and size of slope failures, shape of slopes, local and regional geology and tectonics, as well as recorded ground shaking recordings and other seismo-tectonic information.
- Records of design of cut slopes and comparison of the performance of stabilised and unstabilised slopes, where such information was available.
- Observations of modification of earthquake shaking due to topographic and near-fault effects on ground shaking over the height of slopes.

Table 3.1 presents a summary of the key findings from the literature review of slope performance in past worldwide earthquakes.

Table 3.1 Summary of observations of slope performance from key worldwide earthquakes

Earthquake event	Salient points from observations of earthquake damage	References
1983 Coalinga, California • M6.4 • Thrust fault • Hilly to mountainous terrain	• Strong ground motions recorded at crest and base of 20m high 3H:1V cut slope; topographic amplification ≈ 1.2 at crest, at period T ≈ 0.4-1 s. Amplification up to ~10 x observed, particularly for frequencies 1-6Hz and 7Hz. • Topographic de-amplification ≈ 0.85 at toe, at period T ≈ 0.4-1 s. • Corresponds to wavelengths ≈ 4–9 slope heights. • Weathered sandstone at the surface with harder underlying Pliocene sandstone.	Celebi (1991) Stewart and Sholtis (2004)
1985 Central Chile • M_s7.8 • Thrust fault • Mountainous terrain	• Horizontal amplification ~10 x of ground motion at frequencies 2–4Hz and 8Hz for ridge crest relative to adjacent canyon.	Celebi (1991)
1989 Loma Prieta, California • M7.1 • Strike slip fault • Mountainous terrain	• Directivity effects; stronger ground motion to the northwest. • Failures occurred in deeply weathered or fractured basement rock comprising metasedimentary and granitic rock facies. • Thousands of landslides were recorded, up to 130km from epicentre. • Landslides mostly occurred in steep, rugged and heavily vegetated mountains where they have historically occurred in seismic events and high intensity rainfall.	Shephard et al (1990)

Earthquake event	Salient points from observations of earthquake damage	References
	• Earthquake occurred after 2 dry years and minimal rainfall in the then current season. • Most common form of failure were rock falls and shallow rock and soil slides. • Hundreds of deeper seated rotational slumps and translational block slides were observed but typically had moved less than 1m.	
1990 Luzon, Philippines • M_S7.8 • Sinistral strike-slip faulting • Hilly to mountainous terrain	• Extensive landsliding triggered by earthquake in mountainous areas to north and west of fault rupture, resulting in severe disruption to transportation routes. • Landslides were mainly shallow (<1m deep) translational slides in soil mantle and weathered bedrock. • Amplification of ground motions was apparent due to concentration of extensive landsliding at the crests of steep slopes and ridges. • United States Geological Survey recorded aftershocks and reported higher ground motions in Baguio (mountainous/hilly region), but unclear if directivity effects contributed to this.	Hopkins et al (1991)
1992 Landers, California • M_S7.5 • Dextral strike-slip faulting • Hilly to mountainous terrain	• Fault trending NNW-NW. Vertical and oriented 10° west of north. • Shallow focal depth with two major sub events – sub events combine to have magnitude M_w7.4.	Berryman (1992)
1994 Northridge, California • M6.7 • Thrust fault • Hilly to mountainous terrain	• Pronounced hanging wall effect: 50% increase in PGA on hanging wall over distance range of 10–20km relative to median attenuation for the earthquake. Peak ground acceleration (PGA) on footwall not significantly different from median attenuation over the same distance. • Most triggered landslides were shallow (1–5m thick), highly disrupted shallow falls and slides of rock and debris within Late Miocene to Pleistocene, uncemented or very weakly cemented clastic sediment. • Deeper (>5m thick) rotational slumps and block slides were triggered, often as reactivations of pre-existing landslides. Generally, deeper slumps and block slides were far less common and primarily occurred in more cohesive or competent materials. • Landslides strongly clustered near ridge crests (56% in upper quartile of slopes). • Landslides in the epicentral area occurred preferentially on south-facing slopes. The dominant dip of geological strata is to the south, implying geological control on slope failure (eg bedding plane failure). • Pacoima Canyon: mainly block slides and falls (defect-controlled failures) in Cretaceous igneous rocks. PGA at crests of slopes >1.5g; PGA at base of slopes ~0.4g (nearby free-field ground motions suggest no deamplification at base of slope). • Slope stability analyses suggest unamplified PGAs insufficient to trigger failure of slopes that were observed to have failed – indicates importance of topographic amplification effect on rock slopes.	Abrahamson and Somerville (1996) Gao et al (1996) Harp and Jibson (1996) Harp and Jibson (2002) Meunier et al (2008) Parise and Jibson (2000) Sepulveda et al (2005a)
1995 Aegion, Greece • M_S6.2 • Normal faulting	• Low angle (33º) normal faulting earthquake. • High PGA (0.54g), long period (0.40–0.50s) ground motion. • Rupture directivity effect – PGA in direction of rupture 4 x PGA in opposite direction at similar distance from epicentre.	Bouckovalas et al (1999)

Earthquake event	Salient points from observations of earthquake damage	References
• Hilly to mountainous terrain	• Soil amplification peaks at periods 0.1–0.3s and 0.4–0.7s. • Presence of fault escarpment (step-like topography) appeared to have amplified the intensity of ground shaking in its vicinity.	
1999 Chi-Chi, Taiwan • M7.6 • Thrust fault • Hilly to mountainous terrain	• Landslide intensity shows interaction between structural controls on topography and tectonics/seismicity. • Most slope failures were shallow disaggregated landslides – failure at base of root zone. The dominant failure mechanism was shallow sliding along a stepped path of interconnected fractures. Some discontinuity-controlled failure mechanisms, especially in hard metamorphic rocks along Central Cross-Island Highway. • Most landslides occurred on the hanging wall block – increased motion on hanging wall (peaked at fault trace). • 90% of failures on slopes >45º. • 70% of landslides in Tertiary sedimentary rocks. • Failures generally located at crest of slope (34% in upper quartile of slope). • Slope height more important than angle. • Slope orientation relative to incoming seismic waves important. Landslide rates highest on slopes facing away from earthquake epicentre. • Local convexities on slope profile (eg gorge or cut slope?) can introduce important changes to pattern of surface acceleration, eg amplification of vertical component of incoming S waves. • Inferred amplification ratios ~5–10 x (lack of data to corroborate). • PGAh >0.15g and PGAv > 0.2g = trigger levels for slope failure? PGA alone not satisfactory to predict failure. Distance from fault plane and epicentre provide additional correlation. • Extensive landsliding along Central Cross-Island Highway. Many highway slopes (including cut slopes) were weakened by earthquake shaking with subsequent ongoing instability (rock fall) from aftershocks and rainfall. • Well-designed rock slope support measures (shotcrete and rock bolts) performed well. Anchored retaining walls generally performed better than gravity walls. • Ground failures precipitated structural failures of bridges and tunnel portals. • Surface rupture of 83km, with a N-S trend which turned into a ENE to E-W trend at northern end. • EW (strike-normal) components were larger than N-S (strike parallel) components – fault directivity effect. • Long period motions and large velocity pules recorded at northern end of fault surface rupture resulting from forward directivity effects. • Ground motion greater at hanging wall than foot wall, more damage on hanging wall. • Landslides generally occurred on steep slopes with PGA >0.4g. • Large landslide at Tsaolin Dam - occurred down dip slope in shale and was reported to be 200m thick. Failure caused a lake to build up – new post-event hazard. • Landslides occurred in elevated quaternary terraces on slopes between 30º and 35º. • Tsao Ling landslide formed a landslide dam – earthquakes and heavy rain have previously caused landslides in the area. Failure was due to block slides along interbedded mudstones and sandstones. Sufficient material located at top of slide which could cause another landslide dam at same site – post-event hazard.	Brunsdon et al (2000) Foster and Campbell (2000) Huang et al (2001) Hung (2000a) Hung (2000b) Khazai and Sitar (2003) Koseki and Hayano (2000) Lee and Loh (1999) Meunier et al (2008) Oglesby and Day (2001) Sepulveda et al (2005b) Wang et al (1999) Wu et al (2009)

Earthquake event	Salient points from observations of earthquake damage	References
	• Transition from thrust to significant left-lateral slope north of the fault. • The surficial faulting and near-source ground velocity and displacement are dominated by the interaction between the faulting process and the free surface of the earth.	
1999 Athens, Greece • M_s5.9 • Normal fault • Hilly to mountainous terrain	• Amplification of seismic motion of ~50% for cliff of 30º slope and 40m height. • Damaging effects tend to increase when steep relief or complicated topography is present. • Forward-directivity effects present in ground motions experienced at sites east of the rupture zone. • Rupture terminated beneath a mountain range, whose orientation is nearly perpendicular to strike of the activated fault. Mountain seems to have acted as a barrier, and the sudden interruption and possible turning of the rupturing process would have a similar effect to an impact, generating high-acceleration high-frequency ground motions. • Damage distribution was characterised as being strongly uniform.	Bouckovalas and Kouretzis (2001) Assimaki et al (2005)
1999 Izmit, Turkey • M7.4 • Dextral strike-slip fault • Hilly to mountainous terrain	• Pure right lateral focal mechanism (strike-slip). • 110–130km surface rupture – trending E-W to ENE-WSW. • PGA recorded between 0.23–0.41g. • General lack of rock fall and landslides on susceptible slopes. • Fault trace runs mostly along coastal plain and sedimentary basin, to south topography rises up into range of steep sided hills, exceeding 30º. • Very little slope instability observed. • No significant landsliding in road cuts observed. • Motorway is cut into steep hillsides in highly fractured rock–- no indication of instability. Rock netting not damaged.	Sharpe et al (2000)
2001 Southern Peru • M8.3 • Subduction earthquake • Mountainous terrain	• Hill slope subsidence and slope damage damaged main highways within the 300km long earthquake rupture zone. Damage to slope below motorway shown. • Very little earthquake induced landsliding, one 100m high rock slide observed near epicentre • One PGA recorded showing 0.3g. Estimated that this represents the maximum value.	Stirling et al (2003)
2002 Denali, Alaska • M7.9 • Dextral strike-slip fault • Mountainous/ alpine terrain	• The majority of landslides were shallow rock falls and rock slides from steep slopes. • Much lower number and concentration of triggered landslides than expected for earthquake of that magnitude. Landslides concentrated in narrow 30km wide zone around fault rupture. • High frequency energy generation was greatest in western part of fault rupture zone, but decreased markedly to the east.	Harp et al (2003) Jibson et al (2004) Jibson et al (2006)
2004 Niigata Ken Chuetsu, Japan • M6.6 • Thrust fault • Hilly to mountainous terrain	• Very high concentrations of landslides; Miocene to early Pleistocene sedimentary rocks – weak, friable claystone and siltstone interbedded with sandstone and conglomerate. • Most landslides occurred on hanging wall (steep uplifted terrain). • Most landslides were relatively shallow (1–2m deep), slope-parallel failures of colluvial and residual soils mantling steep slopes (>55º). • High antecedent rainfall was a major contributor to large concentrations and densities of landslides (Typhoon Tokage in days before earthquake). Evidence for rainfall-triggered landslides exacerbated by seismic ground shaking.	Deng et al (2008) Kieffer et al (2006) Konagai et al (2005) Scawthorn et al (2005)

Earthquake event	Salient points from observations of earthquake damage	References
	• Landslide failure mechanisms include shallow translational soil failures, deep rotational bedrock failures, large rock-block slides, slump-flow complexes and rapid debris flows. • Most widespread type of failure consisted of translational slip of the regolith and highly weathered (HW) bedrock materials on very steep slopes (upper 5–10 feet of soil), with slip concentrated along interface between significant root growth and underlying HW bedrock. • High antecedent moisture conditions also led to common slump-flow complexes within colluvium-filled gullies. • Some deep bedrock landslides controlled by rock-mass structure; other failures occurred along curved shear surfaces more characteristic of soil slumping. • Cuesta topography is common – resulting in large scale landslides on dip-slopes and shallower slump/rock fall from steeper side of cuesta. • Road network in mountainous area was severely damaged – poor performance of slopes above the road. Most observed landslides causing road damage are estimated to have volumes of a few hundred to a few thousand cubic metres; collective volume posed significant problem to reopening.	
2005 Kashmir, Pakistan • M7.6 • Thrust fault • Mountainous/ alpine terrain	• Thrust fault mechanism: Hanging wall side of fault severely affected by landslides; 42% of landslides occurred on hanging wall block within 10km of fault (cf 10% on footwall at same distance). • 65% of landslides occurred in elevation range 850m–1,750m, compared total relief of 450m–4,470m. • ~60% of landslides on slopes 20–40º. • 61% of landslides on concave slopes. • 65% of landslides occurred in shale, siltstone and limestone, as well as younger colluvium, terrace and scree deposits. • Largest earthquake-induced landslide = 80 x 106m_3, within Miocene sandstone, mudstone, shale and limestone. Also significant landsliding in upper weathered zone of Paleocene limestone and shale above Muzaffarabad Fault. • Topographic amplification effects observed (eg extensive fracturing of slope crests). • Extensive damage to road network caused by failure of steep cuttings (improperly designed) and natural hillslopes above the road.	Champati Ray et al (2009) Dellow et al (2007) Harp and Crone (2006) Konagai et al (2006) Qureshi and Koseki (2006)
2006 Kiholo Bay, Hawaii • M6.7 • Oblique normal fault • Mountainous terrain	• High concentrations of rock falls and slides in steep canyons. • Variable correlation between observed distribution of landslides and peak ground motions; stronger correlation between landslides and modelled dynamic shear strain. • Homogenous geology.	Harp et al (2014)
2007 Niigata Chuetsu-Oki, Japan • M6.6 • Reverse fault • Hilly terrain	• A typhoon rain front passed through the region immediately before the earthquake. • Slope failures consisted of shallow translational slides, debris slumps and deep-seated rotational slides. • Notable large failures of cuts above roads and railways, particularly in HW mudstone (plastic fine-grained soil). • The area affected by landslides underlain by Neocene sedimentary rocks (unconsolidated mudstone and tuff).	Collins et al (2012) Gratchev and Towhata (2008) Orense et al (2008)

Earthquake event	Salient points from observations of earthquake damage	References
	• Minimum PGA of 0.2g to initiate landsliding. • Geological factors controlling high landslide frequency – dip slopes, weathered coastal zone, young (Tertiary) strata.	
2007 Pisco, Peru • M8.0 • Subduction earthquake • Mountainous terrain	• Significant slope failures blocked highways with debris (disrupted landslides including rock falls, rock slides, soil falls, soil avalanches and disrupted soil slides). • Widespread damage to South Pan-American Highway from landslides and rock falls (as well as liquefaction and lateral spreading). Regional and rural road networks mainly affected by slope failures and rock falls. • Rock fall from steep cut slopes common.	Hopkins et al (2008) Johansson et al (2007) Johansson et al (2008) O'Connor et al (2007)
2008 Wenchuan, China • M7.9 • Thrust fault • Mountainous terrain	• Widespread earthquake-induced landsliding. Shallow soil slips, landslides, rock avalanches, shallow rock slides, rock falls. Large landslides in competent limestone/sandstone cap on ridge tops underlain by weaker shale/phyllite (topographic effects); rock slides in carbonate rocks; rock slides in weathered shale; debris flows; very large defect-controlled landslides in bedded limestone/dolomite/shale sequences. • Ground shaking results in initial tensile shattering/fracturing of rock mass across steep, high back scarps, following by shearing and sliding along basal failure surface. Different response observed of upper (source) area of slopes with very large landslides relative to toe. • Landslides near epicentre often characterised by 'throw-like collapse' – combination of vertical accelerations causing tensile failure of rock mass and horizontal acceleration causing ejection/toppling failure of block. • Majority of landslides on slopes between 20–50º. • Most landslide hazards occur in river valley and canyon section below the elevation of 1,500 to 2,000m, particularly in the upper segment of canyon slopes (convex knick point on slope profile). • Thin ridge, isolated or full-face space mountains show pronounced topographic amplification effects. Collapses and landslides most likely to occur in these areas. • Landslides generally observed in soft rocks, collapses and block failures observed in hard rocks. • Pronounced hanging wall effect – higher PGAs in hanging wall block, cf footwall at equal distance from fault rupture: - <20km of fault: n/a because no station within 20km on hanging wall - 20–70km: PGAs higher on hanging wall - >70km: no significant difference - Hanging wall effect not observed from peak ground velocity (PGV), therefore the hanging wall effect may have been related to frequency contents of strong motions, and only existed in some frequency bands (unlike Chi-Chi with more pronounced hanging wall effect for PGA, PGV and peak ground displacement (PGD)). • Directivity effect - attenuation of PGA more gradual in NW direction. Attenuation of EW vs NS components of PGAh differ: may be related to source mechanism? • Strong topographic amplification effects. Landslides concentrated on hanging wall side of fault; direction of landslide displacements also showed preferred orientation perpendicular to fault rupture. • Horizontal amplification factor of PGA ~2x for intact rock slope.	Che and Ge (2012) Chigira et al (2010) Gorum et al (2011) Huang and Li (2008) Huang et al (2011) Huang et al (2012) Ji et al (2009) Li and He (2009) Li et al (2013) Liu et al. (2013) Liu and Li (2009) Lu et al (2010) Lu et al (2013) Sun et al (2011) Tang et al (2010) Wang et al (2008) Wang et al (2009) Wang et al (2010) Wang et al (2011) Wang et al (2012a) Wang et al (2012b)

Earthquake event	Salient points from observations of earthquake damage	References
	• Vertical amplification factor ~0.9 x horizontal factors. • Slopes with heights >200m and/or angles 30–45º showed a strong dynamic response. • Double surface slope (ie mountain profile) show a larger dynamic response than single surface slope (ie terrace); concave slopes show larger dynamic response than straight slopes. • Observed & inferred critical PGAs for triggering of large/severe landslides: PGAh >0.21g, PGAv >0.12g. • Ground motion thresholds for landslide initiation: PGA ~ 0.07g; PGV ~ 0.5m/s; Ia ~ 0.2m/s. • Threshold ground motion parameters for strong earthquakes of same order of magnitude as those observed for moderate earthquakes. • Modelled response of rock slopes: 85% of the slope height subject to PGAv ≥ 2/3 PGAh, and 32% of the slope height subject to PGAv ≥ PGAh – important for seismic design codes. • Slopes stabilised with rock anchors, anchored retaining walls/foundation beams or lateral loaded piles with prestressed anchors observed to have performed well. • Initiation of landslides can be influenced significantly by seismic acceleration component normal to sliding surface, especially in the area with large vertical acceleration. • Complicated block slide-rock avalanche in Donghekou area (23Mm^3): - dolomite limestone and siliceous phyllite - prominent, planar joints dipping nearly vertically and striking parallel to the landslide scarp (easy to trigger landslide by strong seismic shaking) - direction of the main sliding almost same as dip of sliding surface - data indicates that PGA values induced by a single micro-earthquake increase three times from toe of slope to its top - this landslide could be triggered only if other external triggering factors, such as earthquake and rainfall, are considered or the down-dip sliding force during the earthquake was beyond the critical acceleration friction force - suggestions that vertical ground motion could have significant effects on the stability analysis of earthquake-induced landslides - there is a significant influence normal to the sliding surface on earthquake-triggered landslide initiation. • Larger PGA values closer to the edges of fault and on hanging wall side.	Xiao et al (2010) Yin et al (2008) Yin et al (2011) Yu et al (2010) Yuan et al (2013) Zeng et al (2011) Zhou et al (2010) Yuan et al (2015)
2008 Iwate Miyagi-Nairiku, Japan • M_w6.9 • Thrust fault • Mountainous terrain	• Shallow thrusting to the west (fault rupture plane). • Types of landslides triggered were primarily deep-seated rotational slides in weathered bedrock; collapses of corner buttresses composed of both rock and weathered rock and soil; rock fall and rock avalanches; shallow transitional slides and shallow debris flows. • Shallow landslides were common at road cuts in mountainous terrain. Typical failure plane inclination was 50–70º. Usually of sufficient size to close road. Small isolated falls uncommon. • Massive landslide near Aratozawa Dam (50 million cubic metres) carried a 3.5km section of road downslope. Height of head scarp is 50–150m • Large amount of disintegrating material at toe. Comprised of weakly cemented volcanic ash and volcaniclastic material. 1.2km length, 800m wide, 50m depth. Terrain is suggestive that similar historic landslides were reactivated.	Kayen et al (2008) Miyagi et al (2008)

Earthquake event	Salient points from observations of earthquake damage	References
	• Large landslide triggered in Neogene to Quaternary volcanic tuff, sandstone and siltstone materials. Failure mechanism described as 'block glide' – whole landslide mass slid on 2º failure plane. • Numerous other large landslides within 15km radius of epicentre. • Rock fall at a dam abutment killed worker. • Local amplification effects recorded. • Shallow regolith slides of soil and weathered material sliding on top of more competent bedrock were common at road cuts and occasionally mobilised into a debris flow. • Onshore sallow focus and surface rupture that resulted in severe landsliding damage close in to the epicentre. • Landslide damage was observed equidistant to the epicentre in all directions • Landslides were principal cause of road closures. Highway suffered numerous large landslides that swept away portions of the road and brought down a bridge. • Large rotational slides blocked numerous small lakes and formed natural dams. • Rock avalanche comprised of house sized blocks that fell onto the highway. Rock fall typically associated with slopes in excess of 50º. • Manmade embankment failure of road beds was the primary cause of road closures. • Failure of western slope abutment lead to collapse of a bridge.	
2009 L'Aquila, Italy • M6.3 • Normal fault • Hilly terrain with terraces	• Slope failures were localised and minor, with modes including ravelling and sloughing of road cuts, quarries and natural slopes, permanent displacement of fill embankments, and rock falls. • Typical ravelling-type failures of cut slopes in strong and fractured limestone involved uppermost weathered blocks bounded by soil-filled joints. • General performance of cut slopes in limestone bedrock was excellent and minor surficial failures were not widespread. • Quarry and road cut faces in weakly cemented sand and gravel were affected by ravelling, shallow slides and slumps. • Earth-retaining structures also performed satisfactorily, with only minor damages at few locations.	Lanzo et al (2010)
2009 Padang, Indonesia • M_w7.5 • Oblique thrust fault • Volcanic plateau and caldera, hilly terrain	• Earthquake shaking effects were clearly directional (E-W). • Energy was strongly directed east of the epicentre. • Earth-flow landslides triggered by earthquake buried several villages. • Two main locations of failures. - earthflows along steep slopes that lead from coastal plain to inland volcanic plateau (failures of volcanic tuffs up to 70m deep, formed moderately steep slopes) - rock slides at steep escarpments around Lake Maninjau caldera (which also previously collapsed in M6.4 West Sumatra earthquake in 2007). • Previous rock falls were evident at the toe of some failures.	Bothara et al (2010)
2010 Maule, Chile • M8.8 • Subduction earthquake • Mountainous terrain	• Uncharacteristically low landslide density for a large magnitude earthquake. Rock falls and shallow disaggregated slides (eg ravelling) occurred on natural and cut slopes; minimal impact on infrastructure. • No damage of any significance to slopes stabilised with rock bolts, mesh, shotcrete etc. • Sporadic failures in road cuts observed – size and characteristics reflected the	Bray and Frost (2010) Wick et al (2010) Cowan et al (2011)

Earthquake event	Salient points from observations of earthquake damage	References
	height of the cut and the competency of the source material – more competent rock exhibited larger boulder size within the failed mass while less competent materials exhibited more disaggregated masses of smaller particles. • Tertiary sediments and Quaternary marine/beach sediments form steep coastal bluffs – these slopes are susceptible to shallow ravelling and sloughing, but failures were concentrated in only a few localities. • Deep-seated block or rotational slides were generally absent or rare. • Earthquake-triggered rock falls observed in Argentina, 400+ km from epicentre. • Maximum recorded PGA of 0.65g. • Only two major slips were reported following the earthquake. This low number is thought to be a result of the long period of dry weather Chile had experienced prior to the earthquake.	
2010 Sierra Cucapah, Mexico • M_w7.2 • Normal faulting with dextral slip • Hilly/ mountainous terrain	• Spatial pattern of mass movements reflects fault dynamics – landslides associated with rupture of thrust fault differs from those associated with strike-slip. • This earthquake ruptured several NW trending transform faults, normal faulting with dextral slip (high angle faults). • Extremely arid landscape and sparse vegetation cover constrained to valley bottoms and slope gully systems. • PGA in excess of 0.4g. • Mesozoic crystalline basement rock. • Mountain range have max elevation of 73º, average slope is 18º. • 452 landslides identified. • Dip slip component to east at dip angle of 66º. • Landslide density demonstrated a strong exponential relationship with increasing slope angle. • Steepest gradients and PGAs in the upper elevations but not at the crests of slopes. • Clear increase in landslide activity for slopes that are aligned with fault orientation. Evident that landslide density on slopes oriented parallel to fault experience landslide densities roughly four times that of slopes that are perpendicular to fault. • Uplift is more effective as a trigger to failure than subsidence. • Landslide density highest in proximity to fault lines (not epicentre). • Peak PGA of 0.53g. • Strong motion was felt uniformly at all points equidistant from the fault trace rather than just near the epicentre.	Barlow et al (2015) Meneses et al (2010)
2010 Haiti • M7.0 • Combination of thrust and left-lateral strike-slip • Hilly/ mountainous terrain	• Asymmetric landslide distribution north vs south of fault (hanging wall vs footwall). • Amplification of ~10x of observed PGAs in certain frequencies. Also modelled 20% deamplification at toe of slope. • Importance of coupling of topographic and soil amplification effects. • Topographic amplification effects can be equally as important for microzonation as amplification by shallow sedimentary layers.	Assimaki and Jeong (2013) Jibson and Harp (2011) Hough et al (2010)
2011 Van-Tabanli, Turkey	• Recorded deformation of shallow highway embankments <1.5m • Some more extensive failures through highway cuttings on shallow angled	Cetin et al (2011)

Earthquake event	Salient points from observations of earthquake damage	References
• M7.1 • Oblique thrust fault • Hilly terrain	slopes. Maximum vertical offset of 40cm with lateral deformation up to 15cm (just at one site). • Rock fall recorded, approx. diameter of rocks 1–1.13m. Rolled down moderately steep grassed slopes onto road. • Moderately large landslides observed. • Main shock along WSW-ENE reverse fault with north dipping fault plane.	Alaluf et al (2012)
2011 Tohoku, Japan • M9.0 • Subduction earthquake • Hilly terrain	• Landsliding intensity was lower than expected for a M9.0 earthquake. • 80% of landslides occurred in Quaternary and Neogene rocks (Miocene or younger). Steep natural and cut slopes in volcanic tuff and siltstone/sandstone materials were particularly affected by landsliding. • The earthquake occurred during the dry season – landslides occurred in unsaturated slopes and flow-type failures were largely non-existent (excluding lateral spreading). • The majority of landslides were disrupted-type failures, originating at or near the crests of slopes (topographic effect?). Other common mechanisms of natural slope failures = shallow/surface landslides, deep-seated landslides and rock falls.	Miyagi et al (2011) Tiwari et al (2012) Wartman et al (2013)
2012 Samara, Costa Rica • M7.6 • Thrust fault • Hilly to mountainous terrain	• Rupture began at surface and propagated down dip of the fault to the northeast. • Peak accelerations decrease to northeast of surface rupture (directivity). • Soil amplification (volcanic soils) and topographic effects observed.	Rollins et al (2013)
2013 Lushan. China • M_s7.0 • Thrust fault • Mountainous terrain	• Slopes consisting of deeply weathered and fractured sandstones and mudstones were the most susceptible to co-seismic landslides. • Most common failure mechanisms were rock falls and shallow, disrupted landslides in top few metres of weathered bedrock and colluvium on steep slopes (>45º). • Types of failures categorise into rock fall, rock slides, rock avalanche, soil fall, disrupted soil slides, soil slumps and slow earth flows. • Rock falls from steep road cuts and natural slopes were very common and caused considerable damage and disruption to roads. • Landslides were not concentrated on the hanging wall block. • Landslides generally occurred at the following conditions: - elevations between 800 and 1,600m - slope angle greater than 15º - slope aspects of east, south-east and south - failed from middle slope position - sandstone, conglomerate and siltstone of the Neogene, Paleogene and Cretaceous - PGA values equal to 0.32g or higher.	Tang et al (2015) Xu et al (2015)
2015 Gorkha, Nepal • M_w7.8 • Thrust fault • Mountainous terrain	• Due to the shallow depth and low angle dip of the rupture plane hilly and mountainous areas located north of the surface projection of the fault plane are on the hanging wall block and likely to be affected by hanging wall effects. • Topography effects dominated to a large extent ground response and ground failure effects. • Dry season, yet still widespread landsliding – estimated several tens of thousands of triggered landslides.	Collins and Jibson (2015) Hashash et al (2015)

Earthquake event	Salient points from observations of earthquake damage	References
	• Most landslides involved near-surface regolith and weathered/fractured bedrock, and appear to have mobilised primarily as ravelling failures, translational block slides, and rock falls. Failure surfaces were generally parallel to the slope and 1–10m deep. • Landslide concentrations were highest near the epicentre of the main Gorkha, Nepal earthquake, but significant landslide concentrations extended about twice as far to the east than to the west. This likely was the result of the eastward-directed fault rupture of the main shock as well as the occurrence of the M7.3 aftershock east of the main shock • Extensive damage and closures to highways from landslides on natural slopes and rock falls along road cuts, particularly: - Araniko Highway extending east from Kathmandu to the Nepal-China border at Kodari suffered severe landslide damage. Landslide effects became progressively severe with increasing elevation northward. Landsliding and rock fall damage along the Araniko Highway was nearly continuous within several kilometers of Kodari and the Nepal–China border. - Translational block slides and rock falls closed the highway in numerous locations. The majority of observed landslides were rock fall and rock slides resulting from blocks sliding and releasing along joint planes. - The majority of landslide prevention works such as gabion retaining walls and subsurface drainage networks implemented in previously triggered landslide sites appear to have performed. - Lamosangu-Manthali Highway in close proximity to the epicentre of the M_w7.3 aftershock, was significantly affected by shaking. - The characteristics of landslides were similar to those observed in other areas – rock falls that blocked several sections of the road, ravelling, and ground fissures and settlement of road fills.	
2016 Kumamoto Earthquake, Japan • M_w6.0, 6.2 and 7.0 • Strike-slip fault • Volcanic mountainous terrain and alluvial flats	• Landslides on steep hillsides, appear to have been triggered near the top of the ridges (indicative of topographical amplification) with flow of debris down to significant distances. • Some rocks that have come off the slope indicate potentially large vertical accelerations have dislodged the rock blocks off the slope and onto the road below. • Benched slopes in quarries appear to have performed better than unbenched steep slopes in quarries. • Failures in rock slopes appear to be controlled by dominant defects, with failures in the form of rock slides and large size rock fall. • Some rock falls appear to be toppling type failures, likely to have been exacerbated by high vertical accelerations. • Many key bridges destroyed by landslide debris run-out, rock slides, and undermining of abutments from landslides below. • Significant large landslides on relatively gentle hillsides, 10–25º, volcanic ash and pumice deposits. • Large debris flow which has flowed a few kilometres through the valleys and affected development on alluvial debris fans and adjacent areas. • Lack of close alternative routes have severely affected the transportation network in the earthquake epicentral area. • Landslides/lateral spreading on relatively flat terraces with volcanic ash deposits, seriously damaging residential development. • Landslides have led to disruption of key arterial highways that have remained	Chiaro et al (In press)

Earthquake event	Salient points from observations of earthquake damage	References
	closed for more than a month after the earthquake events (and probably will remain closed for much longer), and this has led to significant disruption to transportation routes in the area. • Many retaining wall failures in the earthquakes in both steep terrain, as well as those supporting roads and development in gentle terrain. • Retaining walls that failed are largely gravity walls, but included in one instance a reinforced earth wall with steel strips.	

3.3 Research into topographic effects

The literature review also included a review of New Zealand and international research on the behaviour of slopes subject to earthquake shaking, including the distribution and effects of topographical amplification of ground shaking and the variation of seismic shaking over the height of high slopes. The results of literature research is summarised below.

3.3.1 Early studies

Early numerical studies on the effect of topography on seismic response were for simple topographic configurations (generally isolated two-dimensional ridges on the surface of a homogeneous half-space) carried out using finite element, finite difference, boundary and discrete wavenumber methods (eg Boore 1972; Smith 1975; Sanchez-Sesma et al 1982; Bard 1982). Matuschka (1980) commented on topographic amplification effects observed from Atene seismometer stations in an M6.7 earthquake north of Wellington, New Zealand in 1973.

Geli et al (1988) reviewed these studies and others, and noted that observed topographic effects on seismic ground motion are often underestimated by numerical analyses of simplified topographic conditions. They concluded the disagreement between predicted (theoretical) and observed amplifications is due to complex interaction between geological structure and topographic geometry, as ridges with observed topographic effects are not isolated but generally in a series of subparallel ridges (akin to a ‘quasi periodic’ structure). Geli et al attempted to resolve this difference by modelling the combined influence of neighbouring topography and subsurface layering. Their results show amplification at hill tops relative to the base, with the crest:base amplification ratios exhibiting a 1st maximum for frequencies corresponding to wavelengths slightly longer than the mountain width. They also note that the hill sides undergo complex amplification-deamplification patterns and also significant differential motions, especially in the upper part of the hill.

Çelebi (1991) analysed spectral ratios of earthquake ground motions to quantify the topographical amplification effects. These results show horizontal amplification of motion up to ~10 at frequencies 2–4Hz and 8Hz for ridge crests relative to adjacent canyon bases.

3.3.2 Recent studies

The first systematic parametric studies found in the literature were by Ashford et al (1997) and Ashford and Sitar (2002), providing valuable insights to the effects of the parameters influencing the problem. Through their study of earthquake damage to steep coastal bluffs in brittle, weakly cemented, sandy soils they concluded that soil amplification effects in the free field behind the slope crest dominate the response, and consequently it is important to differentiate between topographic and soil amplification. They consider topographic amplification to be the amplification at the crest relative to the free field

behind the crest, rather than comparing the ground motion at the slope crest to the motion at the base. This involves separation of the topographic amplification effects from the natural frequency of the region behind the crest. Parametric analysis of effects of slope inclination (i), height (H), wave type (P, SH and SV), wavelength (λ), and angle of wave incidence (b) shows that the peak amplification of motion at the slope crest occurs at a normalised frequency H/λ = 0.2. Ashford and Sitar (2002) use these results to propose a simplified procedure for carrying out seismic slope stability analysis to take topographic effects into account.

Bouckovalas and Papadimitriou (2004; 2005; 2006) analysed step-like (terrace) topography for vertically propagating SV waves. Their results showed:

- Horizontal acceleration generates significant parasitic vertical acceleration due to reflection of incoming SV waves on the inclined free surface forming reflected P, SV and Rayleigh waves. These all have a strong vertical component, and arrive with a time lag and phase difference at different points of the ground surface so their superposition onto the incoming SV waves leads to intense amplification or de-amplification variability at neighbouring points behind the crest within a few tens of metres (ie H/2), especially for high frequencies.
- De-amplification near the toe of the slope suggests that topographic effects may be overestimated when comparing crest:toe ground motions, and consequently an appropriate free-field site is required to establish the extent of topographic amplification.
- Topography effects fluctuate intensely with distance away from the slope, so that detecting them on the base of field measurements alone becomes a very demanding task, requiring a dense seismic array.
- The slope angle and normalised height (H/λ) have a significant effect on horizontal and vertical amplification as well as the distance to the free field in front and behind the slope. Topography effects become important for normalised height ratios H/λ>0.16 and slope inclinations i>17°. If these conditions are met, the peak values of topography aggravation factors for the horizontal and vertical ground acceleration behind the crest usually vary between $A_{h,max}$ = 1.20–1.50 and $A_{v,max}$ = 0.10–1.10 respectively, while free field conditions behind the crest are usually met at a distance D_{ff} = (2–8)H.

In contrast to the findings of Ashford et al (1997) and Ashford and Sitar (2002), Bouckovalas and Papadimitriou (2006) note that the presence of bedrock below the slope has an important effect on topographic amplification and cannot always be decoupled from the effect of the free-field site period.

Bouckovalas and Papadimitriou (2004; 2006), note the few seismic codes that at the time dealt with slope topography aggravation (EC8 and PS-92) are reasonable with regard to the increase of peak horizontal accelerations. Nevertheless, the authors noted that the codes overlook the generation of parasitic vertical acceleration and dangerously underestimate the distance from the slope where topography effects become negligible and propose a provisional series of modifications to the seismic code provisions in Eurocode 8 (EC8).

The same authors also propose new criteria for significant topographical aggravation, not purely based on the geometry of the slope as in the existing code provisions, but also include the predominant wavelength (parameter H/λ) which takes into account local soil conditions and a local crucial characteristic of the seismic excitation. Yet, for usual cases of slopes that have Vs >400m/s (stiff soils or soft rocks) and for common seismic excitations with a predominant period larger than 0.20s, the code provisions for lower bounds are in broad agreement with their proposed criteria H > 13m and i > 17° for 20% topographic aggravation (also referred to in this report as ‘topographical amplification’).

Assimaki et al (2005) carried out an extensive study of the topography effects and seismic behaviour of the Kifissos Canyon slopes during the Athens 1999 earthquake. They highlighted the following issues from their research:

- The non-uniform damage observed in the town of Adames, located along the crest of Kifissos River slopes could not be explained by topography effects only. The damage could not be explained by topographic aggravation reasons or structural reasons, as the town was located along the vertex of a practically two dimensional feature and was relatively uniform in terms of quality of structures. The study took into account actual soil profiles developed from available geotechnical data, shear-wave velocity profiles and actual ground motions from aftershocks.
- The horizontal and lateral heterogeneity of the soil profile play a significant role in the topographic aggravation of soil motion next to the crest of the slope in comparison to that of the free field.
- The effects of soil conditions affect the spatial distribution, aggravation level and frequency content of the surface response next to the crest.
- The nonlinear soil behaviour of the soil has a decisive role in the degree of topographic motion aggravation. They showed that one-dimensional nonlinear soil amplification effects of seismic motion can be as high as 60% in some frequency bands, even for typical stiff sites such as the soil profiles in Adàmes, which are characterised by an average shear-wave velocity of Vs=400m/s.
- Topographic aggravation of seismic motion is a function of local soil conditions and seismic motion intensity. As a result, elastic theoretical/numerical simulations and weak motion data may not be applicable to describe topography effects for strong seismic events, especially the amplitude of high frequency components.
- The equivalent-linear method with frequency-dependent dynamic soil properties may be used to describe soil amplification for horizontally stratified media, even for the case of weakly heterogeneous formations. Nonetheless, it cannot simulate the 2-D wave field direction, and therefore cannot be used to describe the surface response of 2-D topographic features to strong ground motion, in terms of peak amplitude, spatial distribution of motion, and frequency content.
- The parasitic vertical acceleration component can attain quite substantial amplitude close to the crest of cliff-type topographies on the order of magnitude of the primary far-field surface response; its amplitude is even further enhanced for the case of heterogeneous media characterised by soft surface formations and subjected to strong seismic input.
- Assimaki et al (2005) also concluded that weak motion data can be successfully used as a valuable guidance in reconnaissance studies, but they are not adequate to describe topography effects associated with strong-motions.
- Assimaki et al (2005), proposed a possible scheme for a frequency- and space-dependent factor, referred to as the topographic aggravation factor. Multiplied by site-specific design spectra, the space-dependent topographic aggravation factor spectrum would provide modified spectra to account for wave diffraction and constructive interference phenomena observed, for example, at a ravine's ridge. They believe that the high-frequency region of such a spectrum should reflect the excess enhancement of these components of motion, attributed to material heterogeneity and soil nonlinearity. Furthermore, the topographic aggravation factor spectrum should be supplemented by another design parameter, the parasitic vertical topographic aggravation factor, to account for the parasitic vertical acceleration. Assimaki et al (2005) stated that limited number of configurations, soil conditions, and incident motions analysed, not complemented by an extensive strong-motion

database of case studies on topography effects, did not allow generalisation of their conclusions for design purposes.

The effects of geological structure on the seismic behaviour of the slope were also demonstrated by Stewart and Sholtis (2005). They studied a simple two dimensional slope in Coalinga California, with a pumping plant structure at the base. In their study they used strong ground motions recorded during the 1983 Coalinga earthquake mainshock and two aftershocks. Ground accelerations recorded at the crest of the slope were significantly larger than those at the base, which is attributed to three factors: soil-structure interaction effects (on base motions, which were recorded on the pumping plant structure), as well as differential ground response and topographic amplification effects.

To isolate the topographic effects on the ground motion at the crest and base of the slope, the soil structure interaction and differential ground response effects were removed using established engineering models. Geologic amplification significantly contributed to the amplification observed at the crest relative to the base for periods up to about three seconds. Topographic effects are most pronounced for T=0.4–1.0s (wavelengths equal to 4–9 slope heights), which is reasonably consistent with the recommendations of Ashford and Sitar (1997). Across the period range of T=0.4–1.0s, approximately half of the observed amplification is due to geologic effects in each of the three events.

The maximum topographic amplification at the slope crest is found to be approximately 1.2 (ie 20% greater than the anticipated motion at a level site), in agreement with the models proposed by Ashford and Sitar and the maximum topographic de-amplification at the slope base is on the order of 0.85–0.9 (ie 10–15% less than the anticipated motion at a level site).

Meunier et al (2008) examined landslide distribution maps from recent large earthquakes for patterns of damage relating to topographic parameters, supplemented by numerical analysis of the effects of ridge and valley topography on seismic wave propagation.

Modelling of seismic waves travelling in a ridge-to-valley topography shows that diffraction and interference of seismic waves in topographic ridges causes amplification of ground accelerations near ridge crests. Oblique incidence of seismic waves causes the amplification to shift away from ridge crests and into the ridge flanks facing away from the earthquake epicentre. Secondary amplification maxima are predicted at smaller convex-up knick points within ridge flanks.

The modelling results show maximum amplification of peak ground accelerations occurs in the upper quartile of slopes facing away from the wave source, with deamplification along the base of the slope facing towards the incoming seismic wave. Local convexities on the slope profile can introduce important changes to the pattern of surface ground acceleration, such as amplification of the vertical component of incoming S waves.

The modelling results were largely matched by observations from large earthquakes in California (1994 Northridge), Taiwan (1999 Chi-Chi) and Papua New Guinea (Finisterre mountains) where in all epicentral areas, earthquake-induced landslides were strongly clustered around ridge crests, where peak ground accelerations are likely to have been the greatest.

Buech et al (2010) assessed the dynamic response of a bedrock ridge in Canterbury, New Zealand to local and regional earthquakes. The ridge responded most to signal components close to the second mode (first harmonic) of vibration of the calculated natural resonant frequency, corresponding to a wavelength equal to the half width or mountain height ($\lambda_1 \approx 0.5\ w_{mtn} \approx h_{mtn}$). The field experiments showed high variability in amplification effects, with maximum amplification along the ridge crest and de-amplification at the slope toe and mid height.

Ktenidou et al (2011) carried out 2-D finite difference modelling of the city of Aegion, Greece, which consists of a simplified step-like topography in bedrock with a sedimentary basin located below the slope. Ktenidou et al then compare the modelled topographical amplification results to those predicted by the European seismic design codes that specifically address topographic effects. Their modelling showed the French code AFPS90 was insufficient to predict the modelled results, both in terms of degree of amplification and the width of the zone of influence behind the slope crest. EC8 successfully predicts the amplification level for SH waves over a short distance from the slope crest; a wider envelope needs to be applied (equal to half the height of the slope) for EC8 to predict the amplification for SV waves.

Papadimitriou (2011) summarises the conclusions of previous case studies, field measurements and numerical analysis and recognises that the problem is multi-parametric. In an effort to analyse the influence of the different parameters involved he analysed 2-D uniform slopes, trapezoidal canyons and hills (see figure 3.1), examining the following important parameters of the problem as his and others' previous studies had concluded in the past:

- slope inclination, i
- incidence angle, β
- wavelength, λ
- height, H, and width, B, of 2-D slopes, trapezoidal canyons and hills
- the relative magnitude of slope height compared to the wavelength, H/λ.

Figure 3.1 Slope geometries described by Papadimitriou (2011)

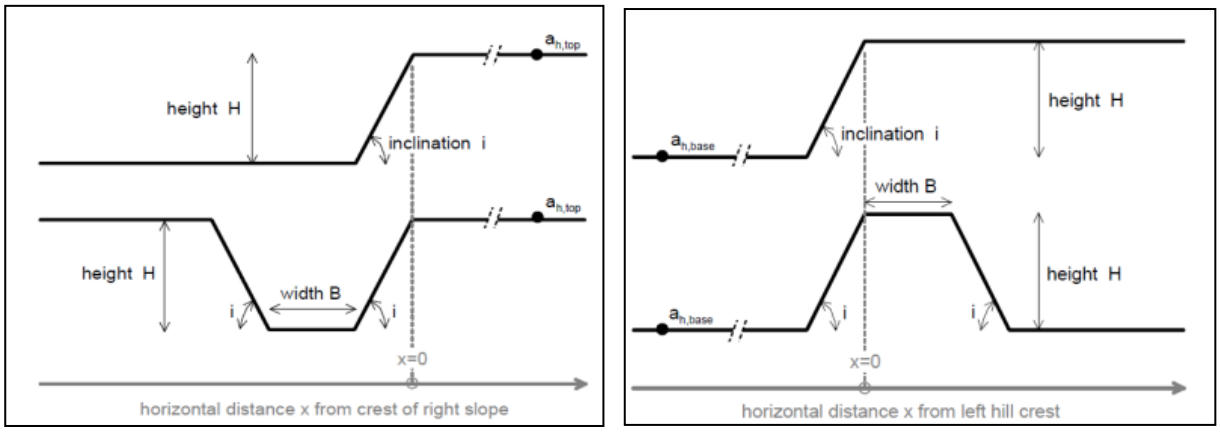

Papadimitriou's parametric study concluded that trapezoidal canyons and slopes with the same H/λ and i produce similar aggravations of horizontal and vertical accelerations in front of their toe and behind their crest. Canyons show larger amplifications of the parasitic vertical accelerations compared with the respective slope. Trapezoidal hills on the other hand, show higher aggravation of the horizontal acceleration at their top, compared with slopes with the same i and H/λ, on average by 30% or more. In parallel, in front of their toe, hills show larger or equal aggravations of the horizontal and vertical acceleration, again compared to the respective slope.

The maximum aggravation factors for the peak horizontal and peak parasitic vertical accelerations on the top of 2-D hills were found to increase with decreasing normalised top hill width B/λ. Papadimitriou (2011) recommended that mandatory provisions for 2-D topography features should be included in EC8, defined by multi-variable relations in terms of inclination, normalised height H/λ and width B which prove

the significant problem parameters, as per earlier studies of Bouckovalas and Papadimitriou (2004; 2005; 2006) and not by assigning fixed values.

Burjánek et al (2011) analysed amplification effects at sites of existing instability in the Swiss Alps, using 76 regional earthquakes (ML 0.5–2) at epicentral distances of 10–40km and estimating site-to-reference spectral ratios based on ambient vibrations. These analyses show that ambient vibrations are strongly polarised at certain frequencies in the unstable areas, and ground motions in areas of instability are amplified in specific orientations relative to the stable part of the slope.

The first peak in site-to-reference spectral ratios is at the same frequency f_0 at all stations in the direction perpendicular to cracks mapped at the ground surface. They observe that the pattern of amplification within areas of instability is comparable to normal mode vibration of sedimentary basins, and therefore suggest that the volume of unstable rock mass is effectively damaged rock with air-filled voids (defects) which therefore reduces the elastic moduli. This results in a seismic impedance contrast across the boundary between the intact and heavily fractured rock masses, trapping incoming waves and producing standing waves (normal mode vibration). Burjánek et al conclude that amplification of ground motions due to internal structure of the area of instability is of primary importance rather than the topographic shape of the slope.

Kaiser et al (2014) present analyses of ground motions recorded in the Port Hills suburbs of Christchurch in the Canterbury earthquake sequence. Their analyses show topographic amplification at 1–3Hz at ridge tops, with the wavelength of amplification strongly correlated with the ridge width and the degree of amplification linked to ridge shape, with sharp, narrow ridges showing the strongest amplification. Significant local variability of high frequency ground motions was observed, as well as variability resulting from the site-to-source azimuth, with the greatest amplification observed when sources were aligned with the major ridge axis, resulting in preferential amplification in the ridge-perpendicular direction.

Massa et al (2014) present a review of research into topographic effects, supplemented by analysis of the seismic response of bedrock ridges in Italy, to investigate correlations between topographic parameters and the fundamental frequency and topographic amplification of the sites. Their results show a negative correlation between the width of the ridges and the fundamental frequency, and a positive correlation between the shape ratio and both the fundamental frequency and topographic amplification. They note the significant effects structural defects such as open fractures or tectonic contacts are observed to have on the response of topographic features, and conclude that topographic effects may be due to a combination of primary response of a topographic high over an effectively homogeneous medium, or induced effects where structural discontinuities within the topographic feature form sub-blocks with differing periods of vibration.

3.3.3 Summary of findings of previous research

The following points summarise the general conclusions extracted from literature review regarding topographic effects:

- Topography effects are influenced by shape, inclination and height of slope, as well as wave type, wavelength and angle of wave incidence.
- Topography effects are also influenced by the stratigraphy and geology of the slope, such as the presence of softer/weaker rock or soil layer at the top of the slope and presence of rock defects and faults.

- Maximum amplification of peak ground accelerations occurs in the upper quartile of slopes, more so when facing away from the wave source, with de-amplification along the base of the slope facing towards the incoming seismic wave.
- Local convexities on the slope profile can introduce important changes to the pattern of surface ground acceleration, such as amplification of the vertical component of incoming S waves.
- Topography effects fluctuate intensely above the crest with distance away from the slope, so that detecting them on the base of field measurements alone becomes a very demanding task.

A summary of the conclusions from previous numerical analyses for ridge terrain is:

- Ground motion at the top of a slope of a ridge is amplified compared with that at the base; amplification of the horizontal component of ground motion is higher than that of the vertical component. De-amplification is observed at the slope base.
- Amplification of the ground motions at the top of the trapezoidal hills is 30% larger than that of terrace like slopes of the same height and inclination.
- Variations in the wavelengths of incident seismic waves create complex, alternating patterns of amplification and de-amplification on different parts of the ridge slope.
- The maximum amplification factors for the peak horizontal and peak parasitic vertical accelerations on the top of 2-D hills were found to increase with decreasing normalised top hill width B/λ.
- Topographic amplification is negligible for wavelengths much larger than the base width of the topographic feature.
- Amplification at the top of the slope increases with increasing H/L (where H = height of the crest above the base and L = the half-width of the topographic feature).
- Topographic amplification is lower for P waves compared with S waves. In-plane incident SV waves show larger amplification than out of plane solution SH waves.
- Topographic amplification depends on the incident angle of incoming waves: maximum amplification occurs for vertically incident waves ($\gamma = 0°$).

The following points summarise the results from experimental studies for ridge terrain:

- Topographic effects are frequency dependent and were found to increase with decreasing normalised top hill width B/λ.
- Amplification of ground motion observed at the crest increases with increasing H/L.
- Amplification effects are greatest along the direction perpendicular to the axis of the topographic feature (negligible amplification effects are observed along the axis).
- Amplification ratios are usually greater for horizontal components of motion.
- The degree of amplification is dependent on the azimuth of incoming waves relative to the azimuth of the topographic slope (source-to-site direction).
- Amplification functions obtained from seismic noise and strong motion recordings are similar in terms of resonance frequency.
- Experimental results are comparable to numerical analyses in terms of resonance frequency, but usually give higher amplification ratios.
- It is difficult to separate influences of geological and topographic effects on site response.

The following points summarise the results of numerical research into terrace topography:

- The slope angle (i) and normalised height (H/λ) of the slope have a significant effect on horizontal and vertical amplification, as well as the distance to the free field in front and behind the slope.
- Topography effects become important for normalised height ratios H/λ>0.16 and slope inclinations i>17°. If these conditions are met the peak values of topography aggravation factors for the horizontal and vertical ground acceleration behind the crest usually vary between $A_{h,max}$ = 1.20–1.50 and $A_{v,max}$ = 0.10–1.10 respectively, while free-field conditions behind the crest are usually met at a distance D_{ff} = (2–8)H.
- Amplification effects at the crest and de-amplification effects near the toe may lead to overestimation of topographic effects when comparing crest:toe ground motions. Therefore slope ground motions need to be compared to an appropriate free-field site, rather than comparing the ground motion at the crest to the motion at the base, noting that the presence of bedrock below the slope has an important effect on topographic amplification and cannot always be decoupled from the effect of the free-field site period.
- Topographic effects are frequency dependent: peak amplification of motion at the slope crest occurs at normalised frequency H/λ ~ 0.2.
- Intense amplification or de-amplification variability is observed at neighbouring points a few tens of metres behind the crest (ie H/2), especially for high frequencies.
- Even purely horizontal acceleration (vertically propagating SV waves) generates significant parasitic vertical acceleration due to reflection of incoming SV waves on the inclined free surface, forming reflected P, SV and Rayleigh waves. These all have a strong vertical component, and arrive with a time lag and phase difference at different points of the ground surface so their superposition onto the incoming SV waves may lead to amplification or de-amplification of horizontal seismic motion.

3.4 Current design methods and standards

3.4.1 Scope

Design standards available for use in the seismic design of high cut slopes have been searched for and reviewed as part of the literature review. This included New Zealand, European, Canadian and USA standards.

3.4.2 New Zealand

3.4.2.1 NZS 1170.5: 2004

In New Zealand, *NZS 1170.5: 2004 Earthquake actions – New Zealand* (Standards New Zealand 2004) provides guidance on the selection of earthquake loading for structural design actions. Unfortunately it specifically excludes the parts of the built environment associated with slopes including slope stability, liquefaction, retaining walls, dams and bunds.

3.4.2.2 New Zealand Geotechnical Society guidelines

Geotechnical earthquake engineering practice, module 1 (draft) (New Zealand Geotechnical Society 2014) provides guidance on the assessment of liquefaction, but does not provide any advice on the assessment or design of cut slopes, other than saying that 'Ground accelerations caused by earthquake shaking can significantly reduce the stability of inclined masses of soil and rock. Even though the acceleration pulses

may be of short duration, they may be sufficient to trigger rock falls or initiate an incipient failure, especially where the soil or rock is susceptible to strain softening or brittle failure'.

3.4.2.3 New Zealand *Bridge manual*

The *Bridge manual's* third edition (NZ Transport Agency 2014) provides guidance on the selection of seismic design parameters for slopes associated with state highways in New Zealand.

The *Bridge manual* provides charts and formulae for the derivation of the following earthquake design parameters for geotechnical design including that of cut slopes:

- peak ground acceleration
- effective magnitude.

These are provided based on:

- the hazard factor based on the seismicity of the location
- return period factor based on the importance and the road form as indicated in table 3.2.
- site subsoil class (A, B, C, D or E) based on NZS 1170.5.

The *Bridge manual* also requires a site-specific seismic hazard study depending on the value of the soil structures and earthworks (values as at December 2012), as follows:

- less than $3 million – no site specific hazard study is required
- between $3 million and $7 million – a site specific study is advisable
- greater than $7 million – a site specific study is mandatory.

Unweighted peak ground accelerations derived from the above methods are specified for design. No allowance is made in the *Bridge manual* for changes to these design parameters, either to allow for amplification (such as due to topographic effects) or reductions (to allow for incoherence of motions where the slopes are of significant height).

The *Bridge manual* provides earthquake loading parameters by classifying the roads depending on their level of importance. Table 3.2 presents a summary from chapter 2 of the *Bridge manual*, illustrating the annual probability of exceedance for ultimate limit state design of cut slopes. The relevant requirements for fills, retaining walls and bridges are shown for comparison.

Table 3.2 New Zealand *Bridge manual* earthquake design levels for cut slopes

As per AS/NZS 1170.0	as per *Bridge manual*	Cut slopes	Fills	Retaining walls	Bridges
4	Routes critical to post-disaster recovery, providing direct access to and within 10km radius of hospitals, emergency services, ports or airports	1/1000	1/2500, if > 6m high 1/1000, if < 6m high	1/2500	1/2500
3	Primary lifeline route as identified in the *Bridge manual*, categorised based on traffic volumes, strategic importance and redundancy of regional road network.	1/500	1/1000, if > 6m high 1/500, if < 6m high	1/2500, if > 5m high and >100m^2 1/1000, if < 5m high or < 100m^2	1/2500
2	Other than primary lifeline routes.	1/100	1/500, if > 6m high 1/100, if < 6m high	1/1000, if > 5m high and > 50m^2 1/500, if < 5m high or < 50m^2	1/1000
1	Routes where failure will not affect access, on no exit road or serving population less than 50.	1/50	1/100, if > 6m high 1/50, if < 6m high	1/500	1/500

Note: Other design criteria are also provided where the “structure” provides protection to adjacent property, which is not reproduced here.

There is no specific guidance on the design of cuttings other than that it shall be designed in accordance with recognised highway design practice, with the provision of benches, and appropriate measures to mitigate the effects of rock fall or minor slope failures. Reference is made to design of cut slopes similar to that specified for embankments, where a factor of safety of 1.5 for static conditions is specified. Cut slopes are almost always in natural geological materials compared to engineered retaining walls or engineered embankments, and hence have a greater level of uncertainty as to the materials influencing cut slope stability. However, cut slopes are not differentiated in the manual.

Where slopes are to be designed for permitting displacement under earthquake loading, reference is made to the section that provides guidance on the performance of retaining walls and slopes, and a table with displacement limits are specified based on the situation of the wall or slope with respect to the road, road structures or other adjacent structures.

It should be noted that for a given level of importance of the route, the *Bridge manual* requires cut slopes to be designed to a much lower level of earthquake hazard, compared to other road forms along state highways. This is illustrated diagrammatically in table 3.3, which summarises the earthquake design actions drawn from the *Bridge manual* for a critical route into Wellington called the Transmission Gully motorway (Rouvray et al 2015). Access into Wellington has little redundancy and therefore the resilience expectations are very high given the regional context of the route (Brabhaharan 2011). The route has very high cut slopes proposed in a highly seismically active environment, and also straddles a major active fault. Despite the very high resilience expectations and the high cut slopes proposed in an active seismic environment, the current *Bridge manual* requires the design to be considered for a rather low level of seismicity.

Table 3.3 Comparison of earthquake design limit states in the *Bridge manual*

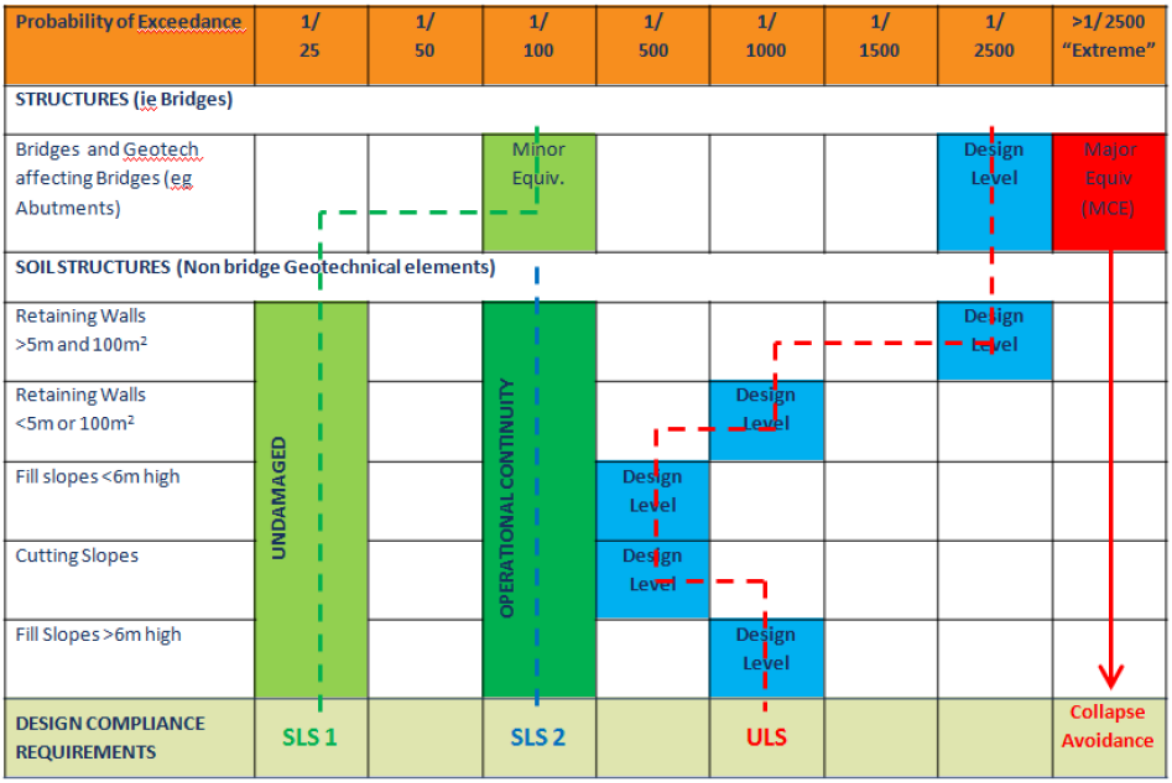

Note: After Rouvray et al (2015). ULS – ultimate limit state, SLS – serviceability limit state, MCE – maximum considered earthquake.

Failure of cut slopes can give rise to closure of important primary lifeline routes for six months or more, for example as reported in the Wellington Region road network earthquake resilience study (Brabhaharan and Mason 2012), and as observed in the closure of SH3 in the Manawatu Gorge for more than 12 months, due to landslides.

Tables 3.2 and 3.3 show that cut slopes of any height are grouped together with low height embankments less than 6m high, and are required to be designed to a much smaller earthquake with the lowest recurrence interval of 500 years for the ultimate limit state (compared to all other forms of highway structures. It is not clear from the *Bridge manual* why cut slopes are required to have a lower level of earthquake performance.

3.4.2.4 Rouvray et al (2015) approach

In a paper presented at the 6th International Conference on Earthquake Geotechnical Engineering, Rouvray et al (2015) set out the approaches they used for the recent design of the Transmission Gully motorway north of Wellington, New Zealand. This is worthy of consideration given the paucity of design approaches in the literature.

Rouvray et al's (2015) paper presents a performance-based design approach, which was developed to meet the requirements specified by the Transport Agency. The design relies on the recurrence intervals specified for different serviceability and ultimate limit states in the current *Bridge manual* (see section 3.4.2.3 above). The authors focus on the whole-of-life costs of the construction and maintenance of the highway, and therefore consider that small more frequent events are likely to govern design, rather than resilience in large earthquakes. Based on this philosophy, they have developed design criteria for rock cuttings, with factors of safety less than 1 considered acceptable for ultimate limit state events where

strains are less than 5% for rock mass failures. Their whole-of-life cost-based design decisions therefore favour a less resilient design for large seismic events, as this approach does not consider the effects on traffic and society or the impacts on the wider economy. It is worth noting various researchers have reported that project whole-of-life costs that ignore the consequential impacts and costs to society and the wider economy are most likely to favour a low-resilience design (Brabhaharan et al 2003).

3.4.2.5 Toh and Swarbrick (2015) approach

Toh and Swarbrick (2015) present a method of assessment of seismic loads considering topographic amplification, as used for the same Transmission Gully project. This method involves selection of a slope crest topographical amplification factor based on the slope angle and slope height, see table 3.4.

Table 3.4 Topographical amplification factor (Toh and Swarbrick 2015)

Slope height	Slope angle		
	<15º	15º–30º	>30º
<50m	1	1.2	2
50–200m	1	1.5	3
>200m	1	2	4

The slope crest seismic acceleration is then reduced by a 'location factor' by linear interpolation between the slope toe and crest to determine a reduced acceleration at the top of a slope failure mechanism involving a rock cutting on the lower part of the slope. This is also further reduced using a 'scale reduction factor' depending on the height of the mechanisms relative to the full height of the slope (crest level – toe level). The modification of the peak ground acceleration by these factors to derive the design acceleration is shown in equation 3.1.

Design acceleration kh

$$= PGAbase \times topographic\ amplification\ factor \times location\ factor \times scale\ reduction\ factor \quad \text{(Equation 3.1)}$$

Where:

- location factor = height from natural slope base to top of mechanism (h)/height from natural slope base to natural slope crest (H).
- scale reduction factor = 1–0.3 (h/H).

While researchers have recognised that the topographical amplification is likely to be highest at the crest, derivation of accelerations at intermediate heights may need to take into consideration the effect of local convexities along the slope profile which are likely to enhance ground shaking locally as noted by Meunier et al (2008). Also it is not clear why the 'scale reduction factor' takes into consideration the full height of the natural slope, rather than just the height of the slope failure mechanism being considered.

Toh and Swarbrick (2015) also suggest that high-quality rock masses are brittle, whereas low-strength fractured rock masses are ductile and do not experience strength loss post yield. From this they conclude that a Newmark sliding block approach to slope displacement can be adopted for rocks, because high-strength rock masses are less likely to have a factor of safety less than 1, whereas fractured low-strength rock masses where the factor of safety is more likely to be less than 1 are ductile and do not experience strength loss post yield and can therefore accommodate displacement without failure.

The assumption that jointed low-strength rock masses, which give factors of safety less than 1, are ductile and can therefore accommodate earthquake induced displacements is inconsistent with the large number of observations of rock slope failures in past earthquakes and subsequent storms as described in section

3.2 and appendix A. The assessment of fractured rocks using the Hoek-Brown failure criterion involves rock where displacement could lead to en echelon failures and breaks in intact rock sections. This in turn would lead to an overall reduction in the strength along the failure surface, leading to the rocks behaving in a brittle manner, with displacement leading to progressive failure of the rock slide. The rock slope weakened by displacement can also fail in subsequent after-shocks or storms as observed in past earthquakes.

3.4.3 Europe

3.4.3.1 Eurocode 8

EC8 (European Committee for Standardization 2004) provides standards for the design of structures for earthquake resistance in the European Union. Individual countries supplement this with their own specific information in the national annexes appended to the Eurocode.

Part 1 provides the basis for derivation of the seismic loads, based on:

- the importance of the structure and associated importance factor
- the reference peak ground acceleration and reference return period chosen by the national authorities for each seismic zone, corresponding to a no-collapse requirement
- ground type (A to E, S1 and S2)
- a topographical amplification factor, for important structures.

It also provides for representation of earthquake motions as a time history.

Part 5 provides for geotechnical structures, including consideration of slope stability associated with natural or artificial slopes, for structures on or near such slopes.

It provides for analyses either by means of:

- established dynamic analyses such as finite element or rigid block models or
- simplified pseudo-static methods, provided that:
  - surface topography and soil stratigraphy do not present very abrupt irregularities
  - the soil is not capable of developing high porewater pressures or significant degradation of stiffness under cyclic loading.

In the pseudo-static analyses method, EC8 proposes the following methods of derivation of seismic inertia forces:

- F_H = 0.5 (peak ground acceleration on rock) x ground type factor S x weight W
- $F_V = 0.5F_H$, if (vertical acceleration / design horizontal acceleration > 0.6)
- $F_V = 0.33F_H$, if (vertical acceleration / design horizontal acceleration < 0.6)

A topographic amplification factor is provided for, if importance factor > 1.

The topographical amplification factors proposed in EC8 are summarised in table 3.5.

Table 3.5 Topographical amplification factors from Eurocode 8

Topographical situation	Topographical amplification factor				
	Sites near top edge			Sites in between top and base	Sites at base of slope
	Slope angle				
	<15°	15°–30°	>30°		
Isolated cliffs and slopes	1	≥1.2		Linear interpolation between base and top edge of slope	1
Ridges with crest width significantly less than base width	1	≥1.2	≥1.4		1

Notes:

- In the presence of a loose surface layer, the smallest value of the factor given in the table should be increased by 20%.
- Seismic amplification also decreases rapidly with depth within the ridge. Therefore for deep seated failures surfaces passing near to the base, the topographical amplification factor may be neglected in pseudo-static analyses.

If serviceability limit state condition is checked by calculating permanent displacements, then the design acceleration is required to be used without reductions.

Annex A of EC8 provides guidance on derivation of topographical amplification factors. These amplification factors are proposed when slopes belong to two-dimensional topographic irregularities, such as long ridges and cliffs of height greater than about 30m. For average slope angles of less than about 15º, the topographic effects may be neglected.

The bibliographical background of the recommended values for topography effect amplification factor proposed in the EC8 is not clear. Following literature review and communications with international experts, our conclusion is that they were derived as an average of the values proposed in a number of precedent studies and published analyses.

Paolucci (2002; 2006) compared 3-D and 2-D numerical analyses results for an actual slope in Italy and compared the results with the topographic amplification factors of EC 8. It turned out that the EC8 recommendations in terms of topographic amplification factors are generally satisfactory, except from specific cases, where the EC8 factor underestimate the numerical value by 40%. These cases include isolated cliffs with heights H > 60m, slopes of similar dimensions of the width (W) and length (L) of the crest (eg $1/3 < L/W < 3$) and slopes with average angle > 30º and maximum angle > 60º. For these cases, a topographic amplification factor ST ≥ 1.7 was suggested, subject to verification with further 3-D numerical simulations. Paolucci further noted that topographic effects are typically 3-D, and few research groups had the capabilities of simulating them with appropriate numerical codes at the time of development of EC8. Therefore, most published results and parametric solutions taken into account for EC8 were derived from 2-D wave propagation analyses.

Bouckovalas and Papadimitriou (2006) note that the parasitic vertical component of the topography amplification factor is of importance and should be taken into account in the proposed topography amplification factors in EC8. They also noted that the horizontal distance to the free field is not clearly defined in EC8. Further, there is no specific suggestion for the reduction of the amplification factor with depth within the slope. They propose to change the slope geometry criteria for applying topography aggravation effects to be a function of the slope height, slope inclination and predominant wavelength of the shear waves λ. However, they concluded that the lower bound of the proposed topography amplification factors in EC8 have good agreement with their analysis for slopes with Vs>400m/s (stiff soils and soft rocks), H>13m and i>17º.

Recommendations for additional provisions and changes to EC8 were also made by the European Technical Committee (ETC-12 2006). The ETC became active in 2003, to provide general and specific comments on EC8 from the point of view of geotechnical earthquake engineering practice, and in light of the latest research at the time. The comments would be utilised during the five-year period of tentative application of EC8, to effect changes. The recommendations of the committee regarding the provisions of EC8 are summarised as follows:

- Characterise cases of irregular (ground surface or bedrock) topography as ground type S3, where the definition of seismic actions requires a special site exploration and study. The simple cases considered in annex A, as well as cases where topography effects are not important (eg average inclination $i<15^{\circ}$ or height H<30m and average shear wave velocity VS>300m/s) should be excluded from this category.
- For cliffs and step-like slopes, the distance behind the crest where topography aggravation persists should be defined. Until more refined studies become available on this topic, it is recommended to use the topography aggravation factors of annex A within a distance H behind the crest and reduce them (linearly) to the free field values (ST=1.00) at distances greater than 5H.
- Add criteria for simple cases of alluvial valleys subjected to weak ground motions.

3.4.3.2 Provisions of the French Seismic Code PS-92

Precedent to the EC8, the French Seismic Code PS-92 (Jalil 1992) included provisions related to the topographic aggravation of seismic motion. The French seismic code introduced a topography aggravation factor τ to the design peak acceleration, ranging from 1.00–1.40 as a function of the slope inclination (I). The factor was applied along the slope as shown in figure 3.2.

The factor was suggested to be applied to the upper part of the slope, of height equal to one third of the height of the slope, measured from the crest (a = AC = H/3). The distance to the free field above the slope crest is defined as a function of the inclination (I) and the height of the slope. Distance CB (b) is the minimum of 20I and (H+10)/4 in metres. Distance BD (c) is equal to H/4.

This French code was subsequently withdrawn, and has been replaced by the Eurocode.

Figure 3.2 Variation of the topography aggravation factor τ, as proposed by PS-92

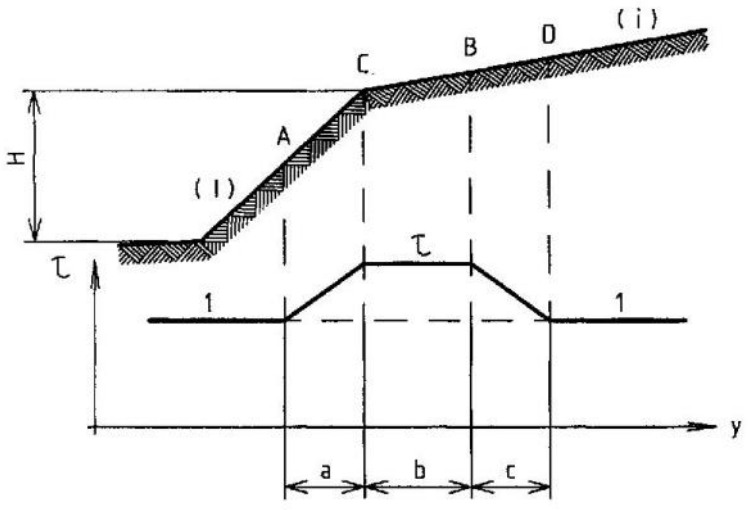

3.4.4 USA – California

The Southern California Earthquake Centre (2002) provides guidelines for analysing and mitigating landslide hazards in California. It was developed by a committee of the Los Angeles Section Geotechnical Group of the American Society of Civil Engineers.

The guidelines provide for derivation of ground motion parameters from either site-specific seismic hazard analyses or from the California Division of Mines and Geology seismic hazard maps. The recommended parameters for the analyses are the maximum horizontal acceleration (MHA), duration of strong shaking (D_{5-95}) and mean period of ground motion (T_m).

The guidelines propose a screening analyses for seismic slope performance, and for sites failing the screening analyses, assessment of slope displacements.

The seismic coefficient used in the screening analyses is calculated as:

$$K_{eq} = f_{eq} \times (MHA_r/g) \quad \text{(Equation 3.2)}$$

Where:

- MHA_r is the maximum horizontal acceleration at the site for a soft rock site condition
- g = acceleration of gravity
- the Californian code introduces a factor, f_{eq} related to the seismicity.

The values of f_{eq} are a function of magnitude (as represented by M) and site-source distance (as represented by r). Magnitude- and distance-dependent f_{eq} values are developed using a model for seismic slope displacements based on a Newmark-type analysis, using the Bray and Rathje (1998) model for estimating Newmark displacements (u) as a function of k_y/k_{max}, k_{max}, and D_{5-95}.

Two threshold values are assumed for the slope displacements of 5cm and 15cm. Based on the above, the f_{eq} values causing the probability that seismic slope displacement would exceed 5cm or 15cm to be 50% are estimated. This methodology for evaluating f_{eq} was developed in order to avoid unnecessary conservatism, with respect to previously followed practice, where a single value for f_{eq} was assumed, thus making implicit, and usually very conservative assumptions about the magnitude of earthquakes causing the design-basis MHA_r. The estimated f_{eq} with the new proposed procedure takes into account large and smaller magnitude earthquakes, as large magnitude earthquakes have longer durations of shaking.

The Californian guidelines make no provision for topographical amplification in their methods.

3.4.5 Discussion

A common element in the international design practice followed for pseudo-static slope stability analysis, is factoring of the horizontal seismic acceleration applied for the calculation of the equivalent acting force on the sliding mass. A factor of 0.5 is used in the EC8, of which we have not been able to clarify the background, and a factor f_{eq} is used in the Californian code.

Amplification of seismic waves due topographic irregularities has generally received limited attention in the context of design codes and standards. Recommendations were found only in the French Code PS-92 and the EC8. Both codes have considered step-like slopes and refer to the topography effects as an amplification of the seismic motion at the upper part of the slope.

Currently EC8 is the only code including recommendations on topographical amplification for slopes. Several authors have identified a number of limitations in the provisions of EC8 such as:

- the recommendations are general and simplifying of a complex phenomenon

- there is no provision to consider de-amplification towards the toe of the slope
- there is no specific definition of the distance to the free field
- the recommendations are considered satisfactory for step-like slopes in stiff soils or soft rocks with H>13m and i>17°. The proposed factors for higher and steeper isolated cliffs or ridges are considered to underestimate the phenomenon.

The focus of EC8 is in providing topographical amplification for buildings built on slopes, near the crest or at some distance from the crest, rather than providing a method for assessing the effect of topographical amplification on the earthquake stability of the slopes themselves.

4 Characterisation of New Zealand's topography and seismicity

The New Zealand land mass is tectonically very active due to its position within the boundary zone between the Pacific and Australian plates. Consequently, the topography of New Zealand is highly variable, from mountainous alpine areas, to lower relief mountains/hills, rolling hill country, rounded and incised peneplains, young volcanic terrain, recent alluvial plains and uplifted marine terraces. We have grouped these differing terrains into three broad categories for areas where transportation corridors pass through hilly terrain. This is presented in table 4.1

Table 4.1 Characterisation scheme for New Zealand topography

Hilly/mountainous terrain		
Characterised by sharp, narrow ridges flanked by steep hillslopes (35°–45°+) and deep valleys.		
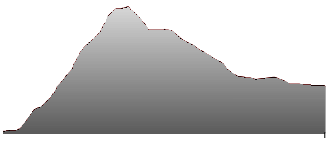 Eastern Bay of Plenty	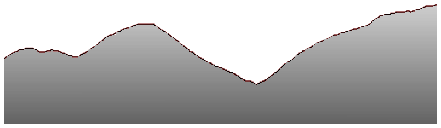 Wellington region	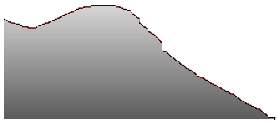 Port Hills
Undulating/rolling hills		
Characterised by rounded slopes (flat to steep slope angles), often with narrow incised gorges at the base.		
 Northland	 Central Otago	
Terraces		
Broad, flat-topped hills or terraces with sharp edges and steep slopes below the terrace edge.		
 Northern Manawatu	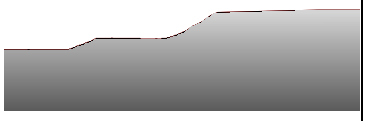 Canterbury Plains	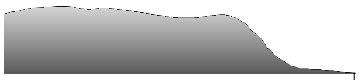 Kaikoura

The geology and seismicity of New Zealand has been characterised for areas where transportation corridors pass through hilly terrain. This is presented in table 4.2, which provides a summary of geological and seismotectonic characteristics for the three topographic types described above.

Geographic areas in New Zealand have been assigned to these terrain categories using regional scale digital elevation models (DEMs)/digital terrain models, supplemented where available with LIDAR data for key areas. These are then subdivided based on their geological and tectonic characteristics, which are described below and shown in figures 4.1 and 4.2. Areas where transportation corridors with major cut slopes are in proximity to major active faults are shown in figure 4.3.

Table 4.2 Summary of topographic, geological and seismo-tectonic characteristics

Geology / Tectonics	Indurated bedrock materials	Soft rock materials	Quaternary deposits
Hilly/mountainous terrain			
Oblique strike slip faults	• North Island axial ranges • Wellington region • Inland Marlborough • Port Hills • Southern Alps	• Coastal Marlborough	
Reverse faults/ subduction zone	• East Cape/eastern Bay of Plenty • Northwest Nelson to Buller • North Canterbury	• Gisborne to Hawkes Bay • Hawkes Bay to Wairarapa	
Normal faults		• South Waikato • Northern Manawatu	• Central volcanic plateau
Undulating/rolling hills			
Oblique strike slip faults			Inland Wairarapa
Reverse faults/ subduction zone	Central Otago		
Normal faults		• Northland	• Central volcanic plateau • Bay of Plenty
Terraces			
Oblique strike slip faults	• Southern Marlborough/ Kaikoura		
Reverse faults/ subduction zone			
Normal faults		• Northern Manawatu • Wanganui	• Coastal Taranaki, Wanganui and Manawatu • Canterbury Plains

Figure 4.1 shows a simplified geological map of New Zealand, with the geological formations grouped into three broad categories: indurated bedrock, soft rock materials, volcanic deposits and Quaternary soil deposits. The geological characterisation is based on the GNS Science 1:250,000 QMAP regional geology maps in conjunction with more detailed mapping where available.

Figure 4.2 shows a simplified seismotectonic characterisation of New Zealand, based on published seismological and tectonic characterisations (eg Litchfield et al 2014; McVerry et al 2006; Oyarzo-Vera et al 2012; Stirling et al 2012; Tarbali and Bradley 2014). The map shows the spatial variability in the styles of faulting/tectonic deformation across the plate boundary zone between the Pacific and Australian plates that spans New Zealand. The seismotectonic regimes vary from the subduction zone and fold-thrust belt in the eastern North Island, strike slip faults through the central part of New Zealand, reverse faults in the north and east of the South Island, normal faults associated with volcanic rifting on the central North Island volcanic plateau, and low seismicity areas in northwest North Island and southeast South Island.

Figure 4.1 Digital terrain model of New Zealand with simplified geology

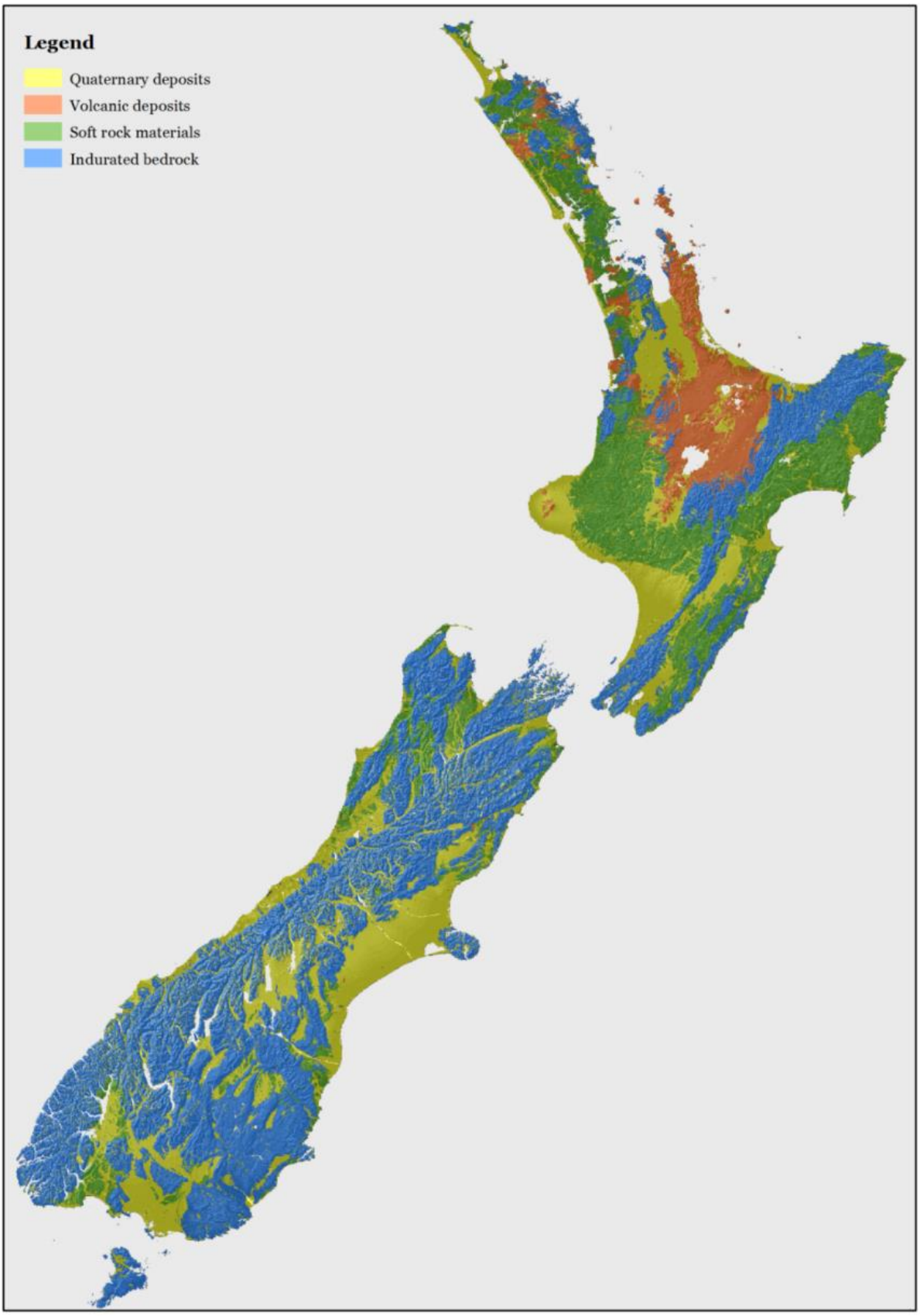

Figure 4.2 Digital terrain model with simplified tectonic domains

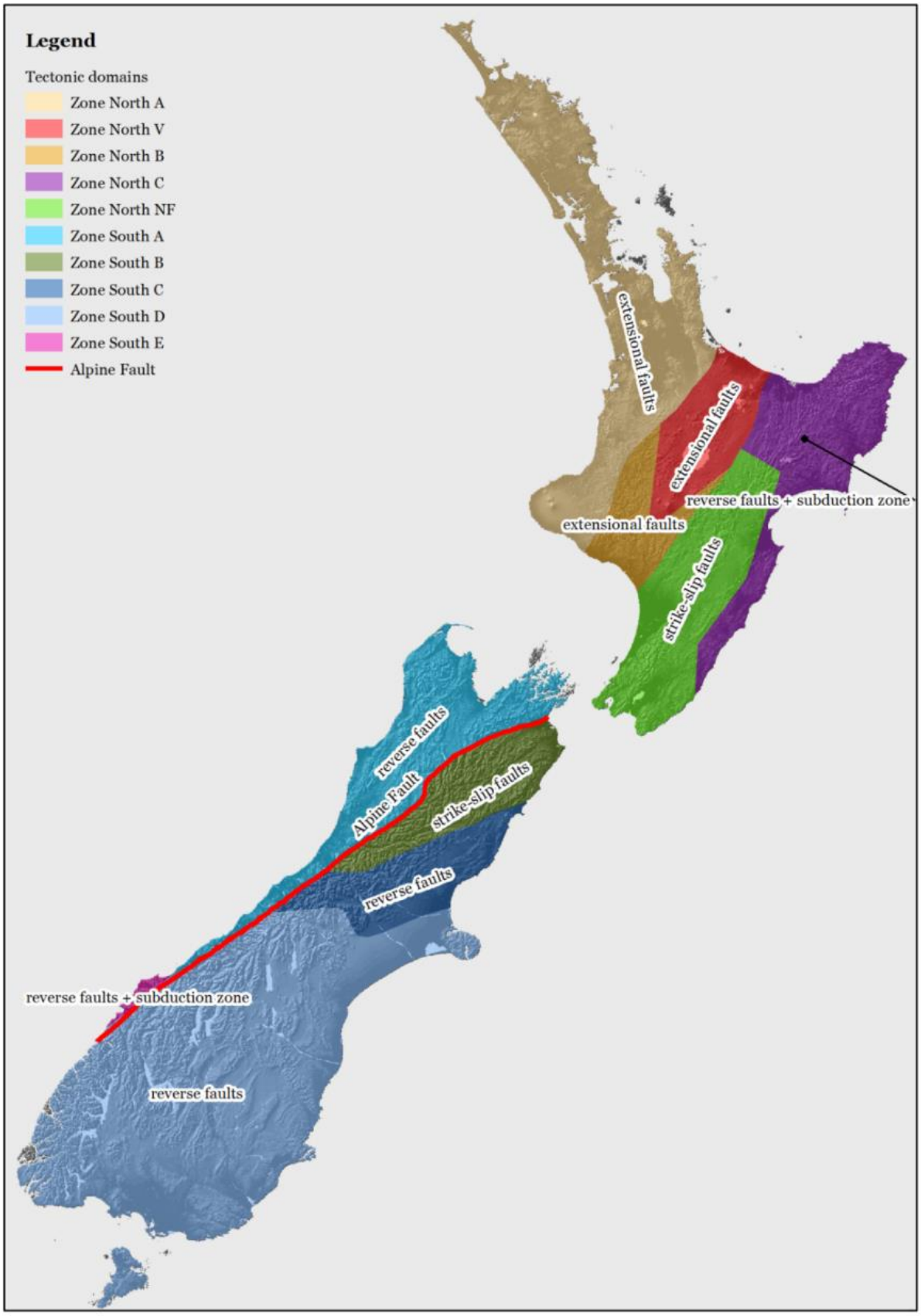

After Litchfield et al (2014), Oyarzo-Vera et al (2012) and Stirling et al (2012).

Figure 4.3 Digital terrain model showing state highways with major cut slopes in relation to active faults

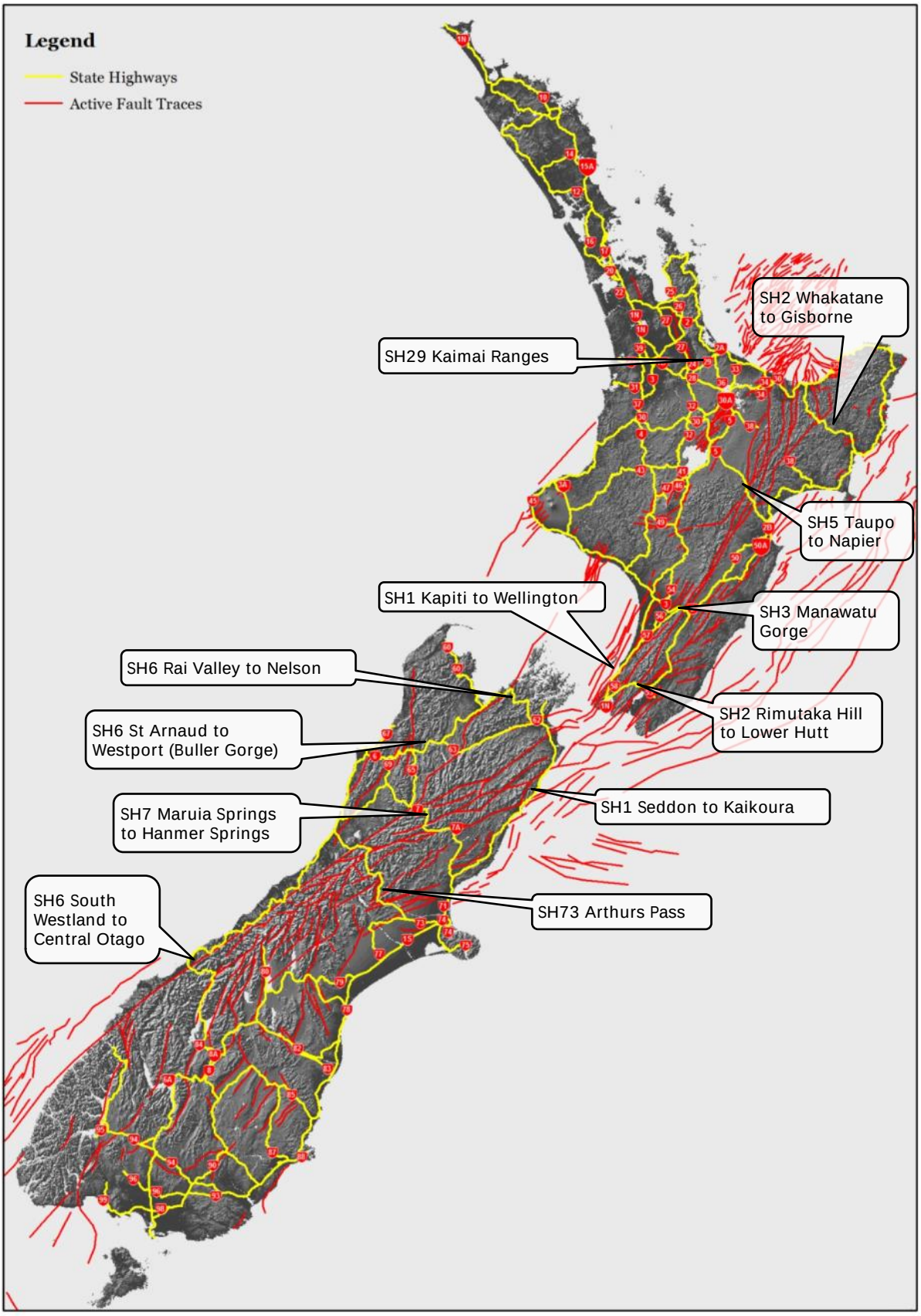

Fault traces after Litchfield et al (2014)

5 Observations from past earthquakes

5.1 In New Zealand

A detailed review of co-seismic landsliding and the performance of slopes during historical New Zealand earthquakes was carried out as part of this research project. The outcome of this review is presented in appendix A; salient points from the literature review of New Zealand slope performance in earthquakes are as follows:

- Co-seismic landslides in New Zealand are predominantly small (~10^3 m^3) to large (~10^5 m^3) disrupted falls, slides, and avalanches of rock, debris and soil.
- Common failure mechanisms involve translational sliding at the interface between bedrock and the overlying soil/regolith, or sliding and release along defects in bedrock.
- Common MM intensities for significant landsliding are MM7–8, with an equivalent PGA of ~0.1–0.5g.
- Shaking intensities of MM6 or greater are sufficient to trigger small to large failures on steep (>50º) unsupported cut slopes more than 3m high.
- The largest landslides (>10^6 m^3) occur on steep to very steep slopes (35 to 60º+) that are more than 50–100m high, in earthquakes with shaking intensities MM9+, with PGAs of 0.35–1.0g or more.
- Landslides tend to be concentrated on the hanging wall side of the fault in reverse/thrust fault earthquakes.

5.2 Worldwide

The literature review of reconnaissance reports and research papers from past worldwide earthquakes, in appendix A, has provided important information on the patterns of slope failure triggered by earthquake shaking. A summary of important observations from slope failures is given in table 5.1 and the key lessons for cut slope performance are discussed below.

Table 5.1 Summary of observations of slope performance in worldwide earthquakes

Earthquake event and key observations
1994 Northridge, California • M6.7 earthquake; thrust fault mechanism in hilly to mountainous terrain. • Most triggered landslides were shallow (1–5m thick), highly disrupted falls and slides of rock and debris within uncemented to weakly cemented Late Miocene to Pleistocene clastic sediment. • Deeper (>5m thick) rotational slumps and block slides were triggered, often as reactivations of pre-existing landslides. • Landslides were strongly clustered near ridge crests (56% in upper quartile of slopes). • Distribution of ground accelerations showed a pronounced hanging wall effect.
1999 Chi-Chi, Taiwan • M7.6 earthquake, thrust fault mechanism in hilly to mountainous terrain. • Most slope failures were shallow disaggregated landslides with failure at base of root zone. The dominant failure mechanism was shallow sliding along a stepped path of interconnected fractures. • Some defect-controlled failures occurred, especially in hard metamorphic rocks on Central Cross-Island Highway. • Most landslides occurred on the hanging wall block, in Tertiary sedimentary rocks. • 90% of failures occurred on slopes >45º; slips generally concentrated in the upper quartile of the slope.

Earthquake event and key observations
• Extensive landsliding occurred along the Central Cross-Island Highway. Many slopes (including cuts) were weakened by the mainshock, with subsequent failures from aftershocks and rainfall. • Well-designed rock slope support measures (shotcrete and rock bolts) performed well.
2004 Niigata Ken Chuetsu, Japan • M6.6 earthquake, thrust fault mechanism in hilly to mountainous terrain. • Very high concentrations of triggered landslides; most were shallow (1 to 2m deep), translational slides of colluvial and residual soils mantling steep slopes (>55º) underlain by Miocene to early Pleistocene sedimentary rocks. • Some deep bedrock landslides. • Most landslides occurred on the hanging wall block. • High antecedent rainfall (Typhoon Tokage in the days before the earthquake). • Poor performance of slopes above the road network in mountainous terrain. Collective volume of landslides caused significant road damage and closures.
2005 Kashmir, Pakistan • M7.6 earthquake, thrust fault mechanism in mountainous/alpine terrain. • Hanging wall side of fault severely affected by landslides. • Most landslides occurred in elevation range 850–1,750m, compared to total relief of 450–4,470m and on concave slopes. Failed slopes predominantly 20º–40º. • Most landslides occurred in shale, siltstone and limestone, as well as younger colluvium, terrace and scree deposits. • Topographic amplification effects observed (eg extensive fracturing of slope crests). • Extensive damage to road network caused by failure of steep cuttings (improperly designed) and natural hillslopes above the road.
2007 Niigata Chuetsu-Oki, Japan • M6.6 earthquake, reverse fault mechanism in hilly terrain. • Slope failures consisted of shallow translational slides, debris slumps and deep-seated rotational slides in areas underlain by Tertiary sedimentary rocks. • Notable large failures of cuts above roads and railways, particularly in HW mudstone (plastic fine-grained soil). • High antecedent rainfall – a typhoon rain front passed through the region immediately before the earthquake. • Minimum PGA of 0.2g to initiate landsliding.
2008 Wenchuan, China • M7.9; thrust fault mechanism in mountainous terrain. • Widespread earthquake-induced slope failures comprising shallow soil slips, landslides, rock avalanches, shallow rock slides, rock falls and debris flows. Landslides near epicentre often characterised by 'throw-like collapse'. • Large landslides occurred in competent limestone and sandstone cap on ridge tops underlain by weaker shale. Large defect-controlled rock slides in limestone-dolomite-shale sequences. • Majority of landslides occurred on slopes between 20º–50º. Slopes with heights >200m and/or angles 30º–45º showed a strong dynamic response. • Pronounced hanging wall, directivity and topographic amplification effects. • Horizontal amplification of PGA ~2 x free field acceleration for rock slopes; vertical amplification ~0.9 x horizontal. • Observed and inferred critical PGAs for triggering of landslides: PGA_h >0.21g, PGA_v >0.12g. • Slopes stabilised with rock anchors, anchored retaining walls/foundation beams or lateral loaded piles with pre-stressed anchors observed to have performed well.
2009 L'Aquila, Italy • M6.3 earthquake, normal fault mechanism in hilly terrain with terraces. • Slope failures included ravelling/sloughing and rock falls of road cuts, quarries and natural slopes. • General performance of cut slopes in limestone bedrock was good (minor superficial failures not widespread). • Typical ravelling-type failures of cut slopes in strong and fractured limestone involved uppermost weathered blocks bounded by soil-filled joints.

Earthquake event and key observations
• Cut slopes in weakly cemented sand and gravel were affected by ravelling and shallow slides and slumps.
2010 Maule, Chile • M8.8 earthquake, subduction mechanism in mountainous terrain. • Uncharacteristically low landslide density for a large magnitude earthquake. • Most landslides were rock falls and shallow disaggregated slides (eg ravelling) on natural and cut slopes. Tertiary sediments and Quaternary marine/beach sediments in steep coastal bluffs susceptible to shallow ravelling and sloughing, but failures were concentrated in only a few localities. • Deep-seated block or rotational slides were generally absent or rare. • Slopes stabilised with rock bolts, mesh, shotcrete etc performed well.
2011 Tohoku, Japan • M9.0 earthquake, subduction mechanism in hilly terrain. • Landsliding intensity was lower than expected for a M9.0 earthquake. • Most landslides were disrupted-type failures, originating at or near the crests of slopes. Other mechanisms included shallow and deep-seated landslides and rock falls. • 80% of landslides occurred in Miocene to Quaternary rocks (siltstone, sandstone and tuff). • The earthquake occurred during the dry season – flow-type failures were rare (excluding lateral spreading).
2013 Lushan, China • M_S7.0 earthquake, thrust fault mechanism in mountainous terrain. • Most common failure mechanisms were rock falls and shallow, disrupted landslides a few metres deep of weathered bedrock and colluvium on steep slopes (>45º). • Slopes consisting of deeply weathered and fractured sandstones and mudstones were the most susceptible to co-seismic landslides. • Rock falls from steep road cuts and natural slopes were very common and caused considerable damage and disruption to roads. • Landslides were not concentrated on the hanging wall block.
2015 Gorkha, Nepal • M_W7.8 earthquake, thrust fault mechanism in mountainous terrain. • Most common failure mechanisms were ravelling failures, translational block slides, and rock falls a few metres deep of weathered and fractured bedrock and colluvium on steep slopes. • Rock falls and block slides from steep road cuts and natural slopes were very common and caused considerable damage and disruption to roads. • Hanging wall, directivity and topographic amplification effects apparent due to landslides distribution and density in the area to the east of the epicentre.
2016 Kumamoto earthquake • M_W6.3 and M_w 7 earthquakes in volcanic terrain and alluvial plains. • Most common landslides mechanisms were shallow failures at the upper parts of steep hillsides. • Large landslides in gentle terrain, lateral displacement of weak deposits and debris flows were also observed in volcanic ash and pumice deposits. • Rock slopes failures were largely defect controlled rock slides, toppling or rock falls.

5.2.1 Types of common slope failures in large earthquakes

The general pattern of damage observed in recent large earthquakes is of widespread slope failures characterised by shallow (generally up to a few metres) landsliding in the surficial layers of regolith and immediately adjacent weak, brittle and dilated rock mass in the upper parts of steep slopes. These are commonly termed disaggregated or ravelling-type landslides.

Example photographs of shallow, disrupted/disaggregated landslides from the 1999 Chi-Chi and 2008 Wenchuan earthquakes are given in figure 5.1.

The common failure mechanisms associated with these types of slope failures are sliding along a stepped path of short-persistence, interconnecting, sub-parallel defects in the surficial zone of weak rock/regolith at or near the base of the root zone. Large or very large landslides are comparatively rare in number and extent compared with the shallow, disaggregated slides. These large landslides are often defect-controlled, where the conditions of seismic wave propagation direction, dip and dip direction of unfavourable discontinuities, and slope orientation are aligned. While defect-controlled failures in bedded, competent bedrock occur less frequently, these tend to be much larger in volume than the shallow disaggregated landslides, and consequently can cause much greater damage. Examples of large, defect-controlled landslides are given in figure 5.2.

Figure 5.1 Shallow, disaggregated landslides –1999 Chi-Chi and 2008 Wenchuan earthquakes

1999 Chi-Chi

2008 Wenchuan

2008 Wenchuan

2008 Wenchuan

Figure 5.2 Large, deep-seated landslides – 1999 Chi-Chi and 2008 Wenchuan earthquakes

1999 Chi-Chi

1999 Chi-Chi

1999 Chi-Chi

2008 Wenchuan

5.2.2 Topographic and geological characteristics

Slopes steeper than 40º to 50º underlain by young (Miocene or younger) sedimentary rocks have been observed to be prone to the shallow, disaggregated/ravelling type of landslides (see table 5.1). Slopes in more competent bedrock are prone to more localised failures (shallow rock slides and rock falls).

The middle to upper parts of hillslopes are most susceptible to landsliding, which is likely to be due to a combination of steep slope angles, weaker rock strength (due to the effects of weathering, dilation, fracturing etc) and topographic amplification of ground motions in those parts of the slopes.

5.2.3 Seismicity effects and seismotectonic regime

Hanging wall, topographic amplification and attenuation/directivity effects result in asymmetric patterns of slope failure around the fault rupture, with larger ground motions and consequently more slope failures located at greater distances from the fault in areas that exhibit these effects (eg Inangahua, Northridge, Chi-Chi, Niigata Ken Chuetsu, Kashmir and Wenchuan events).

The earthquake focal mechanisms are listed in tables 3.1 and 5.1 for past worldwide earthquakes with well documented or important patterns of slope failure; the available dataset shows that thrust faulting is a common factor in earthquakes with widespread landsliding and pronounced topographic effects.

From the recent earthquakes considered, the subduction fault earthquakes although of large magnitude appear to have resulted in less earthquake induced landslides in comparison with the earthquake magnitude.

5.2.4 Antecedent conditions

High antecedent groundwater levels have often been associated with exacerbated landslide damage in large earthquakes (eg 2004 Niigata Ken Chuetsu and 2007 Niigata Chuestu-Oki earthquakes). Conversely, dry conditions have been proposed as a contributing factor in uncharacteristically low levels of observed landslide damage (eg 1999 Izmit and 2011 Tohoku earthquakes).

5.2.5 Post-earthquake triggers

Slopes can be weakened but not fail during strong earthquake shaking, with subsequent change in conditions such as post-event rainfall or aftershocks triggering widespread failures (eg 1999 Chi-Chi earthquake).

The trapping and consequent amplification of seismic waves within the disturbed rock mass of incipient zones of slope failure can also contribute to triggering of large landslides in subsequent events (eg Havenith et al 2003; Burjánek et al 2011; Moore et al 2012).

Stability analysis of slopes for design of large cuttings may require consideration of cumulative effects of a sequence of earthquakes less than the design event, where ground shaking that does not trigger failure produces systematic preferential tensile fracturing in the upper parts of the slope which creates zones of deformed material. These incipient failure zones have degraded properties relative to the surrounding, less-deformed rock, and that in turn can generate geological and topographical amplification effects in subsequent earthquakes, leading to large scale slope failure.

5.2.6 Effectiveness of slope stabilisation measures.

Slope stabilisation measures (eg shotcrete, rock bolts, anchored retaining walls) performed well in the 1999 Chi-Chi and 2008 Wenchuan earthquakes, whereas adjacent unsupported natural and cut slopes suffered widespread shallow landslides and rock falls (eg Khazai and Sitar 2003; Yu et al 2010).

5.2.7 Cut slope design records

The literature review of earthquake reconnaissance reports and research papers did not identify if any cut slope designs had been retrieved and analysed when reporting on or assessing the mechanisms of damage to cut slopes in recent earthquakes. Consequently, forensic examination of the actual performance of cut slopes against their expected design performance could not be carried out. Observation of damage to tunnels and bridges includes examination of design records, but the focus of these tends to be on mechanisms of structural damage rather than performance of any adjacent cut slopes (eg Wang et al 1999).

6 Numerical analysis of topographic effects

6.1 Purpose and scope

Limited, preliminary numerical analyses were carried out as part of the current study to provide a better insight to the variation of ground acceleration along the height of the slope, as well as the effects of cut slopes affecting part of the slope.

Ridge and terrace topographies were both examined in the analysis. The geometry of both topographies examined was varied in terms of slope height and angle (and hence width of base for the ridges). The slopes were assumed to consist of rock, so that high complexity of the model has been avoided and the interpretation of the results concern seismic motion variation due to topography, rather than potential soil amplification effects. However, limited analyses were carried out taking into account the presence of weaker material near the slope surface, at a very preliminary stage, to provide insight into the degree of influence of overburden materials overlying bedrock. The material was assumed to be either soil overburden or HW rock overlying less weathered bedrock.

A case of the ridge topography with a cut excavated at the lower part of the ridge slope was also examined. The objective of this analysis was to investigate if there was variation in the ground seismic motions at the crest of the cut slope (which is not at the crest of the ridge), due to the local topography irregularity.

6.2 Numerical modelling

6.2.1 Software

The numerical analyses were carried out using the Plaxis 2-D finite element software produced by Plaxis bv, The Netherlands.

6.2.2 Boundary conditions

For the Plaxis analysis, the bottom boundary of the model was set as a compliant base while the lateral boundaries were set as a far-field boundary. The compliant base boundary applies the input motion as a traction instead of an acceleration so as to prevent the downward travelling waves from being reflected back into the model. The use of far-field boundary also gives a similar effect of abating horizontal wave reflection at the lateral boundaries.

6.2.3 Application of seismic motions

As Plaxis treats the input motion as an incident wave motion (ie an upward travelling wave) when the motion is applied through a compliant base, the amplitude of the acceleration harmonics applied at the model base were set at 0.3g, which would produce a theoretical 0.6g free-field acceleration amplitude if the motion was applied on a ground profile with a horizontal surface.

The degree of free-field acceleration that is actually observed in the Plaxis simulations are monitored at a point that is at the same elevation as the toe of slope (albeit at a distance away from it).

6.2.4 Geometry of the models

The numerical modelling was carried out for the terrace and ridge geometries to model terrace and hill terrain with high slopes, as illustrated in table 6.1. Ground motions were ‘recorded’ at various locations

(points) in the free-field and along the slope during the analyses, which are also shown in table 6.1. The distance of the terrace – ridge slope toe and crest to the free-field was not thoroughly investigated in this stage of the analyses. Understanding the performance of the common New Zealand, and particularly lower North Island topographies examined was the focus of this current phase of research.

Table 6.1 Summary of geometries modelled in the numerical analyses

Case no.	Type of terrain	Heights and slope angles examined	Model geometry
1	Terrace	• 50m and 45° • 100m and 45° • 50m and 50° • 100m and 50°	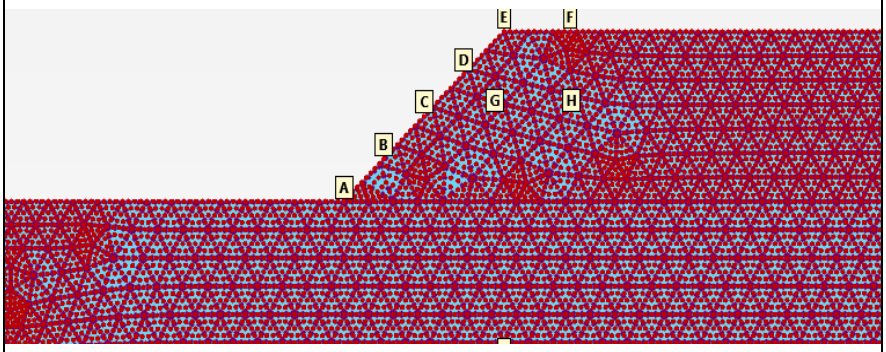
2	Ridge	• 50m and 35° • 50m and 45° • 200m and 35° • 200m and 45° • 400m and 45°	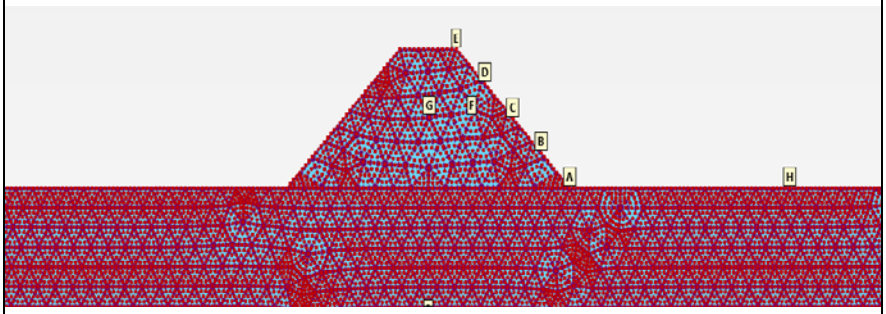

It should be pointed out that the thickness of the model base underlying the geometric profiles studied can influence the horizontal acceleration observed at the selected free-field location in the model, especially for the case of the ridge profile. Upon closer examination of the model outputs, it is noted that, when the thickness of the base is comparable to that of the ridge height, the dynamic excitations would seemingly generate 'rocking' of the ridge that would in turn give rise to large vertical stresses at the ridge toes. These vertical stresses would then travel away from the ridge as horizontal waves. It is surmised here that the presence of these waves is responsible for the influence on the acceleration observed on the surface since the surface can no longer be considered truly free-field.

If the base thickness is set to a smaller value compared with the ridge height (eg 50m for a ridge height of 200m), the peak free-field acceleration observed would become much more consistent with the target value of 0.6g. The results presented in this report are from the analyses with the smaller thickness base that does not influence the free-field conditions.

Limited numerical analyses were also carried out to examine the effects of a weaker layer overlying bedrock on the slopes, either a soil overburden layer or HW rock. The thickness of the weaker layer was modelled as 20m for both cases. The slope behaviour with the presence of weaker layer was modelled for

both the terrace and ridge terrain configurations, as illustrated in table 6.2, which also shows the locations at which the motions were recorded during the analyses.

Numerical modelling was also carried out to examine the effects of a cut slope in the lower part of the ridge, but not extending over its full height. This is also illustrated in table 6.2.

Table 6.2 Geometries modelled with overburden and cut slope in lower part of ridge

Case no	Type of terrain	Heights and slope angles examined	Model figure
3	Terrace with overburden soil layer or HW rock (layer 20m thick)	• 100m and 45º	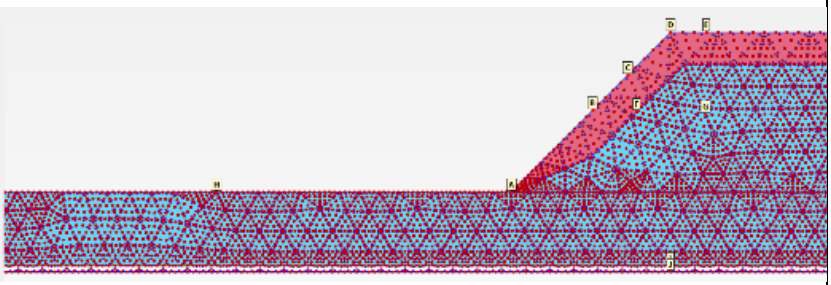
4	Ridge with overburden soil layer or HW rock (layer 20m thick)	• 200m and 45º	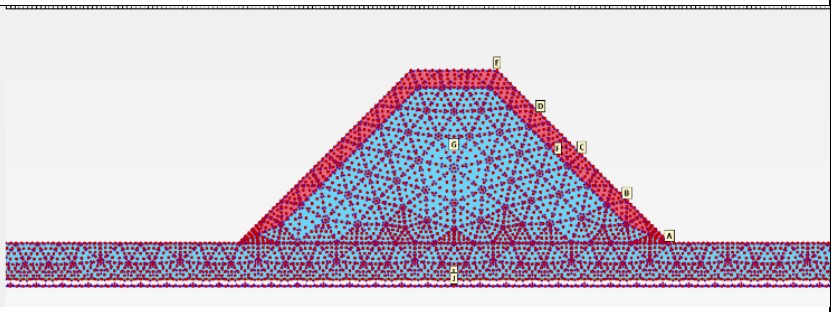
5	Ridge with cut at the lower part of the slope	• Ridge: 200m height with slope angles 27º–35º. • Cut: 45º–50º slopes, 50–100m high.	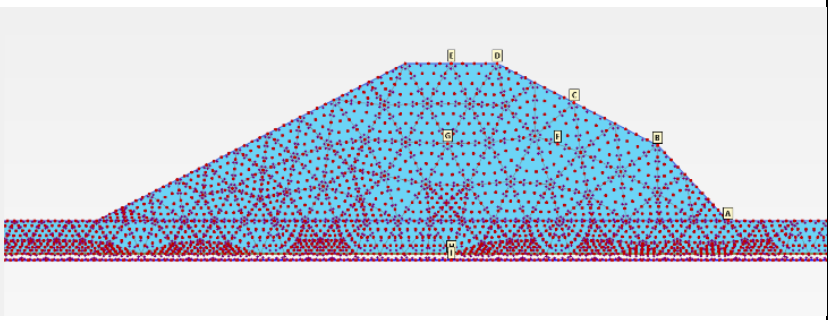

6.2.5 Material parameters

The parent rock, HW bedrock and overburden materials were modelled as linear elastic, with the following material properties:

- The Poisson's ratio for both rock and overburden materials in the model was assumed to be 0.15.
- The Young's modulus for the parent rock material was modelled as 40GPa (equivalent to a shear wave velocity of 2,700ms^{-1}).
- The Young' s modulus for the HW rock material was modelled as 4GPa (equivalent to a shear wave velocity of 500–1,200ms^{-1})

- For the cases with the overburden soil layer, the soil was modelled with a Young's modulus with a lower bound value of 40MPa and an upper bound value of 80MPa.
- Rayleigh damping was applied for both materials, with the α and β parameters selected to be 0.04284 and $0.4341*10^{-3}$ respectively. These damping parameters ensured the damping ratio would stay between 0.5 and 1.5 within the frequency range of 0.5Hz and 10Hz.

6.3 Seismic input motions

6.3.1 Simple harmonics

Most of the numerical model analyses were carried out with simple harmonic seismic input motions, so that the effect of frequency on the topographical amplification could be examined. The simple harmonics free field motion simulated had:

- amplitude of 0.6g
- frequencies of 0.5Hz, 1.5Hz, 2Hz, and 5Hz (and also 10Hz for a limited number of models).

6.3.2 Time histories

Analyses were also carried out using real seismic records to examine the response of the slopes in a wider range of frequencies. The seismic motions used were near source records from the 1992 Landers earthquake, which contained a large intensity of high-frequency components.

One geometry was indicatively examined with the 1992 Landers real-time histories, the ridge of height of 200m and 45º slopes, for comparison.

6.4 Results of the analysis

6.4.1 Derivation of results

During the numerical modelling, the motions induced by the input seismic motions were recorded at the locations (A to H) shown in tables 6.1 and 6.2. These recorded motions were examined to obtain the results of the numerical analyses.

From these recorded results, the amplification factor was calculated with respect to the free-field input motion (equal to 0.6g), as:

- amplification factor = observed amplitude of the acceleration divided by free-field acceleration of 0.6g.

The amplification factor at various locations on the slope were considered as the results of the numerical modelling as the purpose was to examine the effect of topography on the seismic motions.

6.4.2 Terrace and ridge underlain by bedrock, with harmonics inputs

The results of numerical analysis are summarised as follows:

- for the terrace topography consisting of bedrock, case 1 of table 6.1 are summarised in table 6.3 and graphically shown in figures 6.1 and 6.2.
- for the ridge/hill topography consisting of bedrock, case 2 of table 6.2 are summarised in table 6.4, and graphically shown in figures 6.3, 6.4 and 6.5.

Table 6.3 Amplification factor for ground accelerations for terrace with bedrock – case 1

Slope geometry	Amplification factor at different locations on the slope			
	Toe (point A)	Mid height (point C)	Crest (point E)	Inside the slope (point G)
• Terrace 50m high • Slopes 45°–50° • Rock • See figure 6.1	1.0 (at 0.5Hz) 0.8–0.9 (at frequencies ≥1.5Hz)	~1.0 (at all frequencies)	1.0 (frequencies ≤ 2Hz) 1.2 (at 5Hz)	~1.0 (at all frequencies)
• Terrace 100m high • Slopes 45°–50° • Rock • See figure 6.2	1.0 (at 0.5Hz) 0.8–0.9 (at frequencies ≥1.5Hz)	~1.0 (frequencies ≤ 2Hz) 1.2 (at 5Hz)	~1.0 (at 0.5 and 1.5Hz) 1.3–1.4 (at 2Hz and 5Hz)	1.0–1.1 (at all frequencies)

Figure 6.1 Amplification factors for terrace 50m high – 45° and 50° slopes

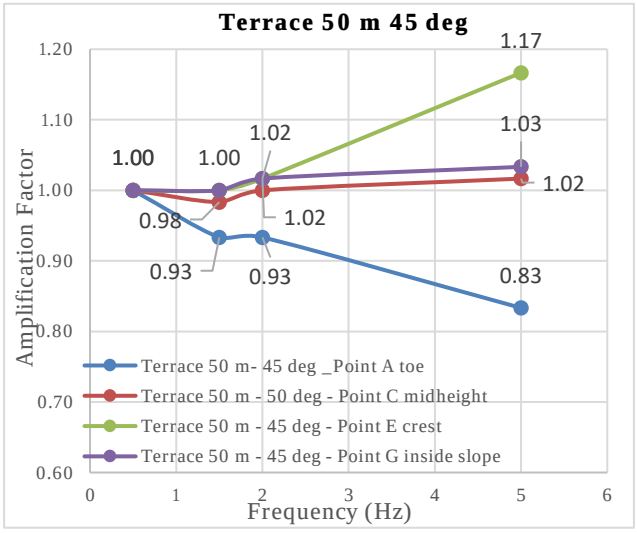

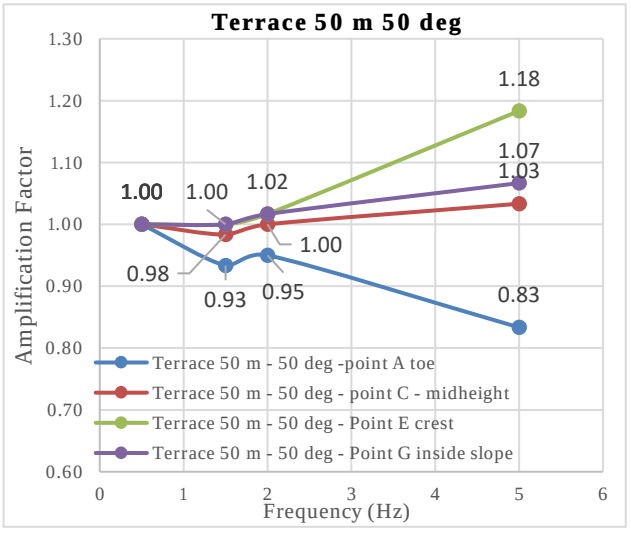

Figure 6.2 Amplification factors for terrace 100m high – 45° and 50° slopes

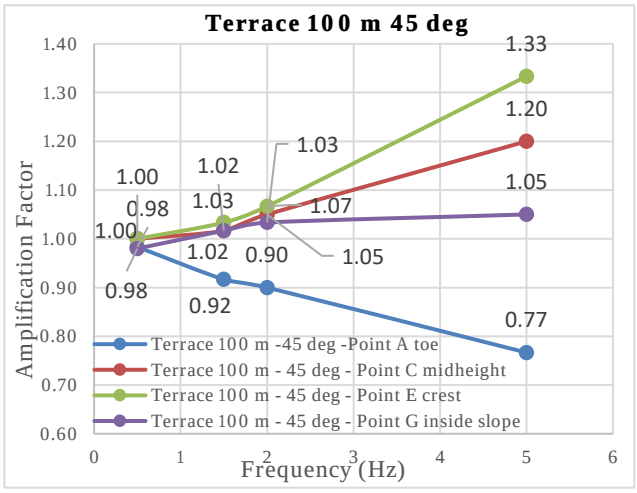

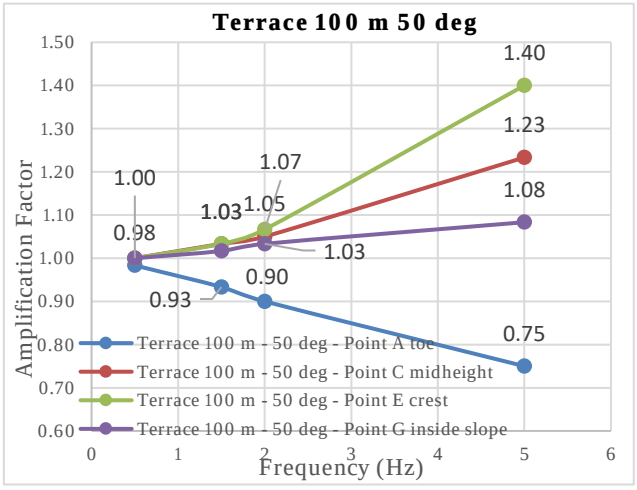

Table 6.4 Amplification factor for ground accelerations for ridge – case 2

Slope geometry	Amplification factor at different locations on the slope			
	Toe (Point A)	Mid height (Point C)	Crest (Point E)	Inside the slope (Point F)
• Ridge 50m high • Slopes 35° and 45° • Rock • See figure 6.3	~1.00 (at all frequencies)	~1.0 (frequencies ≤ 2Hz) 1.2–1.3 (at 5Hz)	1.0 (frequencies ≤ 2Hz) 1.50–1.60 (at 5Hz)	~1.0 (frequencies ≤ 2Hz) 1.50–1.60 (at 5Hz)
• Ridge 200m high • Slopes 35° and 45° • Rock • See figure 6.4	~1.00 (at 0.5Hz) 0.8–0.9 (at frequencies ≥ 1.5Hz)	1.0 (at 0.5Hz) 1.2–1.4 (at 1.5, 2 and 10Hz) 0.8–0.9 (at 5Hz)	1.0 (at 0.5Hz) 1.4–1.7 (at 1.5 and 2Hz) 2.5–3.0 (frequencies ≥ 5Hz)	1.0 (at 0.5Hz) 1.3–1.6 (at 1.5 and 2Hz) 3.0 (at 35° and 5Hz) 0.7–0.8 (at 45° and at 5 and 10Hz)
• Ridge 400m high • Slopes 45° • Rock • See figure 6.5	0.8–1.0 (at all frequencies)	1.0–1.3 (higher amplifications at 1.5Hz and 10Hz)	1.2–3.0 (higher amplifications at 1.5Hz and 2Hz)	1.1–1.4 (at amplifications 0.5, 1.5 and 2Hz) 0.5–0.6 (at amplifications 0.5, 1.5 and 2Hz)

Figure 6.3 Amplification factors for ridge 50m high – 35° and 45° slopes

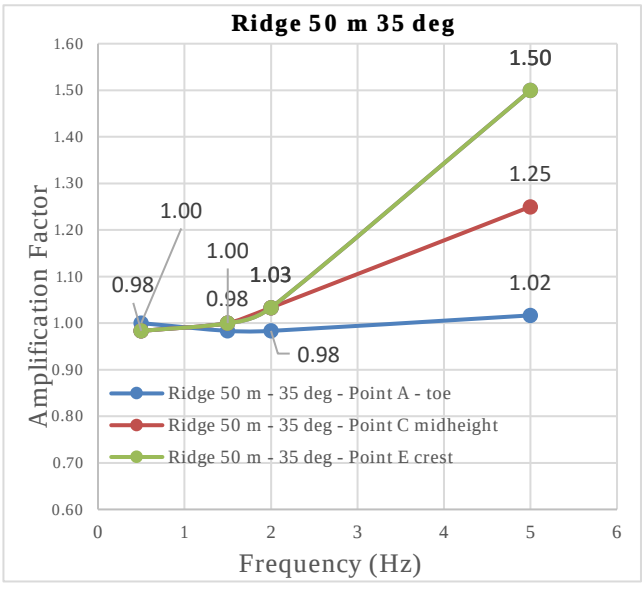

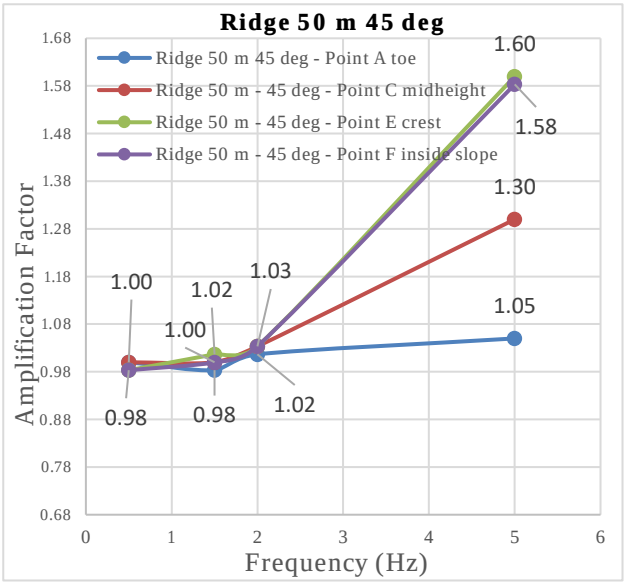

Figure 6.4 Amplification factors for ridge 200m high – 35° and 45° slopes

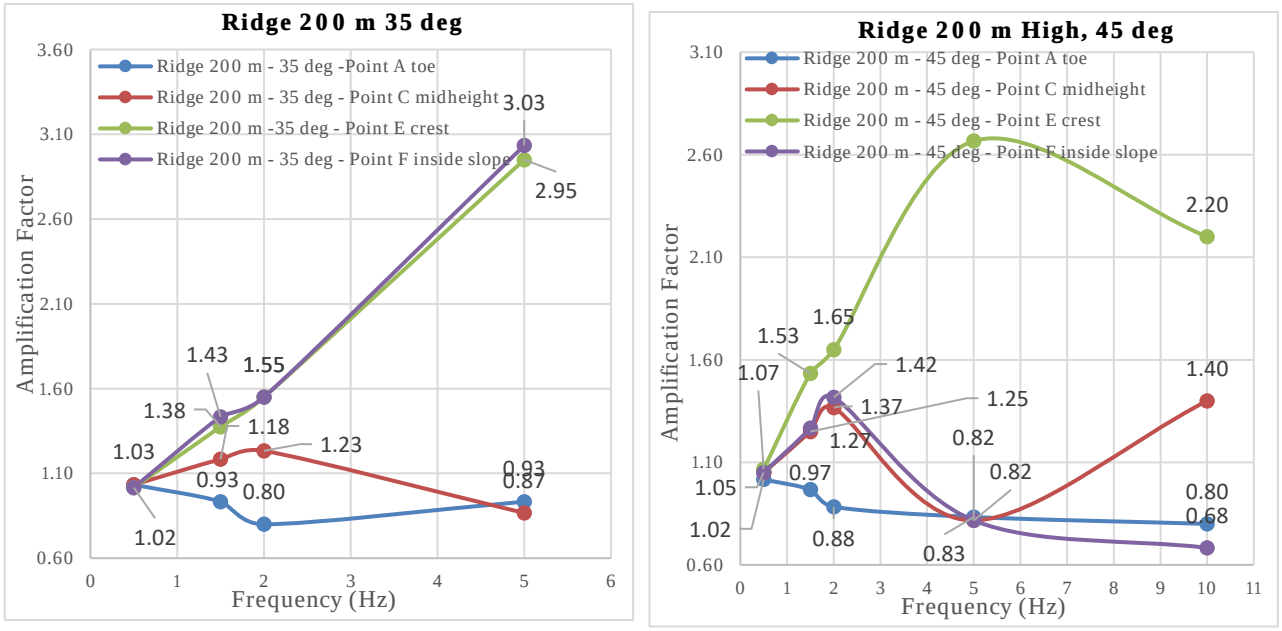

Figure 6.5 Amplification factors for ridge 400m high, 45° slope

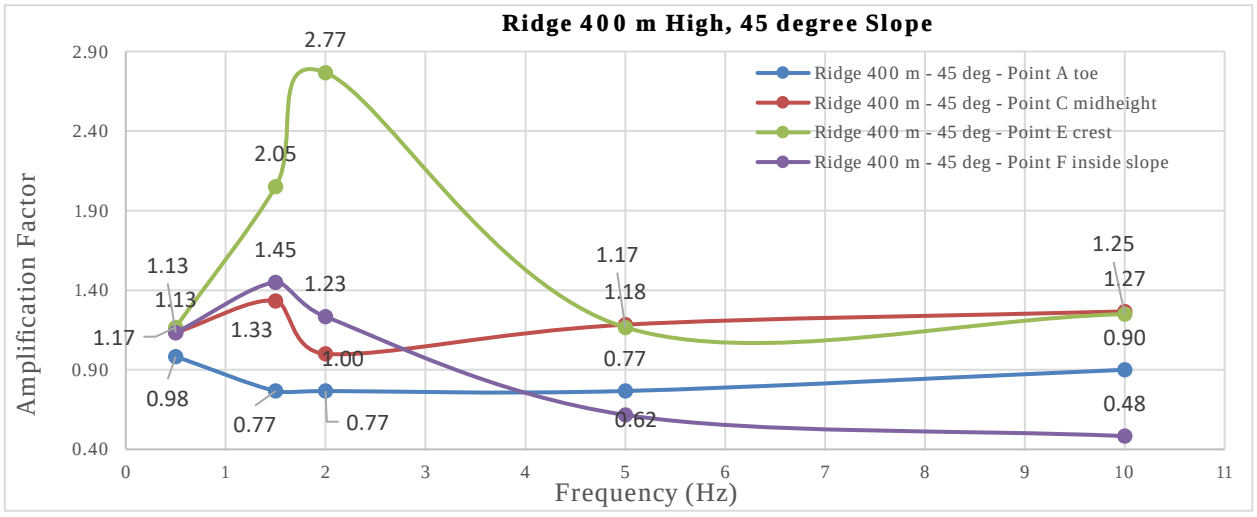

6.4.3 Ridge terrain underlain by bedrock, with time history inputs

The ridge topography, 200m high with 45º slopes, was also examined with numerical analyses using real-time histories from the 1992 Landers earthquake.

Two records (LCN260 and LCN 345) were used from this earthquake sequence for the analysis. The frequency range of both motions was similar and up to 60Hz. The amplitude of the LCN260 was larger.

The results of the analysis are presented in table 6.5 and figure 6.6.

Table 6.5 Amplification factor for ground accelerations for ridge using time histories – case 2

Slope geometry	Time-history	Amplification factor at different locations on the slope			
		Toe (point A)	Mid height (point C)	Crest (point E)	Inside the slope (point F)
• Ridge 200m high • Slopes 45° • Rock • See figure 6.6	LCN 260	0.78	1.04	1.82	0.82
	LCN345	0.86	0.81	1.19	0.88

Figure 6.6 Amplification factors for the ridge 200m high (45° slope angles) using the 1992 Landers earthquake recordings

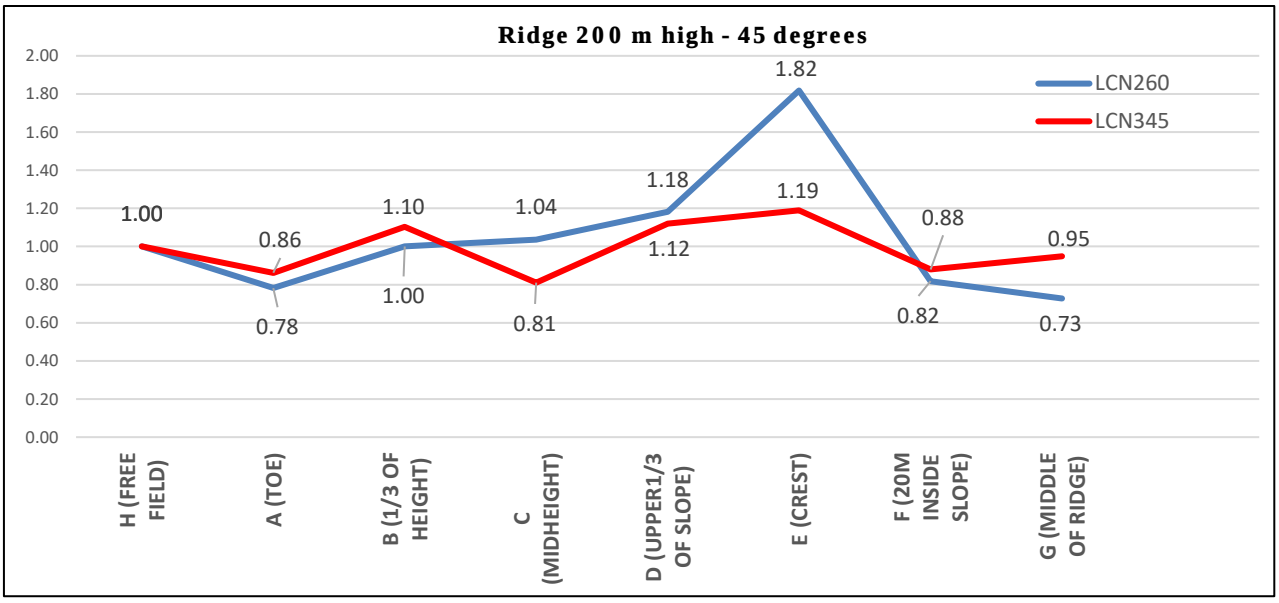

6.4.4 Terrace and ridge bedrock with soil overburden, harmonic inputs

The terrace and ridge topography were also examined considering the presence of a soil overburden layer near the slope surface, cases 3 and 4 of table 6.1. The results of the numerical analysis in terms of ground acceleration amplification factor at different locations of the slope are summarised in tables 6.6 and 6.7 and graphically shown in figures 6.7 and 6.8.

Table 6.6 Amplification factor for ground accelerations for terrace topography with soil overburden – case 3

Slope geometry	Amplification factor at different locations on the slope			
	Toe (point A)	Mid height (point B)	Crest (point D)	Inside the slope (point F)
• Terrace 100m high • Slopes 45°–50° • Rock with soil overburden layer • See figure 6.7	1.0 (at 0.5 and 10Hz) 0.8–0.9 (at frequencies from 1.5 to 5Hz)	1.2–6.0 (higher amplifications at 1.5 and 2Hz)	1.7–13.0 (higher amplifications at 1.5 and 2Hz)	0.8–1.1 (at all frequencies)

Figure 6.7 Amplification factor: terrace 100m high with soil overburden (45° slope)

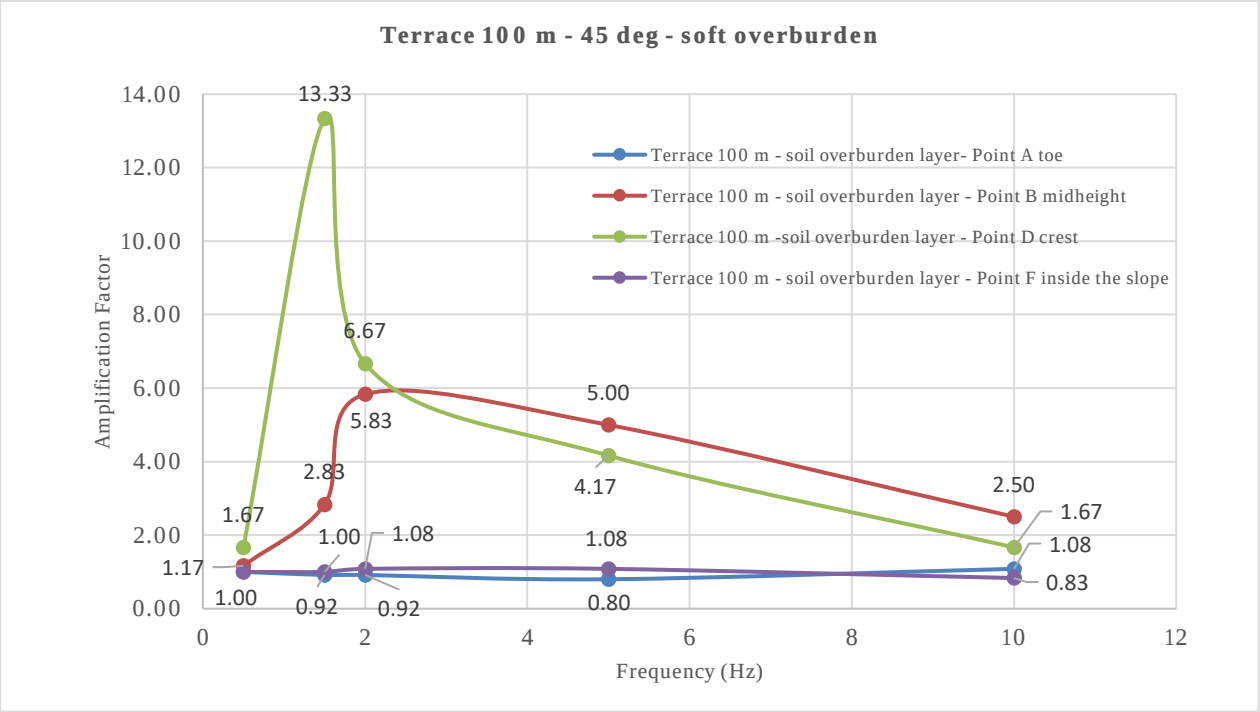

Table 6.7 Amplification factor of ground accelerations for hill-ridge topography with soil overburden – case 4

Slope geometry	Amplification factor at different locations on the slope			
	Toe (point A)	Mid height (point C)	Crest (point E)	Inside the slope (point F)
• Ridge 200m high • Slopes 45° • Rock with soil overburden • See figure 6.8	1.00 (at 0.5Hz) 0.8–0.9 (at frequencies ≥ 1.5Hz)	0.8 (at 10Hz) 1.7–3.3 (at 0.5 and 5Hz) 7.2–13.3 (at 1.5 and 2Hz)	1.7–13.3 (higher amplifications at 1.5, 2 and 5Hz)	1.2–1.3 (at 1.5 and 2Hz) 1.0 (at 0.5 and 5Hz) 0.7 (at 10Hz)

Figure 6.8 Amplification factors for ridge 200m high with soil overburden – 45° slopes

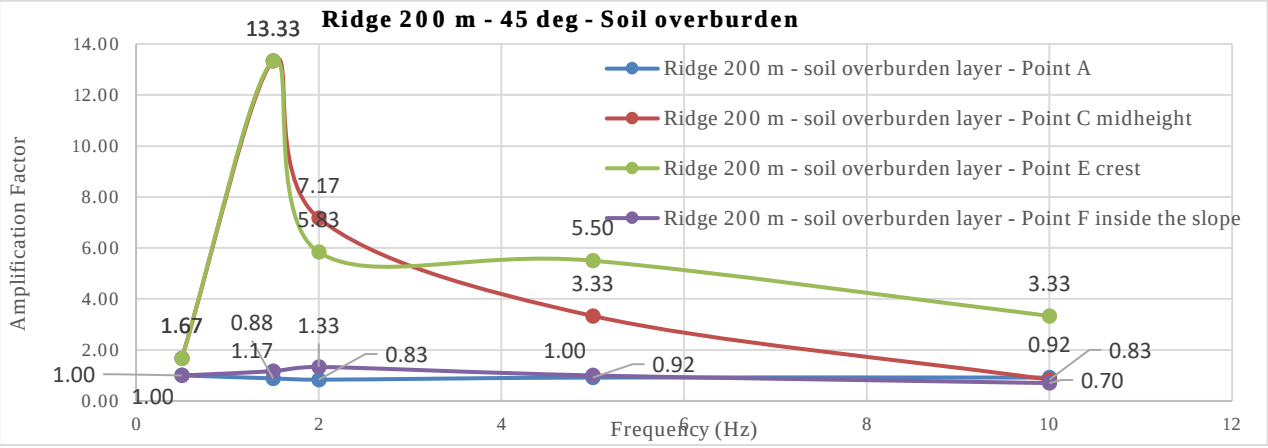

6.4.5 Terrace and ridge bedrock overlain by weathered rock and harmonic inputs

The terrace and ridge topography were also examined considering the presence of a HW rock layer near the slope surface, of a thickness and geometry indicated in cases 3 and 4 of table 6.1.

The results of the numerical analysis in terms of ground acceleration amplification factor at different locations on the slope are summarised in tables 6.8 and 6.9 and graphically shown in figures 6.9 and 6.10.

The results indicate the potential for significant amplification with the presence of weathered rock overlying less weathered rock, which is much larger than the amplification assessed where there is no weathered rock present, see figure 6.2. This is pronounced at the higher frequencies of motion.

Table 6.8 Amplification factor for ground accelerations for terrace topography with bedrock overlain by highly weathered rock – case 3

Slope geometry	Amplification factor at different locations on the slope			
	Toe (point A)	Mid height (point B)	Crest (point D)	Inside the slope (point F)
• Terrace 100m high • Slopes 45º • Bedrock overlain by HW rock • See figure 6.9	1.0 (at 0.5Hz) 0.8–0.9 (at frequencies from 1.5 to 10Hz)	1.0 (at 0.5 and 1.5Hz) 1.1–3.7 (higher amplifications at 10Hz)	1.0–1.1 (at 0.5 and 1.5Hz) 1.25–3.75 (higher amplifications at 5 and 10Hz)	1.0–1.5 (at all frequencies)

Figure 6.9 Amplification factor: terrace 100m high with HW rock overlying bedrock (45° slope)

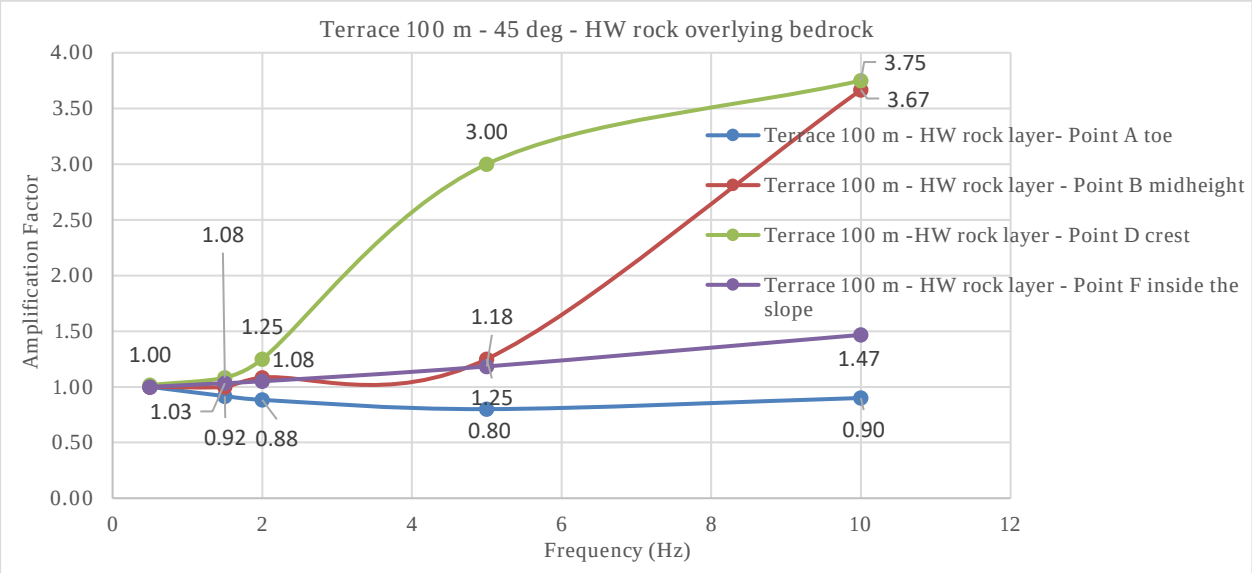

Table 6.9 Amplification factor for ground accelerations for ridge topography with bedrock overlain by highly weathered bedrock – case 3

Slope geometry	Amplification factor at different locations on the slope			
	Toe (point A)	Mid height (point C)	Crest (point E)	Inside the slope (point F)
• Ridge 200m high • Slopes 45º • Bedrock overlain by HW rock • See figure 6.10	1.0 (at 0.5 and 1.5Hz) 0.8 (at frequencies from 1.5 to 10Hz)	1.1–2.27 (higher amplifications at frequencies >1.5Hz)	1.1–4.17 (higher amplifications at frequencies >1.5Hz)	0.5–1.0 (at 0.5, 5 and 10Hz) 1.3–1.5 (at 1.5 and 2Hz)

Figure 6.10 Amplification factor: ridge 200m high with HW rock overlying bedrock (45º slope)

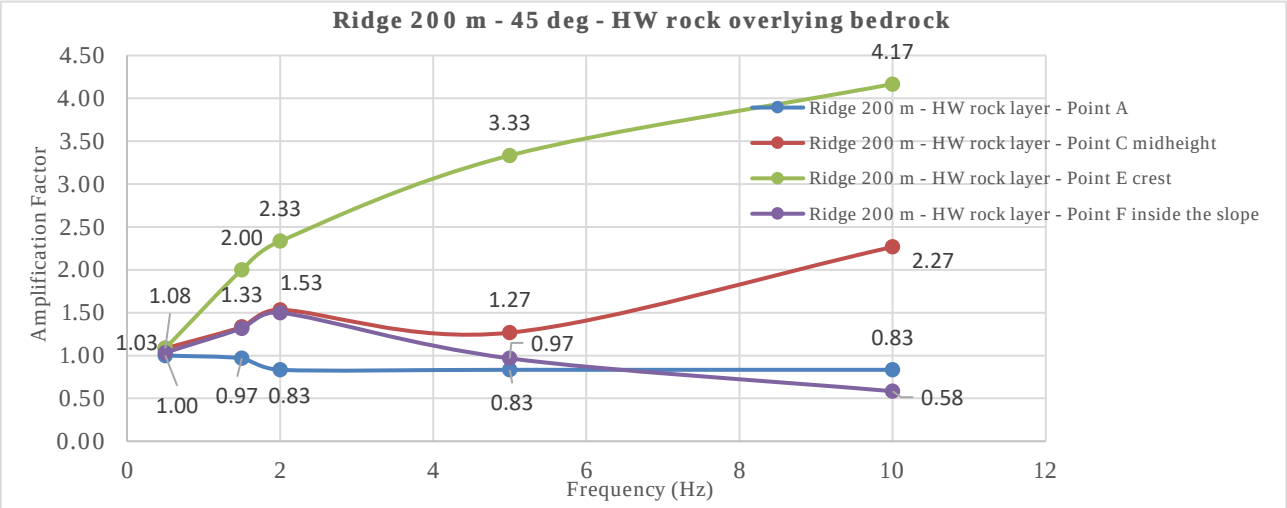

The results in figure 6.10 for ridge topography also indicate a high topographical amplification, where weathered rock is present, compared with the situation where the rock is uniform and unweathered in figure 6.11. The amplification is again pronounced at the higher frequencies of motion, similar to the terrace topography.

6.4.6 Ridge bedrock with lower slope cutting and harmonic inputs

Cut slopes are often formed in a hillslope and do not necessarily extend to the full height of the hillslope. It is therefore important to understand what amplification may be experienced at the crest of cut slopes and along cut slopes which do not extend over the full height of the hillsides.

The ground motions in a 200m high rock ridge with slope angles of 27º–35º, with a cutting in the lower part of the slope (case 5 of table 6.2) was examined. The slope angles for the cutting considered were varied from 45º–50º and the heights from 50–100m.

The results of the numerical analysis in terms of ground acceleration amplification factor at different locations on the slope are summarised in tables 6.10 and and 6.11, and graphically shown in figures 6.11 and 6.12.

The limited analyses considering cuttings that extend partially up the hillside show there is amplification at the crest of the cuttings particularly at high frequencies, but these amplifications are lower than those at the crest of the hillside.

Further analyses of cut slope configurations against the overall height of the hillslopes, and considering the effect of weathered rock or overburden, is necessary to better understand the effects of cut slopes that extend part way up the slope.

Table 6.10 Amplification factor of ground accelerations for hill-ridge topography with 35° slopes and toe cut – case 5

Slope geometry	Amplification factor at different locations on the slope			
	Toe (point A)	Crest of cut (point B)	Mid height (point C)	Crest (point E)
• Ridge 200m high • Ridge slopes 35° • Rock • Cut at the toe at 45° and 50°, 50m high, see figure 6.11.	~1.0 (at 0.5Hz) 0.8–0.9 (at ≥ 1.5Hz)	~1.0 (at 0.5, 1.5 and 2Hz) 0.8 (at 5Hz) 1.3–1.4 (at 10Hz)	1.0–1.3 (at 0.5, 1.5 and 2Hz) 0.9 (at 5Hz) 2.5 (at 10Hz)	1.0–1.3 (at 0.5, 1.5, 2 and 10Hz) 2.8 (at 5Hz)

Figure 6.11 Amplification factors for the ridge 200m high, with 35° slopes and 50° cut 50m high at the toe

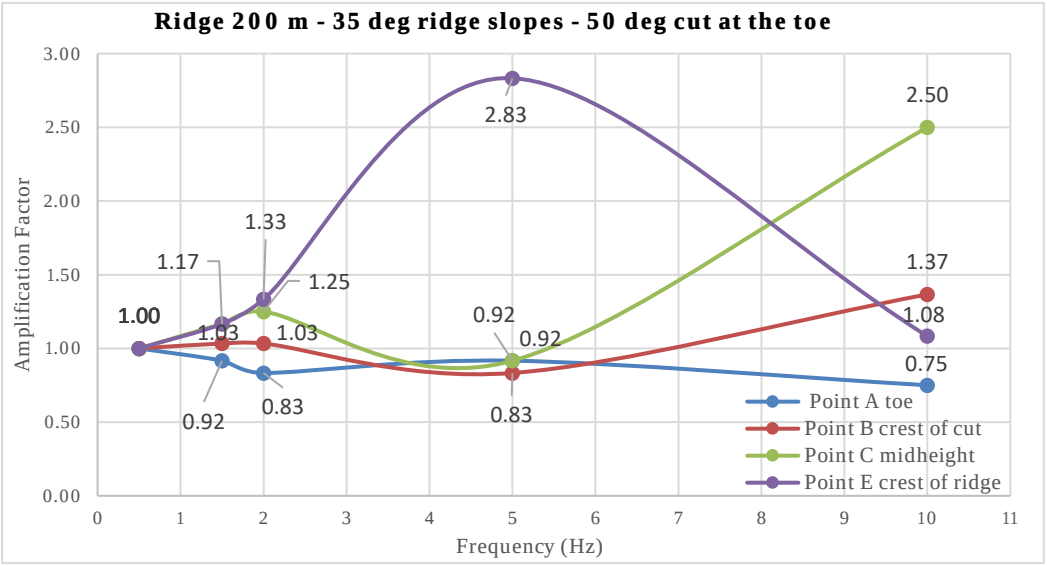

Table 6.11 Amplification factor of ground accelerations for hill-ridge topography with 27° slopes and toe cut – case 5

Slope geometry	Amplification factor at different locations on the slope			
	Toe (point A)	Crest of cut (point B)	Mid height to 3/5 of height (point C)	Crest (point E)
• Ridge 200m high • Ridge slopes 35° • Rock • Cut at the toe at 50°, 100m high, see figure 6.12	~1.0 (at 0.5Hz) 0.8–0.9 (at ≥ 1.5Hz)	1.0–1.1 (at 0.5, 1.5 and 2Hz) 0.9 (at 5Hz) 1.1–1.7 (at 10Hz)	1.1–1.3 (at 0.5, 1.5 and 2Hz) 0.9– .0 (at 5Hz) 0.8–2.2 (at 10Hz)	1.0–1.5 (at 0.5, 1.5, 2 and 10Hz) 2.9 (at 5Hz)

Figure 6.12 Amplification factors for the ridge 200m high, with 27° slopes and 50° cut at the toe, 100m high

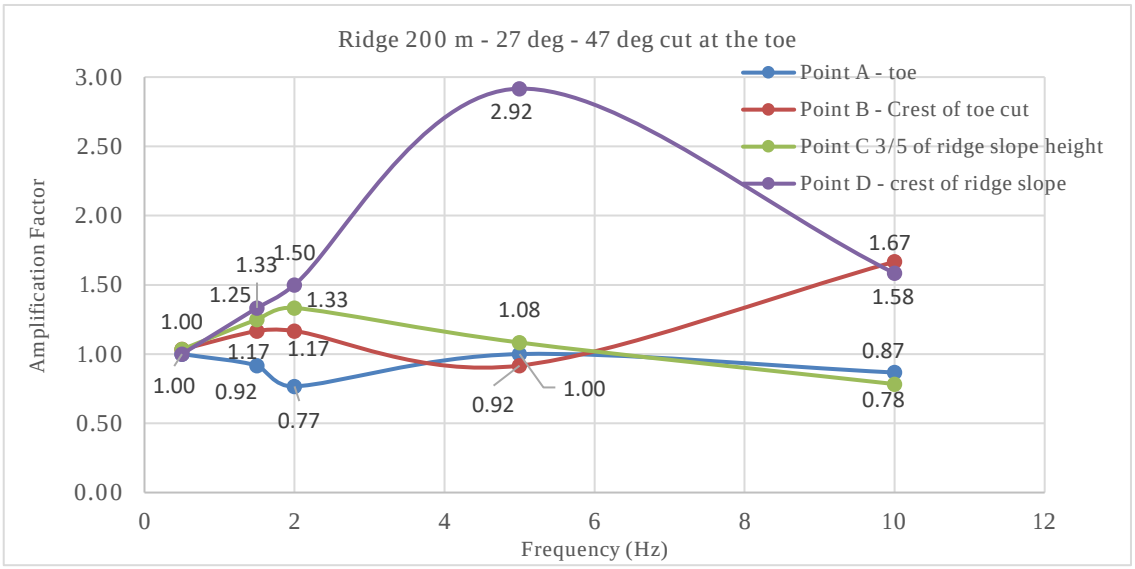

6.4.7 Influence of normalised height and width on amplification factor

The influence of the normalised height of the slope with respect to the harmonics wavelength (H/λ) was examined, as it was identified from the literature review as an important parameter influencing the magnitude of ground motion amplification.

The influence of the normalised height (H/λ) on the amplification factors at the crest of the slope or the top of the ridge are shown in figure 6.13.

Similarly, the influence of the normalised width of the top and the base of the ridge (W/λ and B/λ respectively) on the amplification factor is shown in figure 6.14.

The figures show the strong influence of the normalised heights and widths on the amplification of motions, and generally confirm the indications from literature review based on past research.

Figure 6.13 Influence of the normalised slope height (H/λ) to the amplification factor at the slope crest for terrace and ridge topographies

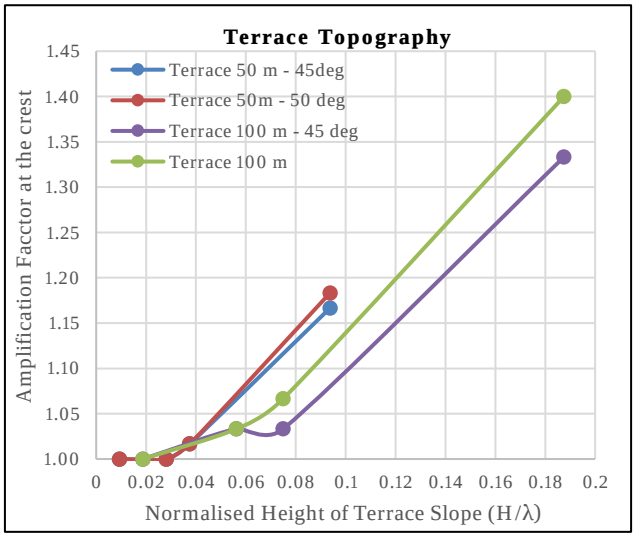

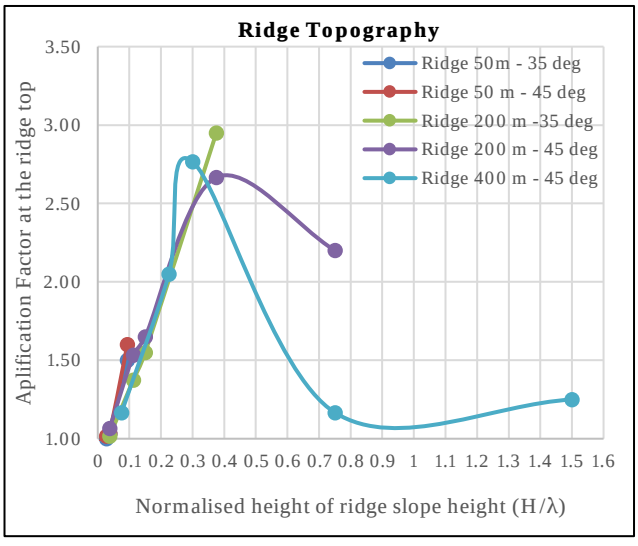

Figure 6.14 Influence of the normalised width of top (W/λ) and normalised width of base (B/λ) to the amplification factor at the slope crest for ridge topographies

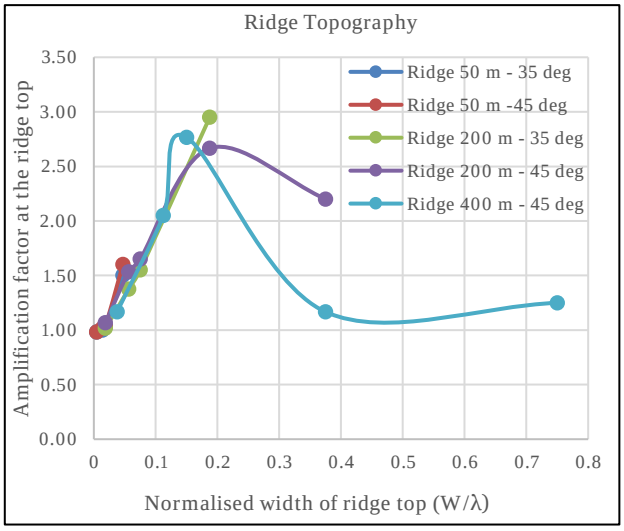

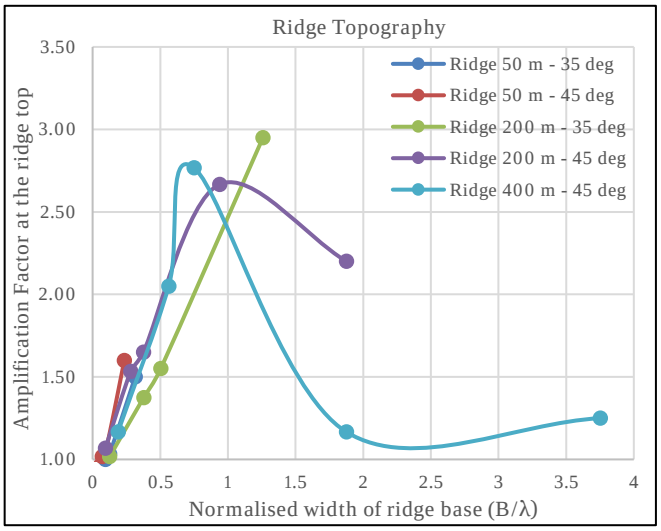

6.4.8 Parasitic vertical accelerations generated in ridge terrain

A significant vertical component of ground acceleration was observed at the top of the ridge topographies, mainly at high frequency harmonics, although the input motions were horizontal only. These vertical accelerations induced by the topography from horizontal input motions are known as parasitic vertical accelerations.

The parasitic vertical accelerations induced were examined at the top of the 200m ridge, for cases 2 and 4 using the horizontal motion harmonics and for case 2 only using time histories from real seismic recordings. It is noted that the vertical component of accelerations was not examined for the terrace topographies.

The vertical ground acceleration values observed in the analysis for the ridge topographies are summarised in table 6.12.

Table 6.12 Vertical ground accelerations at the top of hill-ridge topography

Slope geometry	Vertical ground accelerations						
	0.5 Hz	1.5 Hz	2Hz	5 Hz	10 Hz	LCN260	LCN345
Case 2 of table 6.1 • Ridge 200m high • Ridge slopes 45º • Rock	Negligible	Negligible	Negligible	0.55g	0.78g	0.42g	0.67g
Case 4 of table 6.2 • Ridge 200m high • Ridge slopes 45º • Soil overburden over bedrock	0.50g	4.50g	1.50g	1.50g	2.50g	Not examined	Not examined
Case 4 of table 6.2 • Ridge 200m high • Ridge slopes 45º • HW rock overlying bedrock	Negligible	Negligible	0.48g	0.65g	0.65g	Not examined	Not examined

6.5 Discussion of analysis results

6.5.1 Terrace topography

The conclusions drawn from the analyses of the terrace topography are in general agreement with the conclusions made from the literature review, as follows:

- The slope angles of 45º and 50º examined did not affect amplification factors significantly. A wider range of slope angles need to be examined to better understand the influence of slope angle on the amplification effect.
- The amplification effect was found in our analyses to be mostly influenced by the frequency of the excitation and the slope height, when the slope consists of rock. It was also influenced by the presence of weaker overburden soil material or HW rock overlying unweathered or slightly weathered bedrock.
- De-amplification of the seismic ground motions was observed at the toe of the slope at high frequencies.
- The amplification effect at the upper part of the slope was negligible for the small frequencies (≤ 2Hz) when the slope consists of rock. However, amplification factors of the order of 1.2 and 1.4 are indicated by the numerical analyses for the 50m high and 100m high slopes respectively, for the frequency of 5Hz, when the slope consists of rock.
- Amplification factors comparable to those at the crest, were observed on the ground surface at a distance of 20m behind the crest for the high frequency harmonics, when the slope consists of rock. The literature review indicates that free-field conditions behind the crest are usually observed at a distance of the order of (2 to 8)H, where H is the height of the slope, but this was not tested in this research.
- No amplification was observed inside the slope, at mid-slope height and at a depth of ~20m from the slope surface (point G).
- Amplification factors became significant for normalised slope height $H/\lambda > 0.1$ and maximum for $H/\lambda \approx 0.18$, which is in general agreement with the conclusions of the literature review.
- Significantly higher amplification factors were observed, both at mid-height of the slope and at the crest of the slope, when a weak soil overburden or HW rock layer overlies bedrock, with values up to ~13.0 for the soil and up to ~4.0 for the HW rock. Higher amplifications were observed at frequencies ≥ 1.5Hz.

The vertical component of ground motions was not examined for the terrace topography in this current analysis.

6.5.2 Ridge terrain

The conclusions drawn from the analyses of the ridge topography were:

- The angle of the ridge slopes examined (35º and 45º) did not significantly affect the amplification – de-amplification effects. The amplification effects were mostly influenced by the frequency of the harmonics, the height of the ridge slope and the width of ridge top and base, confirming the indications in the results of the literature review.
- De-amplification at the toe was within the range of 10–20% for high frequencies (>1.5Hz) and was higher for the 400m high ridge. The de-amplification effect could potentially be the result of the

reflection of shear wave off the face of the slope, and the trend with respect to the wave frequency might be influenced by the different modes of vibration. De-amplification was also observed at the mid-height of the slope in certain frequencies (2Hz and 5Hz).

- De-amplification was not consistently observed inside the ridge, at a shallow depth of the order of 20m from the slope surface (point F in case 2 and G in case 5, see tables 6.1 and 6.2). De-amplification was evident inside the ridge, in the middle of it (point G in case 2 and H in case 5, see tables 6.1 and 6.2.
- High amplification effects were observed at the top part of the ridge for all the cases examined, with higher amplification factors occurring for the 200m and 400m high ridges (it is also indicated by the literature that amplification effects increase with the ridge height).
- The amplification of the top of the ridge was about 30% higher than that of the corresponding terrace-like slope, of the same height and inclination, as also indicated by the results of our literature research.
- The amplification factors at the crest did not seem to have a consistent trend (eg increase or decrease) with frequency; higher amplifications were observed for moderate frequencies (1.5Hz and 2Hz) in some cases, especially for the 200m high ridge, while the amplification factors might be lower for higher frequencies. This could be due to the fact that the wavelength in high frequencies might be comparable to the width of the base of the ridge, which affects amplification effects, as also indicated by the results of the literature review.
- Amplification effects in general were found to be negligible for wavelengths significantly larger than the ridge base width (eg for the 0.5Hz harmonics and the 50m and 200m high ridge), as also concluded by the literature research.
- Complex, alternating patterns of amplification and de-amplification on different parts of the ridge slope variating with the wavelength of the seismic excitation, were observed in our analyses, as also indicated by the literature research.
- Considerable vertical component of ground acceleration was observed for some of the cases examined, although the harmonics used in the analysis introduced horizontal motions only to the slope. The presence of a significant vertical component has been indicated by previous researchers, as concluded in the literature review.
- High amplification factors were observed for the ridge topography with weak material, either soil overburden or HW rock overlying bedrock. The amplification factors observed from the analyses were up to 13 for the soil and 4 for the HW rock, with the highest values observed at frequencies ≥1.5Hz.
- Vertical accelerations were recorded for some of the examined cases at the top of the ridge only. The vertical accelerations observed for the bedrock case and the case with HW rock overlying bedrock were of the order of 0.6–0.8g, while for the case with soil overburden were up to 4.5g. The variation of vertical acceleration did not seem to vary consistently with frequency, but appeared to be increasing at the higher frequencies.
- The parasitic vertical accelerations induced appeared at the same ‘dynamic time’ as the ‘horizontal ones’ and in that sense vertical and horizontal ground movements could be considered as synchronous with each other. However the analysis carried out at this stage was very preliminary in terms of the synchronicity of the vertical and horizontal acceleration components, and further cases should be examined to be able to support this conclusion.

- In the case of a ridge with a cut excavated at its toe, of slope angle 45º–50º, the amplification factor was found to be 1.3–1.7 at the crest of the cut, for the higher frequency examined, equal to 10Hz. The amplification factors showed a tendency to increase with increasing height of the slope and increasing difference between the ridge slope angle and the cut slope angle, ie as the irregularity became more pronounced. This may indicate a possible amplification effect when the ridge slope presents local irregularities. This case should be examined with further analysis so that possible amplification effects are quantified with more certainty.
- Higher amplification at the crest was observed for values of the normalised height of the ridge H/λ between 0.1 and 0.4 (where λ is the wavelength). For values of $H/\lambda > 0.4$ a trend of decrease of the amplification factor was observed, as indicated by the results of previously carried out experimental studies.
- Considerable amplification factors at the crest were observed when the normalised width of the top was between the values of 0.05 and 0.2, with the maximum at 0.2. For $W/\lambda>0.2$ a trend of decrease of the amplification factor was observed.
- Similarly, considerable amplification factors (> 1.2) were observed when the normalised width of base (B/λ) was between 0.25 and 1.25. For $B/\lambda>1.25$ a trend of decrease of the amplification factor was observed. The reduction of amplification effects with the increase of normalised width of base is also indicated by the literature research.
- The influence of relationship of the width of the top to that of the base, which is indicated by the literature review, was not thoroughly examined in the analysis carried out in the current stage.

7 Development of guidelines for design of high cut slopes

7.1 Purpose

Draft guidelines for the design of high cut slopes have been developed to aid design for transportation projects in New Zealand. The guidance provides for different design approaches depending on the importance of the transportation corridor, resilience requirements for the route and the scale of the cut slopes and complexity. The guidance includes assessment of suitable topographic amplification factors for typical hilly terrain where highway cut slopes are commonly formed in New Zealand, and factoring of the peak ground acceleration for derivation of equivalent pseudo-static loads for use in design.

It is recognised that this is an area of recent research and development, and there is more research yet required to develop a good understanding of the issues. However, the development of these guidelines will help bring up to date research and current knowledge to the design of major transportation infrastructure involving high cut slopes, currently happening or planned for the near future in New Zealand.

These draft guidelines provide an approach based on the research carried out, and it is envisaged that further discussion and debate may be required to convert these into guidelines published for design use, and for eventual incorporation into design manuals such as the *Bridge manual*, or into design standards.

7.2 Introduction of resilience principles

Resilience is the ability to recover readily and return to its original form from adversity. From an infrastructure and building perspective, this requires us to develop our built environment in a way that reduces damage and the consequent loss or reduction in its functionality, and enhances the ability to recover quickly from such reduction. Brabhaharan et al (2006) adapt this concept for resilience for application to transportation networks as conceptually illustrated in figure 7.1.

Road networks provide a vital lifeline function for society, and their availability is critical for emergency response and recovery after major hazard events. In this context, the concept of resilience of road transportation lifelines is dependent on their vulnerability to a loss of quality or serviceability, and the time taken to bring them back into their original usage state after the reduction or loss of access, as illustrated in figure 7.1. The smaller the shaded area, the more resilient is the lifeline. The greater the area, the poorer is the performance.

Resilience of our built environment can be maximised by early focus on minimising the shaded triangular area in the figure by:

- reducing vulnerability of the transportation network to loss or reduction in functionality in an event
- developing the transportation route so it can be quickly returned to functionality.

Creating a resilient society requires focus on the functionality of our developments after events, by reduction in the loss of use and enable early recovery after events. To achieve a more resilient society, we need to go beyond our focus on life safety from earthquakes, and consider the resilience of the built environment. This requires focus on how a loss of functionality can be minimised, as well as achieving a form that is conducive to quick return to functionality (Brabhaharan 2013).

Figure 7.1 Resilience of route/network

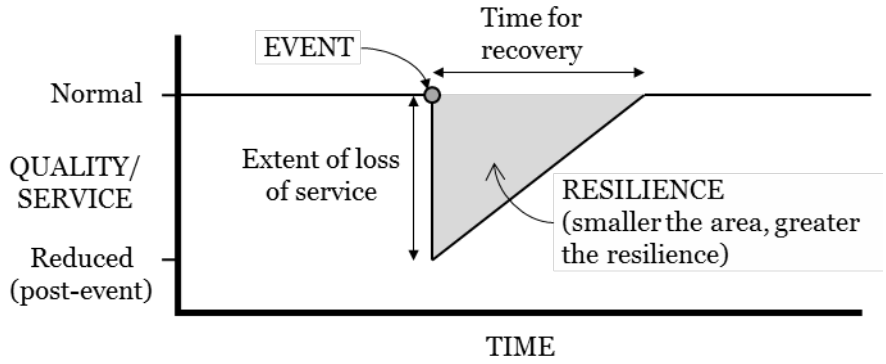

Applying this to transportation routes, the cut slopes should be designed for resilience by:

- adopting a design that has a low vulnerability to failures and closure of the route, by minimising the size of failures
- minimising the size and nature of failures, enabling the functionality of the transportation route to be restored quickly.

It is important to incorporate these resilience principles into the design approach for transportation routes, including cut slopes formed as part of the route.

7.3 Importance of cut slopes

7.3.1 Purpose

Classification of cut slopes is used in these guidelines to:

- select appropriate levels of earthquake shaking (section 7.5)
- adopt an appropriate design approach for cut slopes (section 7.4).

This enables cut slopes to be designed in accordance with the resilience expectations for the transportation facility it affects; and use a level of design which is consistent with the importance of the transportation route as well as the criticality of the cut slope for the performance of the route.

The Australian/New Zealand Standard Structural Design Actions AS/NZS 1170.0 classifies structures in accordance with their importance levels for selection of the design earthquake motions. The *Bridge manual* also classifies highways in terms of importance levels which aims to be consistent with AS/NZS 1170.0.

Classification of the importance of transportation routes in accordance with these New Zealand standards and design manuals ensures that cut slopes (including those which are part of other facilities) are designed and constructed in general accordance with the principles adopted for design in New Zealand. The *Bridge manual* provides more definitive definitions of importance levels for highways, and can be used in conjunction with this guideline. However, there is an anomaly as to how cut slopes are currently considered in the *Bridge manual* (see section 3.4.2), and the guidelines developed here attempts to address this.

7.3.2 Importance level

The importance levels of transportation corridors for use in design are given in table 7.1.

Table 7.1 Selection of importance level

Importance level	Situation
IL 1	Transportation facilities of low importance, eg rural farm roads
IL 2	Transportation routes of normal importance, eg urban roads other than key arterial and collector routes
IL 3	Transportation routes of high importance which are lifelines, or carry significant traffic volumes of more than 2,500vpd
IL 4	Transportation routes providing access to post-disaster facilities and that are expected to provide a service in a post-disaster scenario.

Notes:

1 Importance levels (IL) referred to are those defined in AS/NZS 1170.0.

2 Supplemented by the *Bridge manual* for highways and arterial roads.

The aim of this selection has been to use the existing importance level framework in the New Zealand standards and the *Bridge manual*.

7.3.3 Resilience importance category

Once the importance level is selected based on existing criteria, it is recognised that the resilience expectations even for the same importance level of transportation route vary significantly depending on the regional context of the routes. For example IL3 routes in Christchurch or Auckland would have a lot more redundancy because of the many routes given the terrain, whereas in places like Wellington, Dunedin or Central Otago there is very little redundancy.

Resilience importance categories have been developed to provide for incorporating the local context and resilience expectations into the design process.

The resilience importance category (RIC) of cut slopes along transportation corridors for use in design are given in table 7.2. Resilience importance categories take into consideration the importance level of the transportation route as well as the resilience expectations of the section of route from a regional network context. This recognises that sections of the transportation network may have a higher resilience importance because of the nature of the regional network, its resilience and the availability or lack of alternative routes in the event of incidents.

It is envisaged that the transportation authority would consider the regional context and specify the resilience importance category to be used in the design of cut slopes for a particular transportation corridor.

Table 7.2 Selection of resilience importance category

Resilience expectations	Resilience importance category			
	Importance level			
	IL1	IL2	IL3	IL4
Low Resilience expectations low from the regional context, such as due to availability of many secure alternative routes of adequate capacity.	I	II	III	–[(a)]
Medium Resilience expectations moderate from a regional context, due to some alternative routes but may not have adequate capacity or security in events.	II	III	IV	V
High Resilience expectations high from a regional perspective because of limited or no alternative routes and/or their capacity or security in events is poor.	–[(a)]	IV	V	V

[(a)] IL4 routes are not likely to have a low resilience expectation and IL1 routes are not expected to have a high resilience expectation.

Note:

Importance levels are defined in table 7.1.

Resilience expectations will depend on importance of route and availability of secure alternatives.

The resilience importance category is a function of the transportation route rather than the cut slope or fill embankment.

7.4 Design approach

7.4.1 Outline of design approach

A four-level design approach is presented, to suit the design importance level of cut slopes.

- **Design approach 1** is a simplified design approach suitable for use by practitioners for simple relatively low height cut slopes of relatively low importance.
- **Design approach 2** is a standard design approach for use where performance is important for continued functionality on relatively moderate height cut slopes in simple geotechnical conditions.
- **Design approach 3** is for use where performance is important for continued functionality on relatively higher cut slopes in moderately complex geotechnical conditions.
- **Design approach 4** is for use where performance is critically important for continued functionality, with very high cut slopes, or in complex geotechnical conditions.

A fundamental difference of the design approach given compared with that stipulated in AS/NZS 1170 is that the design is for resilience rather than life safety alone. Cut slopes most commonly affect the functionality of transportation routes, although they can also be critical to life safety in some circumstances.

7.4.2 Selection of design approach

The design approach suitable for a particular cut slope design is presented in table 7.3. A higher level design approach may be adopted for design, but a lower level than indicated is not considered appropriate.

Here the height of the slope is used as a proxy for potential consequences to the transportation corridor due to failure and blockage or safety hazards from rock fall or failures, and the level of difficulty in restoring access in the event of failures.

Table 7.3 Selection of design approach

Resilience importance category (RIC)	Cut slope height			
	< 10m	10–30m	30–50m	> 50m
I	DA1	DA2	DA3	DA3
II	DA1	DA2	DA3	DA3
III	DA2	DA2	DA3	DA4
IV	DA2	DA3	DA4	DA4
V	DA2	DA3	DA4	DA4

Notes:

Resilience importance categories (RIC) referred to are those defined in table 7.2.

The situation or cut height could trigger a design approach.

The design approaches are a minimum expectation, and a higher level design approach may be chosen if the risks are higher, for example due to presence of any structures within the zone of influence either above or below the cuttings.

7.4.3 Description of design approach

The various levels of design approach developed depending on the importance of the route and the scale and complexity of the cut slopes is described in table 7.4.

Table 7.4 Design approaches

Design approach	Situation
DA1	This approach is suited for low height, generally stable cuttings along low importance routes, and where failure will not affect any structures either on the route or on adjacent development. The consequences of failure leading to closure would generally be acceptable and the route can readily be opened through clearance of debris. The design would be carried out by considering the precedent behaviour of cut slopes in the area in similar ground conditions, consideration of critical kinematically feasible mechanisms in rock from logging of the cut face, supplemented by slope stability analyses as required. No specific earthquake design would be required.
DA2	This is a standard approach suited to moderate height cut slopes in simple geology. Performance for continued functionality would be beneficial. The design would be carried out using a combination of precedent behaviour of slopes, including in earthquakes and storm events; detailed logging of rock mass characteristics and defects with associated consideration of kinematically feasible mechanisms; supplemented by stability analyses including consideration of simple earthquake motions from standards or the *Bridge manual* in the design.
DA3	This is a detailed design approach suited to moderate to high cut slopes, or routes where performance is important in hazard events such as earthquakes and storms, or for complex ground conditions. The detailed investigation would include the logging of the ground/rock mass conditions and

Design approach	Situation
	drilling of cored boreholes. Rock defects characterised by field mapping and acoustic/optical televiewer (ATV)/(OTV). Earthquake motions will include assessment of topographical amplification effects. The design will include assessment of kinematically feasible mechanisms controlled by defects, rock mass stability and combined defect and rock mass controlled stability. Soil or rock slope stability will consider complex failure mechanisms and stability analyses. Design would include assessment of displacements and performance of the cuttings.
DA4	This is a detailed design approach suited to high cut slopes, or routes where performance is important in hazard events such as earthquakes and storms, or for complex ground conditions. Adjacent structures may be present. The detailed investigations would include logging of the ground/rock mass conditions and drilling of cored boreholes. Rock defects characterised by field mapping and downhole techniques such as ATV and OTV. Earthquake motions will include assessment of topographical amplification effects. The design will include assessment of kinematically feasible mechanisms controlled by defects, rock mass stability and combined defect and rock mass controlled stability. Soil or rock slope stability will consider complex failure mechanisms and stability analyses. Assessment of topographical amplification effects and stability may be aided by numerical modelling. Design would include assessment of displacements and performance of the cuttings, and the resilience consequences to the transportation route.

Note: The design approaches are a minimum expectation, and a higher level design approach or design actions may be chosen if the risks are higher, for example due to presence of any structures within the zone of influence either above or below the cuttings.

7.5 Selection of ground motions for design

7.5.1 Peak ground accelerations for design

The peak ground accelerations for design are selected based on the *Bridge manual*, to obtain peak ground accelerations that are not weighted by their relevant magnitudes. Spectral accelerations may be considered if there is a dominant period for the site.

The *Bridge manual* provides maps providing hazard factors to derive peak ground accelerations across New Zealand. These represent free-field accelerations before any topographic effects are taken into consideration.

As discussed in section 3.4.2, there is an anomaly in the current *Bridge manual* in that it provides for different hazard levels for different types of structures – bridge, retaining wall, embankments and cut slopes – on transportation routes with a selected importance level. For example for an important transportation route, to design a bridge or wall for a 2,500 year return period earthquake, but only considering the cut slopes (regardless of height) for earthquakes with 1/5th the return period of 500 years, is considered to be inappropriate. It would be prudent for a transportation route importance level to drive the level of hazard it is designed for regardless of the type of structure.

Having set a hazard level, different structures may be designed for a consistent level of resilience, and this may mean accepting a level of performance consistent with that resilience expectation, and perhaps the cost of remediation.

For example, if the resilience expectation is to be able to reopen the route within say three days for a selected ultimat limit state event, then all components forming the route will be designed to perform adequately in the same event, which means that:

- the bridges on the route would be designed to minimise settlement of abutments to a level that can be readily repaired and ensure only minimal repairable damage occurs to critical structural members, which would not compromise access
- the retaining walls would be designed to minimise displacement and consequent damage to the transportation facility and related structures, which could be readily repaired within the required timeframe of three days
- the embankments would be designed to minimise displacements and enable them to be repaired within a short time
- the cut slopes would be designed to minimise the size of failures so they can be cleared within a few days, with the remaining cut slope being stable and measures in place to manage the rock fall hazards.

In line with the above discussion on the importance of designing all components of the route for the same event, the return periods for limit state design of cut slopes in table 7.5 should be consistent with the hazard levels specified in the *Bridge manual* for bridges. Obviously this would need to be discussed at a wider level.

Table 7.5 Return period for limit state design of cut slopes

Resilience importance category (RIC)	Return period (years)		
	Operational continuity	Ultimate limit state (ULS)	Maximum considered earthquake (MCE)
I	100	250	–
II	150	500	–
III	250	1,000	1.5 x ULS
IV	500	2,500	1.5 x ULS
V	500 min with site specific consideration	2,500	1.5 x ULS

Notes:

Resilience importance categories (RIC) referred to are those defined in table 7.2.

Ultimate limit state (ULS) and maximum considered earthquake are as defined in the *Bridge manual*.

Operational continuity as defined in the *Bridge manual*.

The earthquake peak ground accelerations for the relevant hazard levels can be derived from the *Bridge manual*.

The proposed hazard levels are higher than currently provided for in the *Bridge manual*, for cut slopes. As discussed these are too low and will lead to transportation routes that have poor resilience. Therefore, higher hazard levels, but still consistent with the hazard levels for bridges, are proposed to achieve a consistent level of hazard for which the route is designed, regardless of the road form.

Operational continuity is very important from a resilience perspective, and therefore a higher hazard level is proposed in table 7.5, depending on the resilience importance category. This should be considered together with the 'design for resilience' approach noted in section 7.6. These levels would need to be discussed at a wider level. It is noted that seismic performance requirements in chapter 5 of the *Bridge*

manual and the operational continuity requirements in chapter 6, are different, and it would be useful to ensure these are aligned.

While the design hazard level is proposed to be consistent for all elements of the transportation route, the consequences to ensure resilience can be different, for example small cut slope failures can still be accommodated without seriously compromising the resilience of the route, and this approach will help manage the cost of construction to an acceptable level.

7.5.2 Topographical amplification

The numerical analyses and evidence from observations of earthquakes clearly indicate topographical amplification is a key issue that needs to be addressed in design. Understanding and quantifying topographical amplification is an area of recent research and development, and there is more research yet required to develop a good understanding of the issues. However, topographical amplification factors to use in design are given based on up-to-date research and current knowledge, so they can be applied to the design of transportation infrastructure involving high cut slopes, currently happening or planned for the near future in New Zealand.

Cut slopes in steep topography or formed at steep slopes are likely to lead to topographic amplification of the ground shaking. The amplification factor based on the numerical analyses and the literature is higher on ridges than on terrace slopes.

The proposed topographical amplification factor, based on information to date, can be derived from tables 7.6 and 7.7.

Table 7.6 Topographical amplification factors for ridges

Slope angle	Cut-slope height			
	<30m	30–60m	60–100m	>100m
0º–15º	1	1	1	1
15º–30º	1.2	1.4	1.6	2
>30º	1.4	2	2.5	3

Notes:

Topographical amplification factor for ridge slopes

Where the cut slope extends only over part of the ridge slope height, then an appropriate topographical amplification factor for the ridge crest should still be considered, assuming a reduced height ridge.

Table 7.7 Topographical amplification factors for terrace slopes

Slope angle	Cut-slope height			
	<30m	30–60m	60–100m	>100m
0º–15º	1	1	1	1
15º–30º	1	1.1	1.2	1.6
>30º	1.1	1.2	1.4	2

Notes:

Topographical amplification factor for terrace slopes

Where the cut slope extends only over part of the terrace slope height, then an appropriate topographical amplification factor for the cut crest should still be considered, assuming a reduced height slope.

The topographical amplification factor values proposed here only take into account the effect of topography type, slope and height and inclination. It is clear through the literature research there is vast experimental and theoretical evidence that:

- topographical amplification factors are also affected by the predominant wave length of seismic excitation
- a parasitic vertical seismic motion may develop from purely horizontal excitations.

However, from a practical perspective it will be difficult take into consideration the frequencies or wave lengths, as the dominant earthquake frequencies are likely to change depending on the different earthquakes that may affect a particular site, and in a particular earthquake there are likely to be different frequencies.

A similar table could be provided for vertical accelerations, unless there is strong evidence through further research that the vertical and horizontal components are not synchronous. At the present time, there is inadequate research information to allow specification of vertical ground motions for design. However, this could be considered for very important cuttings through numerical time history analyses using both horizontal and vertical accelerations.

7.5.3 Presence of soil overburden

The presence of overburden on parent ground such as bedrock could lead to ground accelerations that are much higher than peak ground accelerations from either:

- the presence of overburden on flat ground, or
- steep rock slopes without any soil overburden.

The combined effects of soil overburden and topography appear to lead to the much higher accelerations observed in practice, and these are also indicated by the limited numerical analyses reported in the literature as well as that carried out as part of this research. Such situations need to be considered with care and the sensitivity of performance checked with higher ground accelerations.

7.5.4 Design ground accelerations for slope design

The numerical analyses and evidence from observations in earthquakes clearly indicate that topographical amplification is present and highest at the crest of slopes. The amplification further down the slope at mid-height or below is much lower, and even de-amplification may be encountered. The evidence of slope failures from earthquakes also suggest that slope failures are predominant at the top of slopes, both ridges and terraces.

It is also clear that the ground accelerations, whether amplified by topography or not, are likely to be different along the height of slopes and the peak acceleration is not expected to be encountered at the same point in time during an earthquake along the height of the slope. Therefore, a lower average acceleration is appropriate for pseudo-static design when large failure mechanisms are considered. To reflect this, design ground accelerations for pseudo-static design are proposed based on consideration of different size mechanisms affecting the slope. These are presented in table 7.8.

Table 7.8 Application of ground accelerations for pseudo-static earthquake design

Situation of failure mechanism	Design acceleration for pseudo-static design
Upper quartile of cut slope	PGA x TAF
Upper half of cut slope	PGA
Full slope	PGA x 0.65

Notes:

PGA = peak ground accelerations, derived from the *Bridge manual*

The topographical amplification factor is derived from consideration of the height of cut slopes and slope angles as suggested in tables 7.6 and 7.7, depending on the situation (ridge or terrace).

Makdisi and Seed (1978) provide average accelerations for embankment dams considering potential depths of the sliding mass. Unlike embankments, steep slopes often involve shallow failures, and this approach has therefore not been adopted for considering cut slopes.

7.5.5 Time history records for design

If numerical analyses using time histories are used in the design, then appropriate time histories that reflect the following should be considered:

- seismo-tectonic regime
- near-fault time history records, where the design ground motions at the site is expected to be experienced during nearby earthquake faults or sources
- frequency content of records representative of expected events that could affect the site
- time histories should be scaled as provided for in NZS 1170.5.

It is also important to monitor the free-field accelerations during numerical analyses to ensure that these are reflective of what is proposed for the site.

7.6 Earthquake design of cut slopes

7.6.1 Design for resilience

In the earthquake design of cut slopes, it would be important to set appropriate performance criteria to achieve:

- a level of performance that is consistent with the resilience objectives set for the transportation route /project
- an economical solution.

Unlike made structures such as bridges, and made earth structures such as embankments, cut slopes are mostly formed in natural materials with their inherent variability and in situ ground characteristics. Therefore, smaller failures, such as small wedge failures in rock, are difficult to prevent, unless a significant expenditure is incurred to protect/stabilise the slope against such small failures.

A resilience-based design would be suitable, such as consideration of the effect of any failures on the level of service or performance of the transportation route, but the time it would take to restore the level of service or access also needs to be considered. It would be more economical to accept such small failures in large events, but design the cut slope to avoid or minimise the risk of large scale failures that would affect the performance of the route for a significant period of time, see figure 7.1.

For example, small failures that affect only the shoulder and can be quickly reinstated, may be accepted as they would have only a small effect on resilience. However, large failures that could close the road, and for long period of time, should be designed against. This is illustrated in figure 7.1. Such an approach would enable the achievement of a resilient transportation route, in a cost-effective manner.

Figure 7.1 Design for resilience of route/network

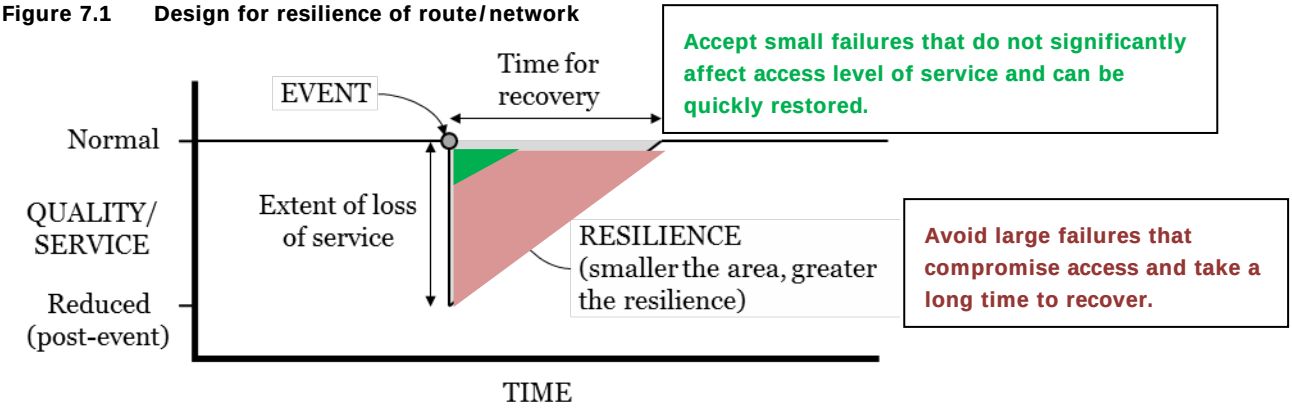

7.6.2 Design for safety

Safety of the users of transportation routes and other people is an important consideration in addition to resilience of access.

The cut slopes should be designed to ensure safety, ie small failures that do not impact on safety may be accepted, and larger failures or mechanisms that impact on safety, should be carefully considered and designed for.

One of the mechanisms, rock fall, can affect safety and should be considered in the design under normal conditions, in storm events as well as earthquake events. This may require rock fall protection measures to be implemented, particularly to allow use of the route to be restored.

7.6.3 Deformation or displacement-based design

Earth structures can be designed for allowing a limited amount of displacement in earthquakes, because the limited displacement occurs when the resistance against instability is exceeded during an earthquake of a short duration. This approach is suited to ductile earth structures such as embankments and reinforced soil walls, and to a lesser extent to natural soils, where there is confidence that the displacement will not be associated with a reduction or loss of the resistance to instability.

Made embankments and retaining walls can be designed using materials that are able to accommodate displacement without significant reduction in their strength. The displacement behaviour of natural soils needs to be understood to ensure they can accommodate limited displacements without an associated loss of strength. Large strain strength properties should be used in the assessment of displacements of slopes in earthquakes.

Usually a Newmark block sliding approach is used to assess displacements. In using empirical or semi-empirical data, it is important to consider using methods to accommodate the local seismicity conditions (eg near fault effects) and making appropriate allowance for these effects.

Rocks are generally brittle and displacement leads to breakage through intact rock through en echelon type failures; this leads to a permanent loss in the strength of the rock mass. Therefore in considering

rock slopes, design based on acceptance of displacements should be avoided, or acceptable displacements limited to very small values.

Cracks associated with displacements in rock and soil materials can also allow infiltration of surface water, leading to a reduction in stability and failure of slopes in storm or rainfall events after the earthquake. Such failures have been observed in a number of earthquakes. Therefore, this needs to be considered in limiting any displacements and associated cracking of ground particularly above cut slopes.

7.7 Comparison with current design standards

The proposed design approach in this guidance is compared against existing standards or guidelines, to illustrate the changes in approach. This is summarised in table 7.9, which illustrates how the proposed guidance, albeit preliminary, uses a novel resilience-based approach to cut slope design, and addresses significant gaps in current design guidance for cut slopes.

Table 7.9 Comparison of proposed guidance with existing design standards

Design feature	**This guidance**	**Existing standards or guidelines**			
		NZS 1170	**NZGS modules**	***Bridge manual* 3rd edition**	**Eurocode**
Importance level	Uses NZS 1170 and *Bridge manual* approach	Provides importance level.	Not addressed.	Provides importance levels based on NZS 1170.	-
Resilience	Resilience-based design approach, importance earthquake motions and performance level.	Not considered beyond importance level.	Not addressed.	Not considered beyond importance level.	Not considered.
Earthquake motions	Consistent across all transportation structures.	Only addresses buildings.	Refers to NZS 1170	Variable earthquake design level for different components of road.	Provided.
Topographic effects	Topography amplification factor. Reduction of TAF along slope based literature or analysis.	Not provided for.	Not provided for.	Not provided for.	Provided for buildings above slope.
Earthquake motions for pseudo-static slope design	Scaling of ground acceleration for deep seated failures, based on international practice.	Slopes not provided for.	No specific guidance for slopes.	No specific guidance.	Provides for arbitrary factor.

8 Conclusions

8.1 Past earthquakes

Past earthquakes in New Zealand and worldwide give us a good indication of earthquake induced landsliding and key observations can be summarised as:

1 Small or large failures in steep unsupported cuts can be triggered by earthquakes leading to MM6 or greater shaking.

2 Significant or widespread landsliding occurs when earthquake shaking exceeds MM7–8 (peak ground accelerations of 0.1–0.5g).

3 Landslides tend to be concentrated on the hanging wall side of the fault in reverse/thrust fault earthquakes. Thrust faults appear to give rise greater shaking for a larger distance from the fault, and hence more landslides.

4 Earthquake induced landslides are predominantly small (~$10^3 m^3$) to large (~$10^5 m^3$) disrupted falls, slides, and avalanches of rock, debris and soil. Common failure mechanisms involve translational sliding at the interface between bedrock and the overlying soil/regolith, or sliding and release along defects in bedrock.

5 Steeper slopes are more prone to landsliding, but the slope angles appear to depend on the local geology, terrain and climatic conditions.

6 Earthquake induced slope failures appear to predominate in the upper parts of slopes and this may be related to the topographic effects as well as weaker ground conditions.

7 Antecedent rainfall and climate appears to have a strong influence on the extent of landsliding in earthquakes.

8 Post-earthquake conditions such as aftershocks and rainfall have been observed to cause further landsliding of slopes weakened, loosened or failures initiated by the earthquake.

9 Slope stabilisation measures such as rock bolts, anchors and shotcrete appear to have been effective against earthquake induced landsliding, but design records appear not to have been available or researched to confirm and understand their effectiveness.

8.2 New Zealand topography and seismicity

The topography in hilly areas with transport corridors has been characterised to include:

- hilly or mountainous terrain with ridge and hill topography
- undulating or rolling hills with more subdued hills
- terraces associated with river/marine terraces or uplifted mountainous areas.

The geology includes indurated rocks, soft Tertiary rocks and quaternary deposits including alluvial and marine deposits as well as volcanic deposits.

New Zealand's seismo-tectonic regions include:

- strike-slip faults
- reverse/thrust faults

- extensional faults including the Taupo volcanic zone
- subduction zone.

These give a wide variety of potential earthquake shaking effects, including the potential for hanging wall effects, where more extensive landslides have been observed on the hanging wall side of the fault rupture.

8.3 Research into topographic effects

There has been research into topographic effects over the last 15–25 years, and this has indicated the complexity of the subject with a wide variety of topographies, geology and seismicity having important effects. Limited additional numerical modelling has been carried out to understand the topographical amplification of motions in terrace and ridge terrains common to New Zealand.

- Topography has a clear effect on ground shaking in steep terrain.
- Topographic effects are frequency dependent: maximum amplification is observed when the incident wavelength is approximately equal to the width of the topographic feature for ridges. For terraces, peak amplification of motion at the slope crest occurs at normalised frequency $H/\lambda \sim 0.2$.
- The ground accelerations appear to be amplified at the crest of the slope, and possibly attenuated at the mid-height of the slope and possibly at the toe and also deeper into the hill.
- Amplification also depends on the incident angle of the seismic waves, with maximum amplification when the waves are perpendicular to the slope.
- Multiple ridges are likely to also vary the topographical amplification, compared with a single ridge.
- Points of significant variation of slope angle and defects within the slope (such as faults) can also compartmentalise blocks of the slope and cause topographic effects.
- Numerical modelling indicates topographic amplification factors which are in the order of 1 to 1.5 or perhaps up to 3, whereas experimental observations indicate much greater topographical amplifications, say up to 10. This discrepancy is not well understood, but is considered at least partly due to the soil amplification effects.
- Various researchers have looked to separate the soil and topographic amplification effects, as well as the distance from the crest they apply to.
- The research outcomes highlight the complexity of the topographic amplification of earthquake motions, which are dependent on a large number of issues and parameters.

8.4 Existing design guidance

There is limited and variable design guidance for the earthquake design of slopes around the world.

EC8 factors down peak ground accelerations. It also provides topographic amplification factor for use in assessing earthquake motions for structures. But does not specifically address how it is to be used in the design of slopes in conjunction with the reduction factors.

The Californian guideline provides an approach to assess a factor for reducing peak ground accelerations based on acceptable levels of displacements. It does not address topographic effects.

In New Zealand, the codes are silent on the design of slopes. The *Bridge manual* provides an approach for using a displacement based design of slopes. But does not provide guidance on topographical

amplification, or the reduction of peak ground accelerations to allow for incoherency of motions when assessing large slopes. Also the design motions adopted for slopes appears to be at odds with that assumed for other structures. The Ashford and Sitar (2002) paper attempts to provide an approach for the design for slopes in a terrace situation.

8.5 Development of design guidelines

Specific resilience-based design guidance has been developed for the design of high cut slopes in New Zealand. This provides for assessment of a resilience importance category based on the importance level of the route and the resilience expectations for the route.

Four design approaches have been developed for use depending on the importance and complexity of the cut slopes, and a method of selection of a suitable design approach is proposed.

The design guidance also proposes selection of earthquake motions based on a consistent approach that is common to the transportation route regardless of the type of road form and structures. Modification of the motions to allow for topographic effects is proposed as an interim measure based on the research evidence to date. Derivation of pseudo static design accelerations for different scale and location of failure mechanisms on the slope are also proposed.

Guidance is also provided on the mechanisms to be considered in the design of steep high cut slopes in rock, soil and failures along the interface between soil and rock. Also guidance is provided on displacement based design and its limitations and caution in using this for rock slopes in particular.

A resilience-based design approach is proposed to achieve an economical design, consistent with the resilience expectations for the transportation route. This would allow acceptance of small failures in earthquakes that do not affect the carriageway and can be quickly cleared and reinstated economically to restore access, while avoiding large failures that impair access and which would take a long time (and cost) to reinstate and recover from.

9 Recommendations

In concluding this research, the following recommendations are made, for consideration by the NZ Transport Agency and other transportation authorities.

9.1 Earthquake design and implementation of design guidance

It is recommended that:

1 The design guidance provided in chapter 7 of this research report be used in the design of high cut slopes along roads and other transportation routes.

2 The design guidance be applied to real design of cut slopes for transportation projects. Such application will identify issues that will help develop and refine the guidance, and also provide case studies to illustrate the application to design practice.

3 The developed design guidance be discussed by the transport sector, and developed and issued for use in design, so that state of the art current practices are applied to develop transportation routes that are resilient to earthquakes.

4 In due course, the design guidance and resilience principles proposed in this research be incorporated into the *Bridge manual*.

5 The design guidance could, alternatively, be published as separate *Design guidelines for the earthquake design of cut slopes*.

6 The design guidance be adopted by the transport sector for their transportation routes.

7 The recommendations for design from this report and guidelines be considered for embedding in earthquake design modules for use more widely in the earthquake design of cut slopes.

9.2 Further research and development

It is also recommended that further research be carried out into specific issues so that this learning can be applied to develop the research guidance and also can be infused into design practice, including:

1 The mechanisms and location of earthquake induced failures be studied through a learning and research reconnaissance study trip to an area affected by extensive earthquake induced landslides, such as the 2015 Gorkha Earthquake in Nepal, to substantiate the observations by one of the authors in China after the 2008 Wenchuan Earthquake and other anecdotal evidence.

2 Extend the limited numerical modelling carried out as part of this research, through further parametric modelling to understand effects such as

   a the distance to the free-field in front of toe and behind the crest of ridge and terrace topographies

   b a wider range of H/λ ratios (H=slope height, λ=predominant wave length) for terraces and W/λ ratios (W=top or base width) for ridges, as well as slope inclinations. In addition, numerical analyses should be performed for a range of shear wave velocities corresponding to common rock types in New Zealand (eg 750–1,500m/s for ‘soft rock’ masses, 1,500–2,500m/s for ‘medium rock’ masses and >2,500m/s for ‘hard rock’ masses

c the horizontal and vertical seismic coefficients for typical failure surfaces (eg lower half of slope, upper half of slope, entire slope), obtained from the average acceleration time history for all nodal points along or within the examined failure

d the effect of cut slopes affecting part of natural hill slopes as topographic irregularities

e effects of combined topography and weathered rock and soil overburden over a range of geometries and material properties

f effect of internal heterogeneities such as fault/shear zones; effects of vertical accelerations and parasitic vertical accelerations developed in the ridge.

3 Further forensic research be carried out into slope failure mechanisms and the effectiveness of slope stabilisation measures. Installation of seismometers be carried out on cut slopes and hillslopes with incorporation into the GeoNet national network and ongoing monitoring, to record future earthquakes and determine the variability of ground motions over the height of hillslopes and the effects of cut slopes on ground motions. This could be considered for forthcoming transportation projects so there is benefit to projects as well as research for the development of guidance.

10 References

Abrahamson, NA and PG Somerville (1996) Effects of the hanging wall and footwall on ground motions recorded during the Northridge earthquake. *Bulletin of the Seismological Society of America 86*, no.1B: S93–S99.

Alaluf, R, R Hernandez, C Donmez, and A Irfanoglu (2012) Learnings from earthquakes – the Mw 7.1 Ercis-Van, Turkey earthquake of October 23, 2011. *Earthquake Engineering Research Institute, EERI special earthquake report*. 17pp.

Ashford, SA, N Sitar, J Lysmer and N Deng (1997) Topographic effects on the seismic response of steep slopes. *Bulletin of the Seismological Society of America 87*: 701–709.

Ashford, SA and N Sitar (2002) Simplified method for evaluating seismic stability of steep slopes. *Journal of Geotechnical and Geoenvironmental Engineering 128*: 119–128.

Assimaki, D and S Jeong (2013) Ground-motion observations at Hotel Montana during the M7.0 2010 Haiti earthquake: topography or soil amplification? *Bulletin of the Seismological Society of America 103*: 2577–2590.

Assimaki, D, G Gazetas and E Kausel (2005) Effects of local soil conditions on the topographic aggravation of seismic motion: parametric investigation and recorded field evidence from the 1999 Athens Earthquake. *Bulletin of the Seismological Society of America 95*, no.3.

Assimaki, D, E Kausel and G Gazetas (2005). Soil-dependent topographic effects: a case study from the 1999 Athens earthquake. *Earthquake Spectra 21*: 929–966.

Bard, P-Y (1982) Diffracted waves and displacement field over two-dimensional elevated topographies. *Geophysical Journal of the Royal Astronomical Society 71*: 731–760.

Barlow, J, I Barisin, D Petley, A Densmore and T Wright (2015) Seismically induced mass movements and volumetric fluxes resulting from the 2010 M_w = 7.2 earthquake in the Sierra Cucapah, Mexico. *Geomorphology 230*: 138–145.

Berryman, K (1992). Reconnaissance field investigation of the Landers earthquake (Ms 7.5) of June 28, 1992, San Bernadino County, California, USA. *Bulletin of the New Zealand National Society for Earthquake Engineering 25*: 230–241.

Blake, TF, RA Hollingsworth and JP Stewart (Eds) (2002) Recommended procedures for implementation of DMG special publication 117 guidelines for analysing and mitigating land slide hazards in California. . Southern California Earthquake Center. 110pp plus appendices.

Boore, DM (1972) A note on the effect of simple topography on seismic SH waves. *Bulletin of the Seismological Society of America 62*: 275–284.

Bothara, J, D Beetham, D Brunsdon, M Stannard, R Brown, C Hyland, W Lewis, S Miller, R Sanders and Y Sulstio (2010) General observations of effects of the 30th September 2009 Padang earthquake, Indonesia. *Bulletin of the New Zealand Society for Earthquake Engineering 43*: 143–173.

Bouckovalas, GD, G Gazetas and AG Papadimitriou (1999) Geotechnical aspects of the 1995 Aegion (Greece) earthquake. *2nd International Conference on Geotechnical Earthquake Engineering*, Lisbon, 10pp.

Bouckovalas, GD and G Kouretzis (2001) Review of soil and topography effects in the September 7, 1999 Athens (Greece) earthquake. *Fourth International Conference on Recent Advances in Geotechnical*

Earthquake Engineering and Soil Dynamics and Symposium in Honour of Professor W.D. Liam Finn, San Diego, California, 26–31March 2001. 10pp.

Bouckovalas, GD and AG Papadimitriou (2004) Numerical evaluation of slope topography effects on seismic ground motion. *11th International Conference on Soil Dynamics and Earthquake Engineering & 3rd International Conference on Earthquake Geotechnical Engineering*, Berkeley, USA, vol 2: 329–335.

Bouckovalas, GD and AG Papadimitriou (2005) Numerical evaluation of slope topography effects on seismic ground motion. *Soil Dynamics and Earthquake Engineering 25*: 547–558.

Bouckovalas, GD and AG Papadimitriou (2006) Aggravation of seismic ground motion due to slope topography. *1st European Conference on Earthquake Engineering and Seismology*, paper no. 1171. Geneva, 3–8 September 2006.

Brabhaharan, P (2006) Recent advances in improving the resilience of road networks. Remembering Napier 1931 – building on 75 years of earthquake engineering in New Zealand. *Annual Conference of the New Zealand Society for Earthquake Engineering*. Napier, 10–12 March 2006.

Brabhaharan, P (2011) *Statement of evidence of Pathmanathan Brabhaharan. Geotechnical Engineering and geology.* Transmission Gully project. 18 November 2011.

Brabhaharan, P and D Mason (2012) Wellington region road network earthquake resilience study. *Opus International Consultants risk study report GER 2012-21*.

Brabhaharan, P (2013) Earthquake resilience through early integrated urban planning and practice. *Annual Conference of the New Zealand Society for Earthquake Engineering. Existing Risks New Realities.* Wellington. April 2013.

Brabhaharan, P, LM Wiles and S Frietag (2006). Natural hazard road risk management part III: performance criteria. *Land Transport NZ research report 296*. 117pp.

Bray, J and D Frost (Eds) (2010). Geo-engineering reconnaissance of the 2010 Maule, Chile earthquake. Geo-Engineering Extreme Events Reconnaissance (GEER) Association. *GEER Association report GEER-022.* 272pp.

Bray, JD and EM Rathje (1998) Earthquake induced displacements of solid-waste landfills. *Journal of Geotechnical and Geoenvironmental Engineering, ASCE, 124*, no.3: 242–253.

Brunsdon, D, R Davey, C Graham, G Sidwell, P Villamor, R White and J Zhao (2000) The Chi-Chi Taiwan earthquake of 21 September 1999. Report of the NZSEE Reconnaissance Team. *Bulletin of the New Zealand Society for Earthquake Engineering 33*: 105–167.

Buech, F, TR Davies and JR Pettinga (2010) The Little Red Hill seismic experimental study: topographic effects on ground motion at a bedrock-dominated mountain edifice. *Bulletin of the Seismological Society of America 100*: 2219–2229.

Burjánek, J, JR Moore, G Gassner-Stamm and D Fäh (2011) Seismic response of unstable mountain rock slopes: topographic site effect? *Proceedings of the 4th International Association of Seismology and Physics of the Earth's Interior and International Association of Earthquake Engineering Internaional Symposium,* Santa Barbara, 23–26 August 2011. 11pp.

Çelebi, M (1991) Topographical and geological amplification: case studies and engineering implications. *Structural Safety 10*: 199–217.

Cetin, K, S Turkoglu, S Oral and U Nacar (2011) Van-Tabanli earthquake (Mw 7.1) October 23rd, 2011 – preliminary reconnaissance report. *Geo-Engineering Extreme Events Reconnaissance (GEER) Association. Preliminary report 2011.* 31pp.

Champati Ray, P, I Parvaiz, R Jayangondaperumal, V Thakur, V Dadhwal and F Bhat (2009) Analysis of seismicity-induced landslides due to the 8 October 2005 earthquake in Kashmir Himalaya. *Current Science 97*: 1742–1751.

Che, A and X Ge (2012) Earthquake-induced toppling failure mechanism and its evaluation method of slope in discontinuous rock mass. *International Journal of Applied Mechanics 4,* no.3: 1–15.

Chiaro, G, G Alexander, P Brabhaharan, C Massey, J Koseki, S Yamada and Y Aoyagi (In press) Report on geotechnical and geological aspects of the 2016 Kumamoto earthquakes. Submitted to the Bulletin of the NZ Society for Earthquake Engineering.

Chigira, M, X Wu, T Inokuchi and G Wang (2010) Landslides induced by the 2008 Wenchuan earthquake, Sichuan, China. *Geomorphology 118*: 225–238.

Collins, BD and RW Jibson (2015) Assessment of existing and potential landslide hazards resulting from the April 25, 2015 Gorkha, Nepal earthquake sequence. *U.S. Geological Survey open-file report 2015–1142,* ver. 1.1, 50pp.

Collins, BD, R Kayen and Y Tanaka (2012) Spatial distribution of landslides triggered from the 2007 Niigata Chuetsu-Oki Japan earthquake. *Engineering Geology 127*: 14–26.

Cowan, H, G Beattie, K Hill, N Evans, C McGhie, G Gibson, G Lawrance, J Hamilton, P Allan, M Bryant, M David, C Hyland, C Oyarzo-Vera, P Quintana-Gallo and P Smith (2011) The M_w 8.8 Chile earthquake, 27 February, 2010. *Bulletin of the New Zealand Society for Earthquake Engineering 44*: 123–166.

Dellow, GD, Q Ali, SM Ali, S Hussain, B Khazai and A Nisar (2007) Preliminary reconnaissance report for the Kashmir earthquake of 8 October 2005. *Bulletin of the New Zealand Society for Earthquake Engineering 40*: 18–24.

Deng, J, Y Tsutsumi, H Kameya, T Sato and J Koseki (2008) Triaxial tests on undisturbed samples retrieved from failed slopes due to 2004 Niigata-Ken Chuetsu earthquake. *Bulletin of the Earthquake Resistant Structure Research Centre 41*: 13–24.

ETC-12 (2006) Proceedings of the Athens Workshop. *Evaluation Committee for the Application of Eurocode 8*, Athens, 20–21 January 2006.

European Committee for Standardization (2004) *Eurocode 8. Design of structures for earthquake resistance, part 1: general rules, seismic actions and rules for buildings. EN 1998-1: and part 5: foundations, retaining structures and geotechnical aspects. EN 1998-5*.

Foster, P and G Campbell (2000) *NZSOLD reconnaissance report – Taiwan Dams March 2000*. New Zealand Society on Large Dams (NZSOLD). 12pp.

Gao, S, H Liu, PM Davis and L Knopoff (1996) Localized amplification of seismic waves and correlation with damage due to the Northridge earthquake: Evidence for focusing in Santa Monica. *Bulletin of the Seismological Society of America 86,* no.1B: S209–S230.

Geli, L, P-Y Bard and B Jullien (1988). The effect of topography on earthquake ground motion: a review and new results. *Bulletin of the Seismological Society of America 78*: 42–63.

Gorum, T, XM Fan, CJ van Westen, RQ Huang, Q Xu, C Tang and GH Wang (2011) Distribution pattern of earthquake-induced landslides triggered by the 12 May 2008 Wenchuan earthquake. *Geomorphology 133*: 152–167.

Gratchev, I and I Towhata (2008) Analysis of a slope failure triggered by the 2007 Chuetsu Oki earthquake. *Proceedings of the First World Landslide Forum*, Tokyo, 18–21 November 2008. Parallel session volume: 227–230.

Hancox, GT (2015) Performance of slopes in past New Zealand earthquakes: literature review and lessons learned from historical earthquakes. *GNS Science consultancy report CR2015/04*. 66pp.

Harp, EL and AJ Crone (2006) Landslides triggered by the October 8, 2005, Pakistan earthquake and associated landslide-dammed reservoirs. *U.S. Geological Survey open-file report 2006-1052*. 13pp.

Harp, EL, SH Hartzell, RW Jibson, L Ramirez-Guzman and RG Schmitt (2014) Relation of landslides triggered by the Kiholo Bay earthquake to modelled ground motion*. Bulletin of the Seismological Society of America 104*: 2529–2540.

Harp, EL and RW Jibson (1996) Landslides triggered by the 1994 Northridge, California, earthquake. *Bulletin of the Seismological Society of America 86,* no.1B: S319–S332.

Harp, EL and RW Jibson (2002) Anomalous concentrations of seismically triggered rock falls in Pacoima Canyon: Are they caused by highly susceptible slopes or local amplification of ground shaking? *Bulletin of the Seismological Society of America 92*: 3180–3189.

Harp, EL, RW Jibson, RE Kayen, DK Keefer, BL Sherrod, GA Carver, BD Collins, RES Moss and N Sitar (2003) Landslides and liquefaction triggered by the M 7.9 Denali Fault earthquake of 3 November 2002. *GSA Today 8*: 4–10.

Hashash, YMA, B Tiwari, RES Moss, D Asimaki, KB Clahan, DS Kieffer, DS Dreger, A Macdonald, CM Madugo, HB Mason, M Pehlivan, D Rayamahji, I Acharya and B Adhikari (2015) Geotechnical field reconnaissance: Gorkha (Nepal) earthquake of April 25 2015 and related shaking sequence. *Geotechnical Extreme Event Reconnaissance (GEER) Association report GEER-040, version 1.1.* 250pp.

Havenith, H-B, M Vanini, D Jongmans and E Faccioli (2003) Initiation of earthquake-induced slope failure: influence of topographical and other site specific amplification effects. *Journal of Seismology 7*: 397–412.

Hopkins, D, WD Clark, T Matuschka and JC Sinclair (1991) The Philippines earthquake of July 16, 1990. Report on field visit by the NZSEE Reconnaissance Team. *Bulletin of the New Zealand Society for Earthquake Engineering 24*: 3–95.

Hopkins, D, D Bell, R Benites, J Burr, C Hamilton and R Kotze (2008) The Pisco (Peru) earthquake of 15 August 2007. NZSEE reconnaissance report, June 2008. *Bulletin of the New Zealand Society for Earthquake Engineering 41*: 109–192.

Hough, S, J Altidor, D Anglade, D Given, M Janvier, J Maharrey, M Meremonte, B Mildor, C Prepetit and A Yong (2010) Localised damage caused by topographic amplification during the 2010 M 7.0 Haiti earthquake. *Nature Geoscience 3*: 778–782.

Huang, CC, YH Lee, HP Liu, DK Keefer and RW Jibson (2001) Influence of surface-normal ground acceleration on the initiation of the Jih-Feng-Erh-Shan Landslide during the 1999 Chi-Chi, Taiwan, earthquake. *Bulletin of the Seismological Society of America 91*: 953–958.

Huang, R and W Li (2008) Research on development and distribution rules of geohazards induced by Wenchuan earthquake on 12th May 2008. *Chinese Journal of Rock Mechanics and Engineering 27*: 2585–2592 (in Chinese with English abstract).

Huang, R, Q Xu and J Huo (2011) Mechanism and geo-mechanics model of landslides triggered by 5.12 Wenchuan Earthquake. *Journal of Mountain Science 8*: 200–210.

Huang, R, X Pei, X Fan, W Zhang, S Li and B Li (2012) The characteristics and failure mechanism of the largest landslide triggered by the Wenchuan earthquake, May 12, 2008, China. *Landslides 9*: 131–142.

Hung, JJ (2000a) Chi-Chi earthquake induced landslides in Taiwan. *International Workshop on Annual Commemoration of Chi-Chi Earthquake*, Taipei, 18–20 September 2000. Vol 3: 23–36.

Hung, JJ (2000b) Chi-Chi earthquake induced landslides in Taiwan. *Earthquake Engineering and Engineering Seismology 2,* no.2: 25–33.

Jalil, W (1992) New French seismic code orientation. Proceedings 10th World Conference on Earthquake Engineering. Madrid, Balkema, Rotterdam. Vol 10: 5867–5873.

Ji, S, Y Tang, D Hu, J Wang and S Tao (2009). Analysis of typical seismic damages of highways in Wenchuan earthquake-induced hazard areas in Sichuan province. *Chinese Journal of Rock Mechanics and Engineering 28*: 1250–1260 (in Chinese with English abstract).

Jibson, RW and EL Harp (2011) Field reconnaissance report of landslides triggered by the January 12, 2010, Haiti earthquake. *US Geological Survey open-file report 2011–1023*, 19pp.

Jibson, RW, EL Harp, W Schulz and DK Keefer (2004) Landslides triggered by the 2002 Denali Fault, Alaska, earthquake and the inferred nature of the strong shaking. *Earthquake Spectra 20*: 669–691.

Jibson, RW, EL Harp, W Schulz and DK Keefer (2006) Large rock avalanches triggered by the M 7.9 Denali Fault, Alaska, earthquake of 3 November 2002. *Engineering Geology 83*: 144–160.

Johansson, J, P Mayorca, T Torres and E Leon (2007) *A reconnaissance report on the Pisco, Peru earthquake of August 15, 2007*. Tokyo: Japan Society of Civil Engineers, Japan Association for Earthquake Engineering & University of Tokyo. 116pp.

Johansson, J, P Mayorca, E Leon and T Torres (2008) Damage in areas affected by the August 15, 2007 Pisco earthquake, Peru. *Bulletin of the Earthquake Resistant Structure Research Centre 41*: 3–12.

Kaiser, A, C Holden and C Massey (2014) Site amplification, polarity and topographic effects in the Port Hills during the Canterbury earthquake sequence. *GNS Science consultancy report 2014/121.* 33pp.

Kayen, R, B Cox, J Johansson, C Steele, P Somerville, K Konagai, Y Zhao and H Tanaka (2008) Geoengineering and seismological aspects of the Iwate Miyagi-Nairiku, Japan Earthquake of June 14, 2008. *Geo-Engineering Extreme Events Reconnaissance (GEER) Association web report 2008*, 83pp.

Khazai, B and N Sitar (2003) Evaluation of factors controlling earthquake-induced landslides caused by Chi-Chi earthquake and comparison with the Northridge and Loma Prieta events. *Engineering Geology 71*: 79–95.

Kieffer, DS, R Jibson, EM Rathje and K Kelson (2006) Landslides triggered by the 2004 Niigata Ken Chuetsu, Japan, Earthquake. *Earthquake Spectra 22*: S47–S73.

Konagai, K, J Johansson, A Zafeirakos, M Numada, A Sadr and T Katagiri (2005) Geotechnical hazard for civil infra-structures in the October 23, 2004 Niigata Chuetsu earthquake, Japan. *Bulletin of the Earthquake Resistant Structure Research Centre 39*: 3–13.

Konagai, K, K Oguni, A Akbar, H Kodama and T Ikeda (2006) Damage and rehabilitation in areas affected by the October 8, 2005 Kashmir earthquake, Pakistan. *Bulletin of the Earthquake Resistant Structure Research Centre 39*: 3–13.

Koseki, J and K Hayano (2000) Preliminary report on damage to retaining walls caused by the 1999 Chi-Chi earthquake. *Bulletin of the Earthquake Resistant Structure Research Centre 33*: 23–34.

Ktenidou, O-J, FJ Chavez-Garcia, D Raptakis and K Pitilakis (2011) Numerical investigation of site effects at Aegion, Greece. *5th International Conference on Earthquake Geotechnical Engineering, paper NIOKT*, 10pp.

Lanzo, G, G Di Capua, RE Kayen, DS Kieffer, E Button, G Biscontin, G Scasserra, P Tommasi, A Pagliaroli, F Silvestri, A d'Onofrio, C Violante, AL Simonelli, R Puglia, G Mylonakis, G Athanasopoulos, V Vlahakis and JP Stewart (2010) Seismological and geotechnical aspects of the M_w=6.3 l'Aquila earthquake in central Italy on 6 April 2009. *International Journal of Geoengineering Case Histories 1*: 206–339.

Lee, GC and C-H Loh (1999) Preliminary report from MCEER-NCREE workshop on the 921 Taiwan earthquake. *MCEER preliminary report*.

Li, X and S He (2009) Seismically induced slope instabilities and the corresponding treatments: the case of a road in the Wenchuan earthquake hit region. *Journal of Mountain Science 6*: 96–100.

Li, W, R Huang, C Tang, Q Xu and C Van Westen (2013) Co-seismic landslide inventory and susceptibility mapping in the 2008 Wenchuan earthquake disaster area, China. *Journal of Mountain Science 10*: 339–354.

Litchfield, N, R Van Dissen, R Sutherland, P Barnes, S Cox, R Norris, R Beavan, R Langridge, P Villamor, K Berryman, M Stirling, A Nicol, S Nodder, G Lamarche, D Barrell, J Pettinga, T Little, N Pondard, J Mountjoy and K Clark (2013) A model of active faulting in New Zealand. *New Zealand Journal of Geology and Geophysics 57*: 32–56.

Liu, H, Q Xu, Y Li and X Fan (2013) Response of high-strength rock slope to seismic waves in a shaking table test. *Bulletin of the Seismological Society of America 103*: 3012–3025.

Liu, Q and X Li (2009) Preliminary analysis of the hanging wall effect and velocity pulse of the 5.12 Wenchuan earthquake. *Earthquake Engineering & Engineering Vibration 8*: 165–177.

Lu, D, J Cui, X Li and W Lian (2010) Ground motion attenuation of M_s 8.0 Wenchuan earthquake. *Earthquake Science 23*: 95–100.

Lu, S, S Li, C Zhai and L Xie (2013) Effects of hanging wall and footwall on demand of structural input energy during the 2008 Wenchuan earthquake. *Earthquake Engineering & Engineering Vibration 12*: 1–12.

Makdisi, FI and HB Seed (1978) Simplified procedure for estimating dam and embankment earthquake-induced deformations. *ASCE Journal GT7*: 849–867.

Massa, M, S Barani and S Lovati (2014) Overview of topographic effects based on experimental observations: Meaning, causes and possible interpretations. *Geophysical Journal International 197*: 1537–1550.

Matuschka, T (1980). Assessment of seismic hazards in New Zealand. Unpublished PhD thesis, Department of Civil Engineering, University of Auckland. 249pp.

McVerry, G, J Zhao, N Abrahamson and P Somerville (2006). New Zealand acceleration response spectrum attenuation relations for crustal and subduction zone earthquakes. *Bulletin of the New Zealand Society for Earthquake Engineering 39*: 1–58.

Meneses, J, R Anderson, J Angel, J Callister, M Creveling, C Edwards, L Everingham, V Garcia-Delgado, A Gastelum, G Guerrini, R Hernandez, M Hoehler, T Hutchinson, D King, I Koutromanos, B Mathieson, S Mazzoni, G McGavin, F Mosele, J Murcia, H Okail, S Okubo, C Poland, J Rodgers, T Sanders, H Stenner, M Sarraf, B Shing, J Smith, A Stavridis, F Turner, D Watkins and R Wood (2010) The El Mayor Cucapah, Baja California Earthquake April 4, 2010. An EERI Reconnaissance Report. *Earthquake Engineering Research Institute, EERI learnings from earthquakes reconnaissance report.* 107pp.

Meunier, P, N Hovius and JA Haines (2008) Topographic site effects and the location of earthquake induced landslides. *Earth and Planetary Science Letters 275*: 221–232.

Miyagi, T, F Kasai, and S Yamashina (2008) Huge landslide triggered by earthquake at the Aratozawa Dam area, Tohoku, Japan. *Proceedings of the First World Landslide Forum*, Tokyo, 18–21 November 2008. Parallel session volume: 421–424.

Miyagi, T, D Higaki, H Yagi, S Doshida, N Chiba, J Umemura and G Satoh (2011) Reconnaissance report on landslide disasters in northeast Japan following the M 9 Tohoku earthquake. *Landslides 8*: 339–342.

Moore, J, V Gischig, F Amann, M Hunziker and J Burjánek (2012) Earthquake-triggered rock slope failures: Damage and site effects. *Proceedings of the 11th International and 2nd North American Symposium on Landslides*, Banff, Alberta, Canada, 3–6 June 2012. 6pp.

Nazari, A, MH Baziar and H Shahnazari (2011) Numerical evaluation of seismic behaviour of neighbouring topography on ground motion response. *5th International Conference on Earthquake Geotechnical Engineering, paper NESNA.* 11pp.

New Zealand Geotechnical Society (2010) *Geotechnical earthquake engineering practice. Module 1 – Guideline for the identification, assessment and mitigation of liquefaction hazards*.

New Zealand Transport Agency (2014) *Bridge manual*. Third edition. Wellington, New Zealand.

O'Connor, JS, L Mesa and M Nykamp (2007) Damage to the highway system from the Pisco, Peru earthquake of 15 August 2007. *Technical report MCEER-07-0021*. 92pp.

Oglesby, D and S Day (2001) The effect of fault geometry on the 1999 Chi-Chi (Taiwan) earthquake. *Geophysical Research Letters 28*: 1831–1834.

Orense, R, M Hyodo, H Kanda and J Ohashi (2008) Geotechnical aspects of the 2007 Niigataken Chuetsu-Oki, Japan earthquake. *Bulletin of the New Zealand Society for Earthquake Engineering 41*: 83–89.

Oyarzo-Vera, CA., GH McVerry and JM Ingham (2012) Seismic zonation and default suite of ground-motion records for time-history analysis in the North Island of New Zealand. *Earthquake Spectra 28*: 667–688.

Paolucci, R (2002) Amplification of earthquake ground motion by steep topographic irregularities. *Earthquake Engineering and Structural Dynamics 31*: 1831–1853.

Paolucci, R (2006) Numerical investigation of 3d seismic amplification by real steep topographic profiles and check of the EC8 topographic amplification coefficients. *Workshop of ETC-12 Evaluation Committee for the Application of EC8*, Athens, 20–21 January 2006.

Papadimitriou, AG (2011) Topographic aggravation of the peak seismic acceleration near two dimensional hills and slopes. *5th International Conference on Earthquake Geotechnical Engineering, paper TAOPA*, 12pp.

Parise, M and R Jibson (2000) A seismic landslide susceptibility rating of geologic units based on analysis of characteristics of landslides triggered by the 17 January, 1994 Northridge, California earthquake. *Engineering Geology 58*: 251–270.

Qureshi, OH and J Koseki (2006) Damage to roads caused by Oct. 8, 2005 North Pakistan Earthquake. *Bulletin of the Earthquake Resistant Structure Research Centre 39*: 79–90.

Rollins, K, K Franke, R Luna, N Rocco, D Avila and A Climent (2013). Geotechnical aspects of September 5, 2012 M 7.6 Samara, Costa Rica Earthquake. *Geotechnical Extreme Events Reconnaissance (GEER) Association Reconnaissance report*, v1.0. 57pp.

Rouvray, B, JCW Toh, R Cammack and B Estrada (2015) Performance based geotechnical design of a seismically resilient motorway: The Transmission Gully Project, New Zealand. *6th International Conference on Earthquake Geotechnical Engineering, paper 324*, 9pp.

Sanchez-Sesma, F, I Herrera and J Aviles (1982) A boundary method for elastic wave diffraction: application to scattering SH waves by surface irregularities. *Bulletin of the Seismological Society of America 72*: 473–490.

Scawthorn, C, S Ashford, J-P Bardet, C Huyck, R Kayen, S Kieffer, Y Kawamata, R Olshansky, P Somerville and J Mori (2005) Preliminary observations on the Niigata Ken Chuetsu, Japan, earthquake of October 23, 2004. *Earthquake Engineering Research Institute, EERI special earthquake repor.*12pp.

Sepulveda, SA, W Murphy, RW Jibson and DN Petley (2005a) Seismically induced rock slope failures resulting from topographic amplification of strong ground motions: the case of Pacoima Canyon, California. *Engineering Geology 80*: 336–348.

Sepulveda, SA, W Murphy and DN Petley (2005b) Topographic controls on coseismic rock slides during the 1999 Chi-Chi earthquake, Taiwan. *Quarterly Journal of Engineering Geology and Hydrogeology 38*: 189–196.

Sharpe, R, D Bradshaw, N Brown, R Van Dissen, D Kirkcaldie, K McManus, T Pham and C Stevenson (2000) Report of the NZSEE Reconnaissance Team on the 17 August 1999 Marmara Sea, Turkey Earthquake. *Bulletin of the New Zealand Society for Earthquake Engineering 33*: 65–104.

Shephard, R, P Wood, J Berrill, N Gillon, P North, A Perry and D Bent (1990) The Loma Prieta, California, Earthquake of October 17, 1989. Report of the NZNSEE Reconnaissance Team. *Bulletin of the New Zealand Society for Earthquake Engineering 23*: 1–78.

Smith, WD (1975) The application of finite element analysis to elastic body wave propagation problems. *Geophysical Journal of the Royal Astronomical Society 42*: 747–768.

Standards New Zealand (2002) *AS/NZS 1170.0: 2002 Structural design actions – part 2: general principles.*

Standards New Zealand (2004) *NZS 1170.5: 2004 Structural design actions, part 5: earthquake actions – New Zealand*.

Stewart, JP and SE Sholtis (2004) Case study of strong ground motion variations across cut slope. *Proceedings of the 11th International Conference on Soil Dynamics & Earthquake Engineering and the 3rd International Conference on Earthquake Geotechnical Engineering*: 917–922.

Stirling, M, R Langridge, R Benites and H Aleman (2003) The magnitude 8.3 June 23, Southern Peru earthquake and tsunami: Reconnaissance Report. *Bulletin of the New Zealand Society for Earthquake Engineering 36*: 189–207.

Stirling, M, G McVerry, M Gerstenberger, N Litchfield, R Van Dissen, K Berryman, P Barnes, L Wallace, P Villamor, R Langridge, G Lamarche, S Nodder, M Reyners, B Bradley, D Rhoades, W Smith, A Nicol, J Pettinga, K Clark and K Jacobs (2012) National seismic hazard model for New Zealand: 2010 update. *Bulletin of the Seismological Society of America 102*: 1514–1542.

Sun, P, Y Zhang, J Shi and L Chen (2011) Analysis on the dynamical process of Donghekou rockslide-debris flow triggered by 5.12 Wenchuan earthquake. *Journal of Mountain Science 8*: 140–148.

Tang, C, G Ma, M Chang, W Li, D Zhang, T Jia and Z Zhou (2015) Landslides triggered by the 20 April 2013 Lushan earthquake, Sichuan Province, China. *Engineering Geology 187*: 45–55.

Tang, H, H Jia, X Hu, D Li and C Xiong (2010) Characteristics of landslides induced by the great Wenchuan earthquake. *Journal of Earth Science 21*: 104–113.

Tarbali, K and BA Bradley (2014) Representative ground-motion ensembles for several major earthquake scenarios in New Zealand. *Bulletin of the New Zealand Society for Earthquake Engineering 47*: 231–252.

Tiwari, B, D Pradel and J Wartman (2012) Performance of slopes and dams in the M_w 9.0 Tohoku, Japan earthquake. *Second International Conference on Performance-based Design in Earthquake Geotechnical Engineering, paper 8.06*. 11pp.

Toh, JCW and GE Swarbrick (2015) The Transmission Gully project: method for assessing seismic stability of large rock cuts in steep terrain, considering topographic amplification. *6th International Conference on Earthquake Geotechnical Engineering, paper 323*. 8pp.

Wang, G, T Kamai, M Chigira and X Wu (2008) Some catastrophic landslides triggered by the May 12, 2008 Sichuan earthquake. *Proceedings of the First World Landslide Forum*, Tokyo, 18–21 November 2008. Parallel session volume: 647–651.

Wang, WL, TT Wang, JJ Su, CH Lin, CR Seng and TH Huang (1999) Assessment of damages in mountain tunnels due to the Taiwan Chi-Chi earthquake. *Tunnelling and Underground Space Technology 16*: 133–150.

Wang, X, G Nie and D Wang (2010). Relationships between ground motion parameters and landslides induced by Wenchuan earthquake. *Earthquake Science 23*: 233–242.

Wang, X, G Nie and M Ma (2011) Evaluation model of landslide hazards induced by the 2008 Wenchuan earthquake using strong motion data. *Earthquake Science 24*: 311–319.

Wang, X, G Nie and S Wang (2012a) Analysis of landslide damage caused by the 2008 Wenchuan earthquake using strong motion data: a case study in the Beichuan county town. *Earthquake Science 25*: 307–313.

Wang, Y, Y Luo, F Wang, D Wang, X Ma, S Li and X Deng (2012b) Slope seismic response monitoring on the aftershocks of the Wenchuan earthquake in the Mianzhu section. *Journal of Mountain Science 9*: 523–528.

Wang, ZZ, B Gao, YJ Jian and S Yuan (2009) Investigation and assessment on mountain tunnels and geotechnical damage after the Wenchuan earthquake. *Science in China Series E - Technological Sciences 52*: 546–558.

Wartman, J, L Dunham, B Tiwari and D Pradel (2013) Landslides in eastern Honshu induced by the 2011 Tohoku earthquake. *Bulletin of the Seismological Society of America 103*: 1503–1521.

Wick, E, V Baumann and M Jaboyedoff (2010) Report on the impact of the 27 February 2010 earthquake (Chile, M_w 8.8) on rock falls in the Las Cuevas valley, Argentina. *Natural Hazards and Earth System Sciences 10*: 1989–1993.

Wu, J-H, J-Sh Lin and C-S Chen (2009) Dynamic discrete analysis of an earthquake-induced large-scale landslide. *International Journal of Rock Mechanics and Mining Sciences 46*: 397–407.

Xiao, S, W Feng and J Zhang (2010) Analysis of the effects of slope geometry on the dynamic response of a near-field mountain from the Wenchuan earthquake. *Journal of Mountain Science 7*: 353–360.

Xu, X, B Shyu, M Gao, X Tan, Y Ran and W Zheng (2015) Landslides triggered by the 20 April 2013 Lushan, China, M_w 6.6 earthquake from field investigations and preliminary analyses. *Landslides 12*: 365–385.

Yin, Y, F Wang and P Sun (2008) Landslide hazards triggered by the 12 May 2008 Wenchuan earthquake, Sichuan, China. *Proceedings of the First World Landslide Forum*, Tokyo, 18–21 November 2008. Parallel session volume: 1–17.

Yin, Y, W Zheng, X Li, P Sun and B Li (2011). Catastrophic landslides associated with the M8.0 Wenchuan earthquake. *Bulletin of Engineering Geology and the Environment 70*: 15–32.

Yu, J, P Yong, S Read, P Brabhaharan and M Foon (2010) The M_s 8.0 Wenchuan earthquake of 12 May 2008 reconnaissance report. *Bulletin of the New Zealand Society for Earthquake Engineering 43*: 41–83.

Yuan, R-M, Q-H Deng, D Cunningham, C Xu, X-W Xu and CP Chang (2013) Density distribution of landslides triggered by the 2008 Wenchuan earthquake and their relationships to peak ground acceleration. *Bulletin of the Seismological Society of America 103*: 2344–2355.

Yuan, R-M, C-L Tang and Q-H Deng (2015) Effect of the acceleration component normal to the sliding surface on earthquake-induced landslide triggering. *Landslides 12*: 335–344.

Zeng, K, J Li, X Liang and J Xu (2011) Collapsing mechanism of rock slopes in Wenchuan earthquake. *Proceedings of 3rd International Conference on Transportation Engineering*: 2044–2049.

Zhou, D, J Zhang and Y Tang (2010) Seismic damage analysis of road slopes in Wenchuan earthquake. *Chinese Journal of Rock Mechanics and Engineering 29*: 565–576 (in Chinese with English abstract).

Appendix A: Performance of slopes in past New Zealand earthquakes: Literature review and lessons learned from historical earthquakes

Prepared by GT Hancox, GNS Science, Lower Hutt

A1 Introduction

This report provides a detailed literature review of coseismic landsliding and performance of slopes and during historical earthquakes in New Zealand. Earthquakes considered in the review comprise 22 events between 1848 and 1995 which caused significant earthquake-induced landsliding, including: Wairarapa 1855, Arthur's Pass and Murchison (Buller) in 1929, Napier (Hawke's Bay) 1931, Wairarapa in June and August 1942, Inangahua 1968, Edgecumbe 1987, and Arthur's Pass 1994 and 1995. Nine other important coseismic landslide events occurring between 2003 and 2015 were also reviewed. These comprise earthquakes in Fiordland in 2003 and 2009, Rotoehu 2004, Christchurch in 2010 and 2011, Cook Strait and Lake Grassmere 2013, Eketahuna 2014 and the Wilberforce Valley in 2015.

The component of the research presented in this report relates to the performance of slopes in past New Zealand earthquakes. The scope of the work undertaken and described in this report includes:

1 A literature search and review of the performance of slopes and coseismic landslides in a variety of New Zealand geological and topographic conditions during past historical earthquakes. Significant earthquakes considered include Wairarapa 1855, Murchison (Buller) 1929, Inangahua 1968, Rotoehu 2004, Fiordland 2003 and 2009, Christchurch 2010–2011, Cook Strait and Lake Grassmere 2013, and Eketahuna 2014.

2 Documentation of the lessons learned (knowledge obtained) from slope failures in past earthquakes for cut slope design, and observations on slope performance, include:

   a occurrence of slope failures (including cut slopes), their distribution with respect to fault rupture (eg hanging wall versus foot wall), and any measured ground accelerations/MM intensities

   b mechanisms of slope failures (coherent or disaggregated, shallow/deep, defect controlled or rock mass failures, and location of failure on slope (top, mid-height or lower slope)

   c sizes of failures and consequences to the built environment

   d recorded or inferred ground condition and ground shaking, topographical effects and seismotectonic regime.

Landslide nomenclature: Landslides are often classified into different types according to the materials involved and the mode of slope movement. Landslide types typically include rock falls, rock slides, soil and debris falls, slides and flows. The classification used in this study is the 'Varnes landslide classification', as defined by Hungr et al (2014) and summarised in annex A.1. Landslide criteria and effects defined in the New Zealand MM intensity scale (Hancox et al 2002; Dowrick et al 2008) are summarised in annex B.1.

A2 Literature review

Landslides have been triggered by many historical earthquakes in New Zealand between 1840 and 2015. Historically, the damage, loss of life and economic effects of earthquake-induced landsliding (EIL) is second only to earthquake shaking. Coseismic landslides have destroyed buildings and damaged many roads, and in the last 100 years at least 22 people have been killed by landslides and rock falls triggered by earthquakes (Hancox et al 2002; 2011; Crozier et al 2009). Earthquakes that have caused significant landsliding in New Zealand are shown in figure A.1. Details of the earthquakes, their associated landslide effects and the main references relating to these events are summarised in table A.1.

Figure A.1 Map showing the locations (epicentres) of historical earthquakes that have caused significant landsliding in New Zealand from 1840 to 2014. The approximate locations of some larger landslides are indicated by small circles. Dashed lines show the extent of the landslide-affected areas (in which landslides occurred) during earthquakes that caused widespread landsliding.

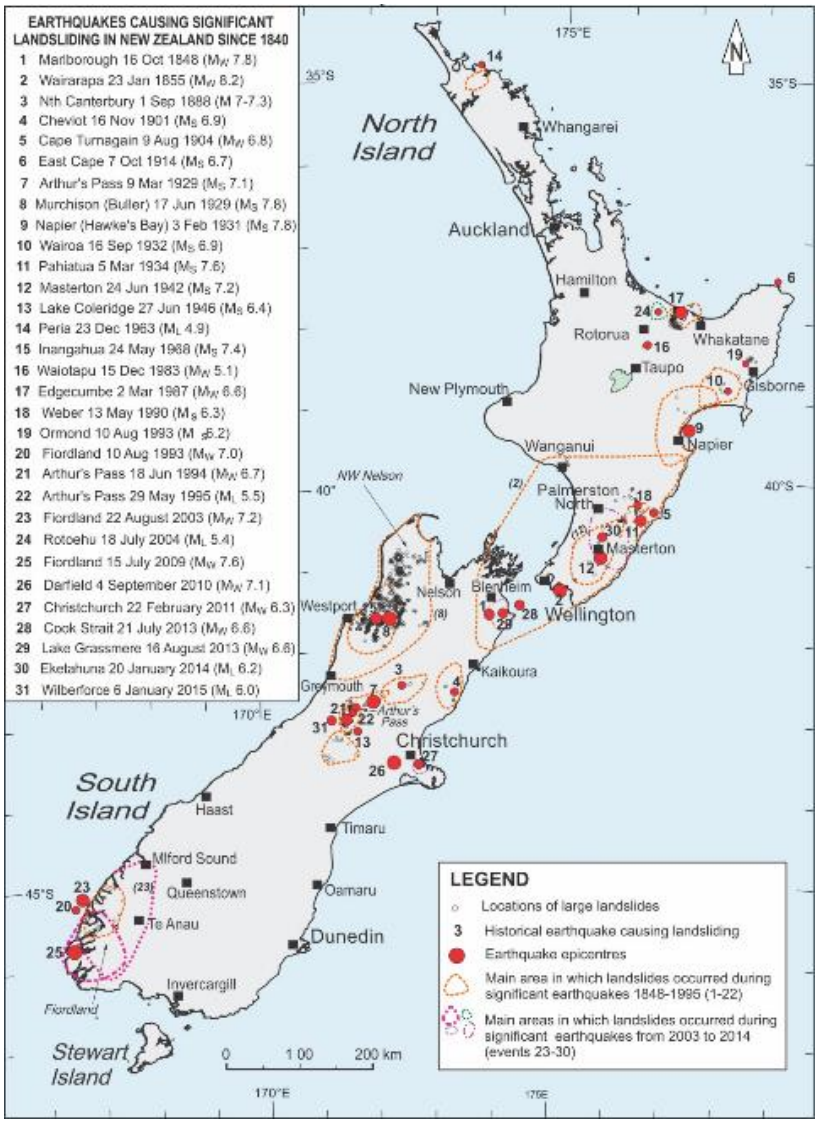

Source: Hancox et al (2002)

Table A.1 Historical earthquakes from 1840–2014 that have caused significant landsliding in New Zealand

Earthquake name (and number)	Date	Magnitude[a] (Max MMI)[1a]	Depth *km*[b]	Summary of landslide effects[c]	Main references
1 Marlborough	16 October 1848	M_w7.4–7.7 (MM10)	12	Surface faulting in Awatere Valley. Many landslides in epicentral area and in Marlborough hill country and coastal cliffs, the SE Wairarapa coast, and the Rimutaka Range.	Grapes et al 1997; Dowrick and Rhoades 1998; Hancox et al 1997; 2002; GeoNet, GNS files[c]
2 Wairarapa	23 January 1855	M_w8.2–8.3 (MM10)	33	Widespread landsliding in southern Rimutaka Range and Wairarapa; at least 17 landslides of ~1–10Mm^3. Landslides occurred over ~20,000km^2 of southern North Island from Wellington city and Lower Hutt to as far north as Wanganui and Hawkes Bay, and NE South Island; landslide locations are mainly poorly defined.	Grapes and Downes 1997; Dowrick and Rhodes 1998; Hancox et al 1997; 2002; Hancox 2005.
3 North Canterbury	1 September 1888	M_w7–7.3 (MM9)	12	Landsliding spread over ~1,600km^2 of mountains southwest of Hanmer Springs, mainly on alluvial terraces edges and steep slopes in Torlesse rocks (greywacke and argillite).	Cowan 1991; Dowrick and Rhodes 1998; Hancox et al 1997; 2002. GeoNet.
4 Cheviot	16 November 1901	M_s6.9 M_w6.8 (MM9)	10	Landslides in epicentral area over ~500km^2 of coastal ranges of north Canterbury (MM8–9); roads blocked by landslides in area; large failures on coastal cliffs near Point Gibson. Most landslides were in Tertiary age rocks (siltstone, sandstone and limestone) on steep (>30º) slopes.	Mckay 1902; Dowrick and Rhodes 1998; Hancox et al 1997; 2002.
5 Cape Turnagain	9 August 1904	M_s6.8 M_w6.7 M_L7.0 (MM8)	16	Landsliding over ~3,500–6,000km^2, mainly on coastal cliffs of Wairarapa, Cape Kidnappers and Bluff Hill in Napier. Failures in the Dannevirke-Weber area were mainly small to moderate falls of Tertiary rocks in road cuts. A very large landslide occurred, or was reactivated on the cliffs at Cape Turnagain.	Downes 1995; Downes 2006; Dowrick and Rhodes 1998; Hancox et al 1997; 2002; GeoNet.
6 East Cape	7 October 1914	M_s6.6 (MM7–8)	12	Significant landsliding in epicentral area at MM7–8. A landslide near Cape Runaway is reported to have killed a shepherd (Morgan 1920).	Morgan 1920; Downes 1995; Hancox et al 1997; 2002; GeoNet.

Earthquake name (and number)	Date	Magnitude[a] (Max MMI)[1a]	Depth *km*[b]	Summary of landslide effects[c]	Main references
7 Arthur's Pass	9 March 1929	M_s7.1 M_w7.0 (MM9)	12	Widespread landslides in mountains from Arthur's Pass to Lake Sumner over ~650km^2 along the Kakapo Fault. Triggered several very large (≥1Mm^3) failures in greywacke rocks, including Falling Mountain (~70Mm^3). Other landslide locations are generally poorly known. MM8 to MM9 inferred in the epicentral area from the landsliding that occurred.	Speight 1933; Yang 1992; Dowrick and Rhodes 1998; Hancox et al 1997; 2002; GeoNet.
8 Murchison (Buller)	17 June 1929	M_s7.8 M_w7.8 (MM10)	10	Widespread landsliding over up to ~15,000km^2 of mountains of NW Nelson. Landslides damaged roads in the Buller River area, resulting in 14 deaths. Triggered the highest number (>10,000) and density of landslides (~200–300/100km^2) of any historical earthquake in New Zealand. Two landslides >100Mm^3; ~50 >1Mm^3.	Dowrick 1994; Henderson 1937; Pearce and O'Loughlin 1985; Hancox et al 1997, 2002; Hancox et al 2014; GeoNet.
9 Hawke's Bay (Napier)	3 February 1931	M_s7.8 M_w7.8 (MM10)	17	Widespread landsliding occurred over ~4,700km^2 to the north, west, and south of Napier. Very large failures in Tertiary mudstone and sandstone on inland and coastal cliffs from ~ 5–72Mm^3, along with numerous smaller rock falls within the MM 8–10 isoseismals. Many roads were blocked by slips, and the Te Hoe River was dammed by a 15Mm^3 rock fall into a gorge.	Baird 1931; Marshall 1933; Henderson; Guthrie-Smith 1969; Dowrick and Rhodes 1998; Hancox et al 1997; 2002; GeoNet.
10 Wairoa	16 September 1932	M_s6.9 M_w6.8 (MM9)	20	Caused landsliding over ~700km^2 north and west-SW of Wairoa. Most were shallow failures, although two very large slides occurred in tertiary rocks, including a 20Mm^3 rotational slide on the coast 30km southwest of the epicentre, and 10km west a 10Mm^3 slide into the Wairoa River (mainly within MM8–9 isoseismals). Landslides closed many roads and disrupted transport in the area.	Ongley 1937; Downes 1995; Dowrick and Rhodes 1998; Hancox et al 1997; 2002; GeoNet.

Earthquake name (and number)	Date	Magnitude[a] (Max MMI)[1a]	Depth *km*[b]	Summary of landslide effects[c]	Main references
11 Pahiatua	5 March 1934	M_S7.6 M_w7.4 (MM9)	12	Minor landsliding in Tertiary age rocks over ~6,500km^2 in northern Wairarapa, southern Hawkes Bay, Manawatu-Wanganui areas, mainly within the MM7–9 isoseismals between Dannevirke and Masterton. Numerous small rock and debris falls affected roads in the epicentral area, and coastal cliffs from Castle Point to Cape Turnagain.	Bullen 1938; Dowrick and Rhodes 1998; Downes et al 1999; Hancox et al 1997; 2002; GeoNet.
12a Masterton (Wairarapa)	24 June 1942	M_S7.2 M_w7.2 (MM8, MM9 at 4 sites)	12	Landslides occurred over 6,500km^2, mainly in Tertiary rocks of the hill country east of Masterton, mainly within the MM8 isoseismal. Most roads east and south of Masterton were blocked by small to moderate rock/debris falls. At least four large to very large (10^5–10^6m^3) landslides occurred, one of which formed a small landslide-dammed lake. Moderate to large slides were noted in greywacke rocks in the Tararua Range. About 65km southwest a rockfall blocked the railway line at Plimmerton; small rock falls were also reported on the railway line from Plimmerton to Paekakariki, in Wellington City, and along the Hutt Road (SH2).	Ongley 1943; Hancox et al 1997, Downes et al 2001
12b Masterton (Wairarapa)	2 August 1942	M_S7.0 M_w6.8 (MM7, MM at 2 sites)	40	Landsliding was less severe than in June 1942 and affected a smaller area (~5,600km^2). Most landslides occurred in hill country south, east, and north of the epicentre. Small rock falls again occurred at Pukerua Bay, Paekakariki and Otaki. Many landslides were on slopes that failed in the June earthquake, but were fewer in number and less damaging.	Ongley 1943; Hancox et al 1997; Downes et al 2001.

Earthquake name (and number)	Date	Magnitude[a] (Max MMI)[1a]	Depth *km*[b]	Summary of landslide effects[c]	Main references
13 Lake Coleridge	27 June 1946	M_S, M_w6.2 (MM7 or possibly MM8)	12	Minor to moderate landsliding over ~1,500km^2 from Lake Coleridge to Lake Heron, and along the banks of the Rakaia River within the MM7 isoseismal. Most of the landslides (volumes up to ~10,000m^3) were at the northern end of Lake Coleridge, where shaking may have reached MM8. Boulders, small slips and cracking damaged and closed some hill country roads in the area.	Eiby 1990; Downes 1995; Dowrick and Rhodes 1998; Hancox et al 1997; 2002; GeoNet.
14 Peria	23 December 1963	M_L4.9 (MM7)	10	Minor landsliding (small soil falls) occurred over ~450km^2, within 20km of the epicentre at MM6–7. All failures occurred on very steep (>50º) natural slopes or cut slopes; no roads were closed by slips.	Eiby 1968; Downes 1995; Hancox et al 1997; 2002.
15 Inangahua	24 May 1968	M_S7.4 M_w7.1 (MM10)	12	Widespread landsliding occurred over ~3,500km^2 centred around Inangahua, Murchison and Westport and north as Little Wanganui within the MM 8–10 isoseismals. Numerous slope failures occurred in the mountains north and south of the Buller River, including extensive rock falls from limestone scarps. Moderate to large slips closed the Buller Gorge road for 10 weeks, and a ~5Mm^3 rock avalanche dammed the Buller River. A rock fall killed two people near Inangahua, and a third person died near Greymouth due to road subsidence. Based on the size, number and density of landslides that occurred (~40–100km^2), the Inangahua earthquake is one of New Zealand's most significant historical earthquakes.	Lensen and Suggate 1968; Douglas 1969; Duckworth 1969; Anderson et al 1994; Dowrick and Rhodes 1998; Hancox et al 1997; 2002; Hancox et al 2014; Parker et al 2015.
16 Waiotapu	15 December 1983	M_S4.6 M_w3.8 (MM5–6)	5	Minor landslides in weak pumice and tuff deposits in the Waioatpu area; boulders on SH5, with little effect on local roads or buildings.	Downes 1995, Dowrick and Rhodes 1998; Hancox et al 1997: 2002; GeoNet.

Earthquake name (and number)	Date	Magnitude[a] (Max MMI)[1a]	Depth *km*[b]	Summary of landslide effects[c]	Main references
17 Edgecumbe	2 March 1987	M_s6.6 M_w6.5 (MM9)	10	Landslides occurred over ~700km² of the area around Edgecumbe from Whakatane to Matata, Kawerau, and Lake Matahina. The failures were mainly small, shallow, soil and rock falls on slopes steeper than 40º up to 30km from the epicentre, within the MM8–9 isoseismals. Rock and debris falls from the coastal cliff blocked SH2 west of Matata. Ridge crest cracking (incipient landsliding) was common on the hills and ridges west of Tarawera River.	Pender and Robertson 1987; Franks et al 1989; Lowry et al 1989; Hancox et al 1997; 2002; GeoNet.
18 Weber	13 May 1990	M_s6.2, M_w6.4 (MM8, one site MM9)	30	Shallow landsliding over ~500km² in weak Tertiary rocks southeast of Dannevirke. Small to moderate size failures of road cuts damaged and closing some roads in the area, mainly within the MM8 isoseismal.	Perrin 1990; Downes 1995; Dowrick and Rhodes 1998; Hancox et al 1997; 2002; GeoNet.
19 Ormond	10 August 1993	M_w6.2 M_L6.7 (MM7–8)	33	Caused minor landsliding over about 30km² in weak Tertiary rocks; minor damage to roads.	Read and Sritharan 1993; Read and Cousins 1994; Dowrick and Rhodes 1998; Hancox et al 1997; 2002; Reyners et al 1998; GeoNet.
20 Fiordland	10 August 1993	M_s7.0 M_w6.8 (MM8)	20	Sparse, widely distributed shallow landslides over ~5,000km²; mainly small narrow slides and falls of soil, rock, and debris, none of which affected the Milford Road (SH94).	Van Dissen et al 1994; Dowrick and Rhodes 1998; Hancox et al 1997; 2002; GeoNet.
21 Arthur's Pass	18 June 1994	M_w6.7 (MM8)	4	Landsliding occurred over ~950km² in steep mountainous terrain in the epicentral area ~10–20km southwest of Arthurs Pass, within the MM8 isoseismal. At least 70 landslides in greywacke/argillite rocks were attributed to the event, the largest of which was ~1–2Mm³. SH73 was temporarily blocked by rock falls in a few places north of Arthur's Pass; the Otira River was briefly dammed by rock fall.	Paterson and Bourne-Webb 1994; Patel and Wood 1994: Dowrick and Rhodes 1998; Hancox et al 1997; 2002; GeoNet.

Earthquake name (and number)	Date	Magnitude[a] (Max MMI)[1a]	Depth *km*[b]	Summary of landslide effects[c]	Main references
22 Arthur's Pass	29 May 1995	M_L5.5 (MM6)	4	Minor landsliding in the epicentral area; failures on some road cuts and road edge fills; landslides fewer and smaller than in June 1994.	Paterson and Berrill 1995; Dowrick and Rhodes 1998; Hancox et al 1997; 2002; GeoNet.
23 Fiordland (Secretary Island)	22 August 2003	M_w7.2 (MM7 or >) (MM8–9 indicated by landsliding)	20	Widespread superficial landsliding on steep slopes over ~10,000km^2 in the mountains west of Te Anau. At least 400 landslides up to ~700,000m^3 in size occurred on very steep slopes within 25km of the earthquake fault plane. Based on landslide effects shaking intensity reached MM8–9 in the epicentral area. Wilmot Pass road blocked by a large landslide; small rock falls on SH94 from Homer Tunnel south.	Hancox et al 2003; 2004; Reyners et al 2003; Power et al 2005; GeoNet
24 Rotoehu (Lake Rotoma)	18 July 2004	M_L5.4 (MM8)	5	Landsliding and ground damage occurred over a 300km^2 area near Lake Rotoehu and Lake Rotoma; at least 100 landslides triggered, mostly very small (<10^3m^3) to small (10^3–10^4m^3) superficial soil slides and falls of unconsolidated scoria and tephra deposits around steeper parts of the lake shorelines, and on road cuts greater than 3m high; some cut slope failures disrupted traffic on roads. The relatively high number of landslides was attributed to slopes in the area being saturated when the earthquake occurred.	Hancox et al 2004; GeoNet
25 Fiordland (Dusky Sound)	15 July 2009	M_w7.6–7.8 (MM7)	12	Small-scale, shallow landslides over ~5,600km^2. Offshore (southward) directivity of seismic energy and low stress release (~0.2MPa; M_E7.0) resulted in fewer landslides than expected, given the magnitude.	Fry et al 2010; Hancox et al 2010; GeoNet.
26 Darfield	4 September 2010	M_w7.1 (MM9)	11	Small to moderate rock falls in the Port Hills affected roads in the area. Sumner Road closed by rock falls.	GeoNet; Quigley et al 2010.

Earthquake name (and number)	Date	Magnitude[a] (Max MMI)[1a]	Depth *km*[b]	Summary of landslide effects[c]	Main references
27 Christchurch (Port Hills)	22 February 2011	M_w6.3 (MM9)	5	About 175km^2 of Banks Peninsula the Port Hills and southeast of southern of Christchurch affected by coseismic landslides and ground cracking caused by the earthquake. The effects included cliff collapses, rock falls and boulder rolls, incipient loess landslides, and retaining wall and fill failures. Four deaths from rock-fall occurred during the main shock and one during an aftershock. Hundreds of houses were damaged by rock-falls and ground cracking within the MM8–MM9 isoseismals. Although the landslides were highly damaging, most of the failures were relatively small in volume (<100m^3).	Dellow et al 2011; Hancox et al 2011; Kaiser et al 2011; GeoNet.
28 Cook Strait	21 July 2013	M_w6.5 (MM8)	13	Minor landsliding occurred across ~700km^2 of Marlborough, mainly to the steep (35º) coastal cliffs within ~15km of the epicentre, and terrace edges in the middle Awatere Valley. The largest landslide that occurred was a ~100,000m^3 rotational slide on the steep mudstone cliffs 1km west of Cape Campbell. Debris falls on White Bluffs and similar cliffs in the area were small (10–1,000m^3).	GeoNet; Hancox et al 2013
29 Lake Grassmere	16 August 2013	M_w6.6 (MM9)	8	Small to moderate rock and debris falls/slides and incipient failures (ridge and slope cracking) occurred over ~3,000km^2. No new larger landslides had formed since the 21 July Cook Strait earthquake.	Van Dissen et al 2013; GeoNet.
30 Eketahuna	20 January 2014	M_L6.2 (MM8)	34	Approximately 130 instances of landslides, rockfalls, and areas of ground cracking were triggered by the earthquake over ~5,500km^2. Most failures were on steep-very steep (~35º–45º or >) natural slopes (cliffs, scarps, terrace edges) and road cuts in a variety of Tertiary rock types; some road closures.	Rosser et al 2015; GeoNet.

Earthquake name (and number)	Date	Magnitude[a] (Max MMI)[1a]	Depth *km*[b]	Summary of landslide effects[c]	Main references
31 Wilberforce	6 January 2015	M_L6.0 (~MM7)	6	Numerous small to moderate rock falls and rock avalanches near epicentre in the mountains 40–50km west of Arthur's Pass. Landslide temporarily blocked Arahura River west of main divide. No landslides reported to have affected roads.	GeoNet; Carey and Rosser 2015.

Notes:

[a] Magnitude values are either: local (M_L); surface wave (M_S); moment (M_W).

[1a] For MM intensities refer to table A.4 or appendix B.

[b] Centroid (centre of fault rupture surface) depths (km) from Dowrick and Rhoades (1998), other listed references, or GeoNet.

[c] The approximate size of landslides referred to in this table and elsewhere in the report are as follows (see appendix 2 also):

Very small (≤10^3m^3); Small (10^3–10^4 m^3); Moderate (10^4–10^5m^3);
Large (10^5–10^6m^3); Very large (1–100 x 10^6m^3); Giant (≥100 x 10^6m^3).

Reporting and documentation of landsliding and ground damage caused by historical earthquakes in New Zealand (figure A.1) has varied through time, and has been described in detail mainly for moderate and large earthquakes (M=7.0 or >) from 2003 to 2015 when landslide reconnaissance studies for GeoNet have been undertaken.

Brief written accounts are given of landslides caused by earlier earthquakes such as the 1929 Arthur's Pass (Speight 1933) and the 1931 (Napier) Hawke's Bay (Baird 1931) earthquakes (table A.1). More detailed accounts are given of landsliding triggered by the 1929 Murchison (Buller) earthquake (Henderson 1937; Pearce and O'Loughlin 1985), although the complete landslide distribution for that event was not mapped. More detailed descriptions are given of landslides caused by recent large (≥M6.5) earthquakes such as: Inangahua 1968 (Lensen and Suggate 1968); Edgecumbe 1987 (Franks et al 1989); Weber 1990 (Perrin 1990); Fiordland 1993 (Van Dissen et al 1994); Ormond 1993 (Read and Sritharan 1993), and Arthur's Pass 1994 (Berrill et al 1994; Paterson and Bourne-Webb 1994). General comments on landsliding were also provided in relation to ground shaking intensities and isoseismal maps of historical (1948–1990) New Zealand earthquakes (Downes 1995).

The first comprehensive analysis of landsliding during historical earthquakes in New Zealand was undertaken by Hancox et al (1997), who carried out retrospective studies of 22 earthquakes that had caused widespread and damaging landsliding (earthquakes numbered 1–22, figure A.1 and table A.). The results of that study are summarised below:

> *Landsliding and ground damage caused by historical earthquakes from 1840–1997 were studied to determine: (a) relationships between landslide distribution and earthquake magnitude, epicentre, faulting, geology and topography, and (b) to develop improved environmental response criteria and ground classes for assigning MM intensities and seismic hazard assessments in New Zealand.*
>
> *It was shown that in New Zealand, very small landslides occur at ~M 5, but significant landsliding occurs only at M 6 or greater. Most widespread landsliding (mainly disrupted slides or falls of rock and soil) were caused by shallow earthquakes <45 km) of M 6.2–8.2. The minimum MM intensity threshold for landsliding was found to be MM6, while the most*

common intensities for significant landsliding were MM7 and MM8. Very large landslides occur mainly at MM9 and MM10, and were used in the study to redefine zones of MM10 shaking for the 1855 Wairarapa and 1929 Murchison earthquakes.

The maximum area affected by landsliding (in which landslides occurred) was found to range from ~100 km² at M 5 to ~20,000 km² at M 8.2. From the area-magnitude relationships the expression: $Log1_0$ A (area km²) = 0.96 M (magnitude) – 3.7 was derived to estimate the average area likely to be affected by landsliding during earthquakes in New Zealand. Overseas earthquakes were found to affect slightly larger areas, possibly because of topographic and climatic differences.

Landslide size was found to be strongly dependent on earthquake magnitude, intensity, and distance from the epicentre. In New Zealand, smaller landslides are formed at maximum epicentral distances of almost 300 km (for M 8.2, at MM6). Large and very large failures occur at distances of up to about 100 km (for M 6 or more, at MM8–MM10). However, during overseas earthquakes landslides can occur at greater maximum distances, probably due to poorly understood interactions between topography, geology, seismicity, and climatic factors (coseismic landsliding in New Zealand was likely to be more widespread and severe during winter than in summer).

Landslide occurrence during earthquakes was also found to be strongly controlled by topography and rock and soil type. Slope failures occurred mainly on moderate to very steep (20°–50°) slopes.

The most common coseismic landslides were rock and soil falls on very steep cliffs, escarpments, gravel banks and terrace edges, and high, steep, unsupported man-made cut slopes. Such features were found to be highly hazardous and more susceptible to rapid failure because of rock defects, low strength, and topographic amplification of shaking. Large (10^5–10^6 m³) dip slope failures in Tertiary sandstone and mudstone often occur on gentle to steep slopes (10°–40°). Very large (≥10^6 m³) rock avalanches were caused by earthquakes of M ≥6.5, on hill slopes steeper than 25°–30° and greater than 100–200 m high, especially on strongly shaken high, narrow ridges.

The good correlation between landsliding and the fault rupture zone indicated by aftershocks suggests that overall landslide distribution can be used to indicate the approximate location of the epicentre and fault rupture zone for some earthquakes, but allowance must be made for topographic effects.

Historical seismicity shows that shallow M 5 and 6 or greater earthquakes that trigger damaging landslides are more likely in northwest Nelson, the central Southern Alps, Fiordland, Marlborough, Wellington, Wairarapa, Hawke's Bay, and East Cape areas. The central North Island, Auckland, Central Otago and Southland are regarded as lower hazard areas. More detailed and expanded environmental response criteria (landslides, subsidence, sand boils, lateral spreads) in the MM intensity scale are proposed, along with provisional ground type classes of varying landslide susceptibility (similar to those for buildings). It is hoped that these can be used for assigning more reliable and consistent earthquake intensities in areas where there were few buildings.

Relationships developed in this study can be used to assess earthquake-induced landslide hazard and risk in New Zealand. Further studies are recommended to incorporate results from this project into a GIS based National Landslide Hazard Model, which could be used to

> *predict landslide hazard in different parts of New Zealand for triggering events such as moderate to large earthquakes and rainstorms. Other research that is recommended includes detailed studies of some earthquakes (e.g., 1929 Murchison, 1855 Wairarapa) to refine the ground type classes, palaeoseismic studies in known 'seismic gaps' on major active faults, and continued earthquake reconnaissance studies in New Zealand and overseas.*

The results of the Hancox et al (1997) study were developed further in a 2002 paper (Hancox et al 2002). The 2002 study incorporated new data included a summary of landslides associated with the 1929 Murchison earthquake, a size/frequency distribution for New Zealand coseismic landslides over the last 150 years, and a preliminary earthquake induced landslide susceptibility, opportunity and hazard model for New Zealand.

Since 2003 support from GeoNet has enabled aerial and ground reconnaissance studies to be carried out by GNS Science after earthquakes that have caused significant landsliding (events 23–31, table A.1). This has enabled landslides triggered by those earthquakes to be mapped, photographed, entered into GIS-databases, and documented in technical reports and papers (eg Hancox et al 2003; 2004; 2010; 2011; 2013; Dellow et al 2011; Van Dissen et al 2013; Rosser et al 2015; Carey and Rosser 2015). These studies have enabled the nature and distribution of coseismic landslides to be mapped with more accuracy than was previously possible. In addition, a detailed retrospective study of landslides triggered by the M_w7.1 Inangahua earthquake of 24 May 1968 was recently completed by GNS Science using 1968 and 1974 aerial photos (Hancox et al 2014; Parker et al 2015). This new landslide dataset comprises 1,400 landslides larger than 2,500m^2 (~50 x 50m), of which 1,154 (82%) are first-time failures, and 246 (18%) are reactivations or enlargements of landslides caused by the 1929 Murchison earthquake. The study determined and analysed relationships between landslides and topography, geology and seismicity, and allowed detailed documentation of the types and effects of the landslides.

The main (maximum concentration) and total areas over which landslides occurred during the Inangahua earthquake are plotted on an area-magnitude graph in figure A.2, along with other historical earthquakes and six major earthquakes that have caused significant landsliding in New Zealand from 2003–2014 (from Hancox et al 2002; 2014).

Figure A.2 Area - magnitude graph showing the relationship of the main and total areas affected by landslides during the 1968 Inangahua earthquake determined in this study (pink), compared with historical New Zealand earthquakes (Hancox et al 2002; 2004), overseas data (Keefer 1984), and six recent New Zealand earthquakes that have caused significant landsliding since 2003 in Fiordland 2003 and 2009, Lake Rotoehu 2004, Christchurch 2011, Lake Grassmere 2013 and Eketahuna 2014.

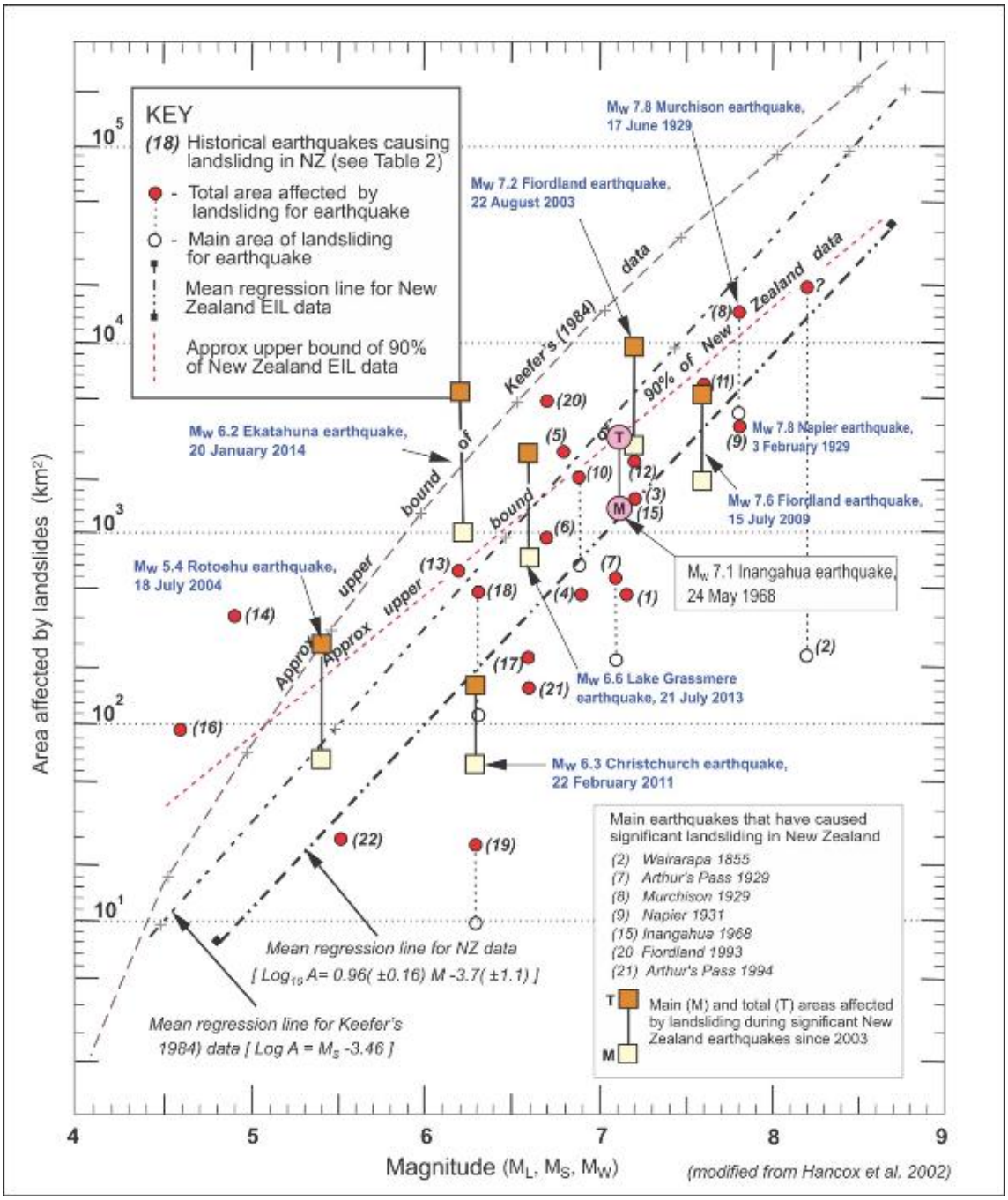

Source: Hancox et al (2014)

Landslide frequency, density and areas affected: The main and total areas of landsliding (1,250 and 3,500km^2 respectively) established for the Inangahua earthquake in the 2014 study is only slightly higher than the previous estimates of 950 and 3,200km^2 (Hancox et al 1997; 2002). However, landslide locations, sizes (m^2), numbers and densities of landsliding were established with greater accuracy. As shown in

figure A.2, the area affected by landsliding during the Inangahua earthquake is slightly above the area–magnitude mean regression line for New Zealand earthquakes, but slightly below the mean regression line for worldwide earthquake data. This is likely to be due to differences in local geology, topography, along with seismogenic and climatic factors.

During some recent earthquakes, however, larger areas have been affected by landsliding than during the Inangahua earthquake (Hancox et al 2014). As shown in table A.2, landslides triggered by the Fiordland earthquakes in 2003 and 2009, Lake Grassmere in 2013, and Eketahuna in 2014 were smaller in size, number and density compared with the Inangahua 1968 and Murchison 1929 earthquakes. This suggests that, although the area affected by landslides is often used to compare landsliding caused by different earthquakes, it may not be the best means of assessing and comparing the extent and severity of the landsliding. The number (frequency), size and density of landslides provides a better measures of the severity of coseismic landsliding, and their potential to damage property and infrastructure, or cause loss of life. In this context the 1929 Murchison and 1968 Inangahua earthquakes are the most significant historical earthquakes that have occurred in New Zealand. [Note: This may seem like common sense, but compared with the 'areas affected by landslides', data on the frequency, density and size of landslides has been less often reported than it perhaps should be.]

Table A.2 Characteristics of landslides triggered by the Inangahua earthquake compared with the 1929 Murchison earthquake and earthquakes that have caused significant landsliding since 2003.

Landslide characteristics	Earthquake					
	Inangahua 1968[a] (M_W7.1)	**Murchison 1929[b], [g] (M_W7.7)**	**Fiordland 2003[c] (M_W7.2)**	**Fiordland 2009[d] (M_W7.6)**	**Lake Grassmere 2013[e] (M_W6.6)**	**Eketahuna 2014 (M_W6.3)**
Landslide numbers by size (m^3)						
• Very small (~1–10^3)[a]	Many[a]	*[h]	354	178	270	89
• Small (~10^3–10^4)	37	*[h]	53	50	88	21
• Moderate (~10^4–10^5)	1,062	*[h]	4	13	0	4
• Large (10^5–10^6)	283	*[h]	11	0	0	1
• Very large (≥10^6)	18	~50º or >[h]	0	0	0	0
Total number of landslides	1,400	10,000 or[h]>	422	241	358	113
Main area affected by landslides (km^2)	1,250	~4,500	3,000	2,000	~750	1,000
Total area affected by landslides (km^2)	3,500	~15,000	10,000	5,600	~3,000[f]	5,500
Density (landslides/100km^2) in main (M) and/or total (T) areas	40[T]–92[M]	~200–300[M]	4.2[T]	4.3[T]	12[T]	2[M]

Notes: [a]Hancox et al 2014. Landslides smaller than 50 x 50m (~2,500m^2) were not mapped in the 2014 study, but many landslides of ~1,000m^3 or less were observed by the author in 1968–69.[M,T] Main and total areas affected by landslides. [b]Hancox et al 2002, [c]Hancox et al 2003; [d]Hancox et al 2010; 2014 [e]Van Dissen et al 2013; [f]Rosser et al 2015; [g]Pearce and O'Loughlin 1985; [h]The numbers and density of landslides triggered by the 1929 earthquake is currently being determined (Hancox et al in prep).

Source: Hancox et al (2014)

A3 Lessons learned from coseismic landsliding in New Zealand

This section documents the lessons learned (knowledge obtained) from slope failures in past earthquakes for cut slope design, and observations on slope performance, including:

- occurrence and distribution of slope failures with respect to MM intensities and ground motions, natural and cut slopes, slope angle (gradient) and the earthquake fault plane
- slope failure mechanism (coherent or disaggregated; shallow or deep-seated; defect-controlled or rock mass failures; location of failure on slope (top, middle or lower slope)
- sizes of slope failures and consequences to infrastructure and buildings
- influence of ground condition, topographic effects and seismogenic factors.

A3.1 Occurrence of slope failures

As shown by Keefer (1984; 2002) earthquakes trigger landslides when the shaking intensity is strong enough for slope failure to occur when combined with unfavourable site conditions (eg steep slopes and weak rocks and soils). In New Zealand, Hancox et al (1997; 2002) have shown that very small landslides can occur during M5 earthquakes, but significant landsliding occurs only at M6 events or greater (annex B.1). Most widespread landsliding (mainly disrupted slides or falls of rock and soil) have been caused by shallow (<~30km) earthquakes of M6.2–8.2. The minimum MM intensity threshold for landsliding is MM6, while the most common intensities for significant landsliding were MM7 and MM8 (pga ~0.1–0.5g). The largest landslides (10^6–$10^8 m^3$) invariably occur on steep to very steep slopes (35º–60º or >) more than ~50–100m high at intensities of MM9–10 (Dowrick et al 2008) with PGAs of ~0.35–1.0g or greater (annex B.1). Escarpments and coastal cliffs in Tertiary sedimentary rocks (figures A.3, A.4 and A.5), volcanic rocks (figures A.6 and A,7), and high mountain ridges (figures A.8 and A.9) have been shown to be particularly vulnerable to landsliding during historical earthquakes in New Zealand.

Figure A.3 During the 1968 Inangahua earthquake extensive large rock falls occurred on the Tertiary limestone escarpment within the MM9 isoseismal 5km west of Inangahua

Photo: DL Homer (1968)

Figure A.4 The Matiri Valley was extensively damaged by landslides during the 1929 Murchison earthquake. The scars of rock falls from Tertiary limestone cliffs bordering the 'Thousand Acres Plateau' (foreground) and many other landslides within the MM10 isoseismal are still visible today

Photo: DL Homer (1993)

Figure A.5 This very large (~33Mm^3) rotational landslide in Tertiary mudstone on the coastal cliffs near the Mohaka River mouth in Hawke's Bay, occurred during the 1931 Napier earthquake within the MM9 isoseismal. The toe of the slide debris, which is 300–400m wide and extends about 1.3km along the coast, originally pushed 200–300m out into the sea, but it has since been cut back by wave action

Photo: DL Homer (1995)

Figure A.6 The February 2011 Christchurch earthquake triggered extensive falls of volcanic rocks on the 60m high cliff behind Redcliffs School (a former quarry site, right) and nearby houses. Two of the five fatalities due to coseismic rock falls occurred in two houses (RF, bottom centre). Although these fatal slope failures were relatively small (~10–100m³) they were highly hazardous because of the proximity of the houses. The shaking intensity on the cliff and ridge crest in this area is estimated to have been MM8 to MM9, with a PGA of greater than 0.4g.

Figure A.7 Houses at the foot of the old sea cliff at Redcliifs were damaged by rock falls, and houses at the top of the cliff were damaged by ground cracking *(C)* during the 22 February mainshock and were undermined during subsequent cliff collapses during aftershocks. Two houses *(H1, H2*), had to be demolished at this site.

Figure A.8 The Lake Stanley rock avalanche (18Mm³) in Palaeozoic conglomerate and volcanics is one of several very large rock avalanches and landslide dammed lakes formed during the 1929 Murchison earthquake, and is located in the Tasman Mountains ~90km north of the epicentre within the MM9 isoseismal. The avalanche had a runout of ~2km and a vertical fall of about 800m from the top of the head scarp to the valley floor.

Figure A.9 During the 1968 Inangahua earthquake a ~5Mm³ rock avalanche of weathered granite occurred in the Buller Gorge within the MM10 isoseismal. Landslide debris dammed the Buller River for a day between Inangahua and Murchison, and the road through the Buller gorge (SH6) was severely damaged (see figure A.10). Boulders and wind blast damaged vegetation up to 50m above road level.

Photo: GNS Science (1975)

Figure A.10 The toe of the very large rock avalanche that dammed the Buller River and ran upslope 50m above SH6, causing severe damage to a 400m length of the highway. This photo shows the remains of the landslide dam and lake a few hours after the dam was overtopped and breached.

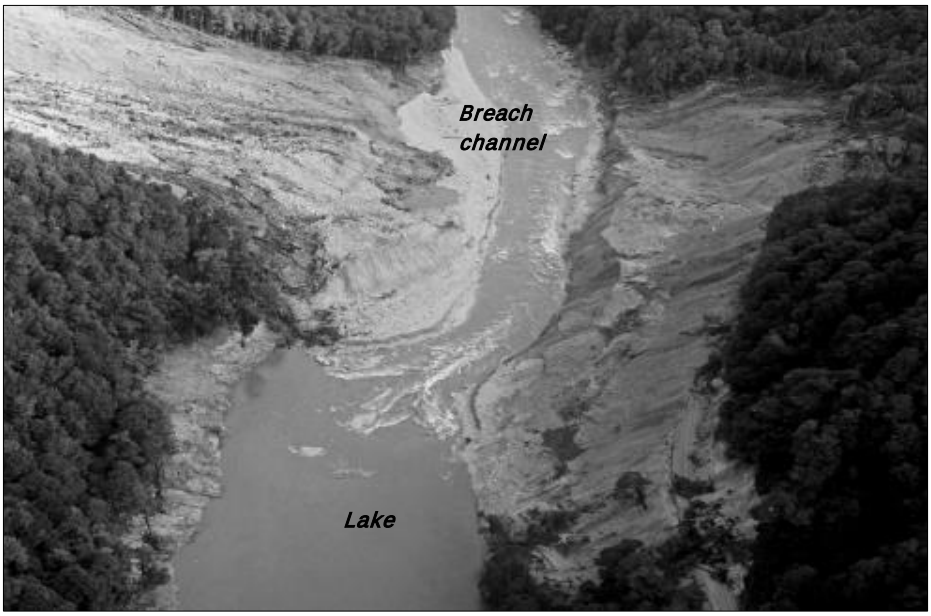

Photo: DL Homer (1968)

Landslides during earthquakes in New Zealand show a strong correlation between rock types and slope gradient. Failures in closely jointed rocks such as greywacke occur on moderate to steep slopes (25–45º or >), while landslides in Tertiary sandstone and mudstone occur on gentle to steep (10–40º) slopes, and on limestone cliffs and escarpments (figure A.3). These aspects are discussed below.

A3.1.1 Coseismic landslides on cut slopes

Studies of historical coseismic landsliding in New Zealand have shown that strong earthquake shaking (MM 6 or >) often causes landslides on steep, unsupported cuts >3m high along roads and railway lines, often causing road closures and disruption of transport. Landslides on road cuts and steep slopes above and below roads have caused significant damage to highways during a number of large earthquakes in New Zealand such as Murchison 1929, Napier 1931, Masterson June 1942, and Inangahua 1968 (table A.1). Of these events, the most severe landslide damage to main roads and railway lines is believed to have been caused by the Murchison and Inangahua earthquakes, as described below.

The newly re-constructed SH6 through the upper Buller Gorge was severely damaged and closed by cut slope failures in more than 50 places, either buried by landslide debris, or drop-outs where sections of the road had slumped into the gorge (figures A.11, A.12, A.13, A.14, A.15 and A.16. The upper gorge road was closed for 10 weeks, and the lower gorge road and Inangahua-Westport railway line was closed for three weeks (Douglas 1969; Duckworth 1969; Hancox et al 2014). Landslides triggered by the 1929 Murchison earthquake also completely buried parts of the road in the Buller Gorge. Slip damage closed the Buller Gorge road between Westport and Reefton for 18 months after the 1929 earthquake. Because of extensive rockfalls and the complete destruction of parts of the road in the Lyell creek area (figure A.16), the road between Murchison and Inangahua was not reopened to wheeled vehicles until 29 April 1931, almost two years after the earthquake (Henderson 1937). Figures A.11 to A.16 illustrate that landslide damage caused by the Murchison and Inangahua earthquakes was more severe than other New Zealand earthquakes, particularly to roads and cut slopes.

Figure A.11 The Inangahua earthquake triggered this large (~120m wide) rotational slide and earth flow in Tertiary mudstone which closed SH6 at Walker Flat 5km west of Inangahua and almost hit a farm house. The failure occurred where the toe of the slope had been cut back *(c)* to widen the road.

Photo: DL Homer (1968)

Figure A.12 This ~3Mm³ rotational landslide in mudstone was triggered by the Inangahua earthquake within the MM10 isoseismal 10km northeast of Inangahua, burying or carrying away a 200m length of SH6.

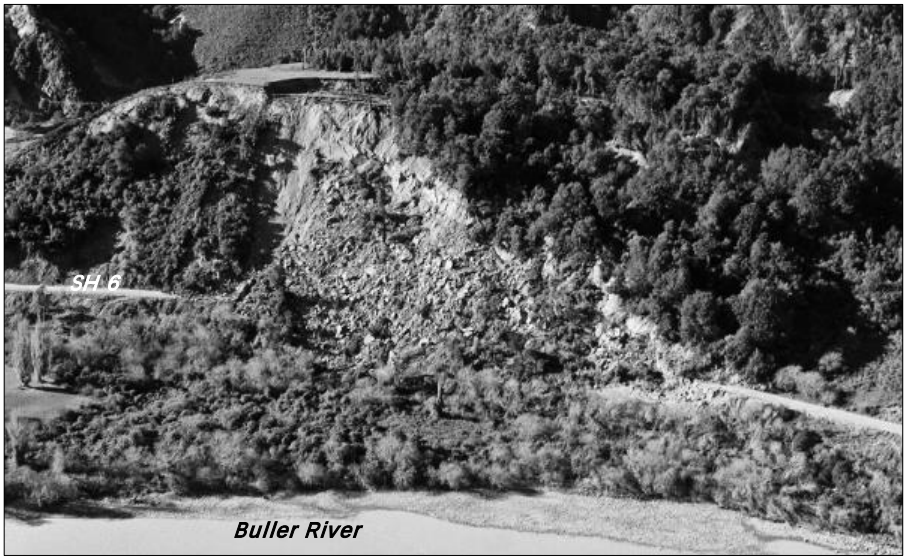

Figure A.13 Rock falls *(rf)* and debris slides *(ds)* from road cuts and bluffs of Tertiary limestone during the Inangahua earthquake buried SH6 for a length of about 1km along the Buller River at White Cliffs, 4km northwest of Inangahua, causing that section of the highway to be relocated well out from the base of the cliffs.

Figure A.14 One of the many steep unsupported SH6 road cuts in the upper Buller Gorge which were badly damaged by rock and debris falls during the Inangahua earthquake. In this photo much of the rock fall debris has been cleared away, allowing the highway to be re-opened to one-lane traffic 10 weeks after the earthquake.

Figure A.15 Multiple debris falls and slides *(dfs)* occurred on the many of the recently-constructed road cuts in the upper Buller Gorge during the Inangahua earthquake. The upper gorge road was also extensively damaged by rock and debris falls during the 1929 Murchison earthquake (see figure A.16).

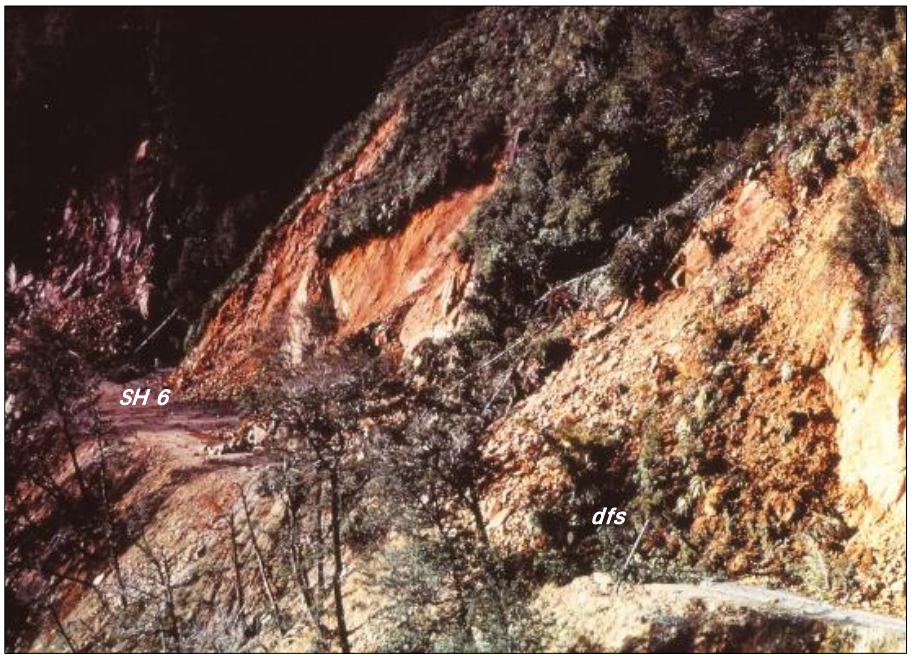

Figure A.16 Extensive rock falls triggered by the 1929 Murchison earthquake completely buried parts of the road in the upper Buller Gorge. Below, the extensive rock falls that covered the gorge road near Lyell Creek.

Photo source: GNS collection

The Wellington City area was very strongly shaken (MM 9) by the 1855 Wairarapa earthquake, resulting in many landslides that affected local roads and a large failure (Gold's Slide) on the Hutt Road (figure A.17). The steep cut slopes constructed since that time along SH1 (figure A.18) and SH2, however, have not been subjected to a large earthquake and were not designed to withstand such an event. An earthquake (~M7.5

or >) on the Wellington fault will probably result in large failures on cut slopes that will damage and close the main roads and railway lines in and out of Wellington city (Brabhaharan et al 1994; Kingsbury and Hastie 1995).

Figure A.17 'Gold's Landslide' (~300,000m³) on the Hutt Road (SH2), which was triggered by the 1855 Wairarapa earthquake, illustrates the potential for similar failures to occur during a Wellington fault earthquake.

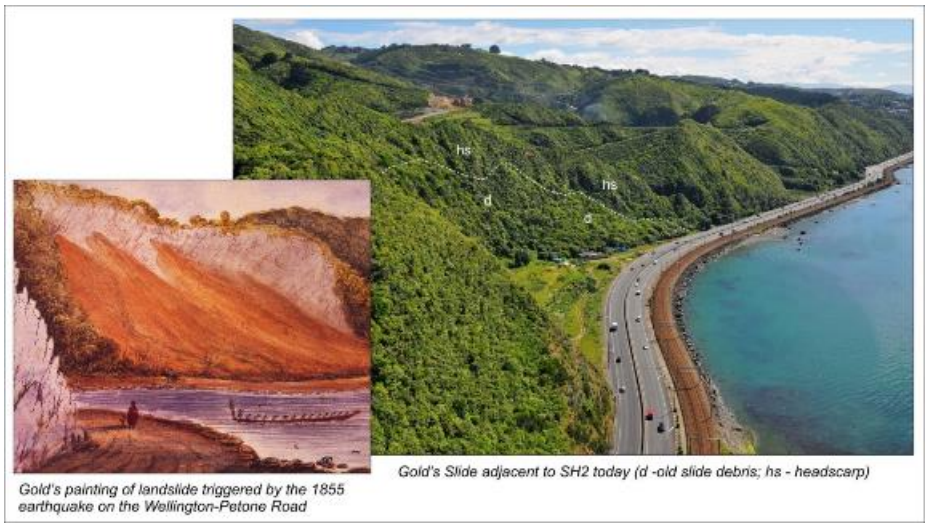

Figure A.18 The steep (60–65°) 60m cut slopes along SH1 in the Ngauranga Gorge (bottom right) are believed to be vulnerable to landsliding during a Wellington fault earthquake (MM9–10,with PGAs of ~0.5 to 1.0g or >). These cuts have not been tested by a large earthquake since they were constructed in the 1950s.

A3.1.2 Coseismic landslides in relation to slope angle

Several studies have shown that slope angle (hillslope gradient) has a significant effect on the stability of slopes, with increased likelihood of failure on steeper slopes during strong earthquake shaking (Keefer 1984; 2000; Hancox et al 1997; 2002; Dai et al 2011). Relationships determined from previous studies of earthquake-induced landslides in New Zealand (Brabhaharan et al 1994; Hancox et al 1997; 2002) were used by Hancox et al (2014) to develop a simple landslide susceptibility model based on slope angle,

slope type and geology). This includes data from a GIS analysis of slope angle in relation to landslides triggered by the Inangahua earthquake (figures A.19, A.20 and A.21), along with the other historical New Zealand earthquakes listed in table A.1

Table A.3 Slope angle and earthquake-induced landslide susceptibility classes in New Zealand.

Slope class	Slope angle (failure %)[a]	Landslide susceptibility	Slope types and characteristics[b]
Low	< 25º (~10%)	Low	Very low to gentle slopes (0–25º) with few landslides; dip-slope slides in Tertiary mudstone and sandstone, and falls on steep gravel banks and terrace edges along rivers in low-lying areas of Quaternary and recent alluvium.
Moderate	25–35º (~30%)	Moderate	Moderate slopes (25–35º). Includes dip slope failures in Tertiary rocks (as above); and debris and rock falls in hard rocks (greywacke, schist, granite etc), especially in gullies and stream channels of hill country.
Moderate to steep	35–45º (~40%)	High	Moderate to steep slopes (35–45º). Steep dip slopes, escarpments, cliffs, and gorges in Tertiary rocks and older hard rocks (greywacke, schist, granites etc) especially in steep hilly, mountainous, and glaciated terrain.
Steep	45–60º (~15%)	Very high	Steep to very steep slopes (45–60º or >), mainly on cliffs, escarpments, headscarps of pre-existing landslides, and high steep, unsupported road cuts and other excavations. Road cut failures are most common in this slope range, but slopes >60º are poorly detected by the 10m DEM based on 20m topographic contours.
Very steep	>60º (~5%)		

Notes:

[a] Slope ranges and failure percentages based on historical New Zealand earthquake-induced landslide data (Hancox et al 2002).

[b] Slope failure percentages and descriptions apply mainly to natural slopes and do not take into account the many smaller falls and slides that occur on steep unsupported road cuts and excavations during strong earthquakes, most of which are under-represented in this model because they are not detected by DEMs based on 1:50,000 topographic maps.

Figure A.19 shows landslides triggered by the Inangahua earthquake in the upper Buller Gorge plotted on a slope angle/landslide susceptibility map derived in GIS by Hancox et al (2014) using the model defined in table A.3, and a 10m digital elevation model (DEM) derived from the 1:50,000 topographic map. This illustrates that the source areas of landslides occur mainly on moderate to steep (35–45º) and steep (45–60º) slopes, with debris runout and deposition zones generally on low to moderate angle slopes (< 25º). Few landslides are mapped on very steep slopes (>60º). This is largely because natural and man-made slopes (road and railway line cuts etc) steeper than 60º could not readily be differentiated by the DEM derived from 20m topographic contours. GIS analysis of the source areas of landslides triggered by the Inangahua earthquake allowed Hancox et al (2014) to determine the percentage frequency of landslides in different slope angle classes for the mean and maximum slope angles across the area in which landslides occurred (figures A.20 and A.21).

Figure A.19 Landslides triggered by the Inangahua earthquake in the upper Buller Gorge (the area of highest landslide density ~15km southeast of the epicentre) plotted on a slope angle and landslide susceptibility map. Most of the failures (78%) were on moderate to steep (25–45º) slopes.

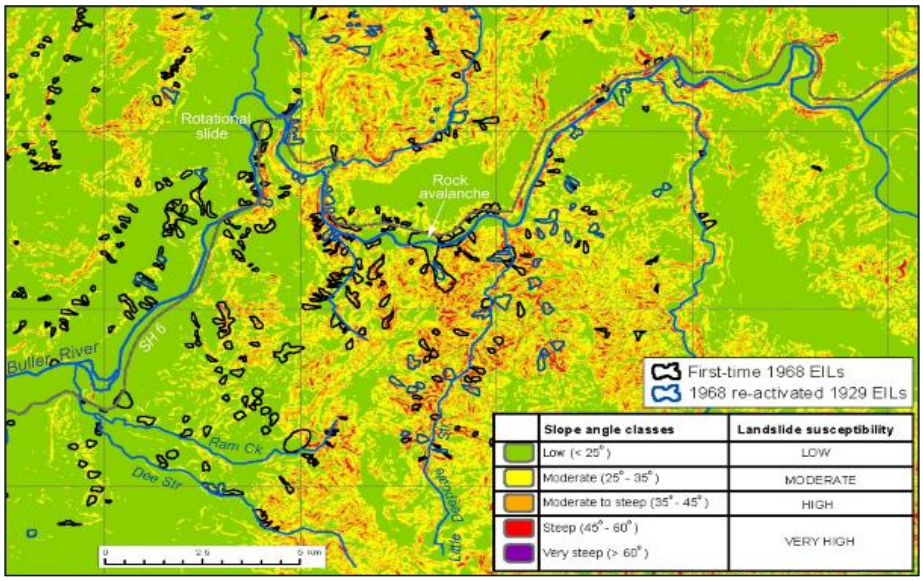

Source: Hancox et al (2014)

Figure A.20 Graphs showing landslide frequency (%) in relation to mean and maximum slope angles in the source areas of landslides triggered by the Inangahua earthquake, slope angle frequency and the slope angle/landslide susceptibility classes.

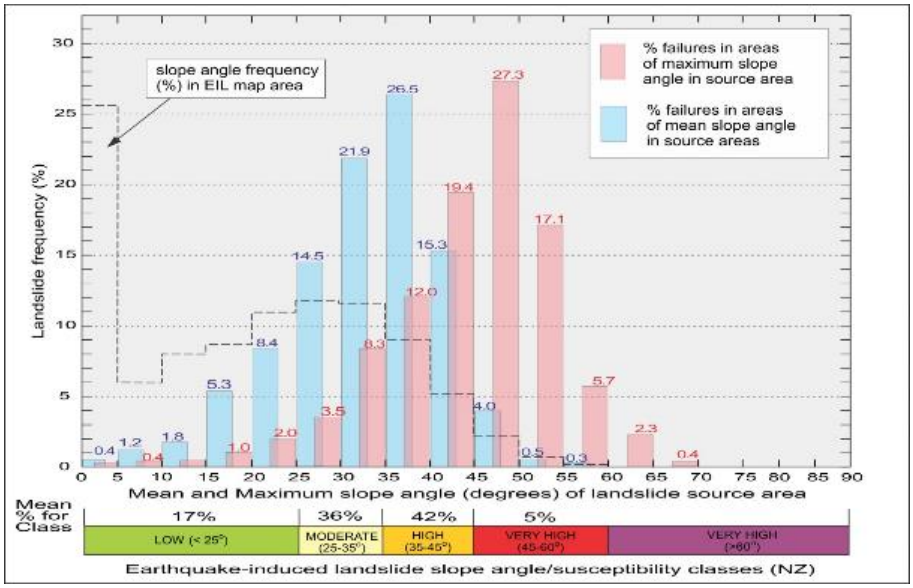

Source: Hancox et al (2014)

As illustrated in figure A.20, the frequency of landslides triggered by the Inangahua earthquake increases with slope angle, with a maximum frequency of ~64% between 30–45º for the average slope angle in the landslide source areas, and 40–55º for the maximum slope angle. As expected, there are fewer landslides (~17%) on lower-gradient slopes (< 25º). However, the graphs also show that few failures (5%) occur on slopes steeper than 60–70º. Field observations suggest that many slopes steeper than 60–70º within the study area, including the road cuts in the Upper Buller Gorge, and particularly the Tertiary limestone

escarpments, such as White Cliffs west of Inangahua (figure A.3), are not identified by the DEM used in the analysis.

These findings are generally consistent with landslide frequency/slope gradient relationships determined in overseas studies of coseismic landsliding (Jibson et al 2000; Keefer 1984; 2002; Dai and Lee 2002; Dai et al 2011; Lin et al 2008; Qi et al 2010), as well as those in New Zealand (Hancox et al 1997; 2002; 2003; 2011; Dellow et al 2011). The landslide frequency/slope angle correlations derived for the Inangahua earthquake are also consistent with slope angle and landslide susceptibility models developed from historical earthquake-induced landslide data in New Zealand (table A.3 and figure A.20).

A3.1.3 Relationship of landsliding to the earthquake fault plane

Past studies of landsliding during historical earthquakes in New Zealand have shown that there is seldom a clear correlation between landslide occurrence and ground surface fault rupture, possibly because the faulting was of limited extent, affected low-lying alluvial terrain that was less susceptible to landsliding, or was of a secondary nature (Hancox et al 1997; 2002). However, these studies found a strong correlation between landsliding and the underlying fault rupture zone indicated by aftershocks, as shown by the 1929 Murchison, 1968 Inangahua, 1990 Weber and 1994 Arthur's Pass earthquakes. This association suggests that in some earthquakes landslide distribution may provide a general indication of the epicentre location and extent of the fault rupture zone of the earthquake.

The association between landslide occurrence and the underlying earthquake fault plane was confirmed by the recent study of the Inangahua earthquake by Hancox et al (2014). The results of the 2014 study showed that landslide distribution during the 1968 earthquake had a strong correlation with the main area of aftershocks and the 30km-long subsurface seismogenic fault plane modelled by Anderson et al (1994), which had at least 4m reverse fault slip and dips 45º northwest under the Inangahua Valley. The 1968 coseismic landslides were mostly concentrated on the hanging wall of the fault plane, and mainly to the west and north of Inangahua. Of the 1,400 landslides that were mapped, 1,154 (82%) of the failures (~92/100km^2) occurred in the main area of landsliding close to the epicentre, the main area of aftershocks, and the underlying seismogenic fault plane (figure A.21).

There is also strong evidence that most large coseismic landslides tend to be located on the hanging (upthrown) wall of reverse fault earthquakes (Abrahamson and Somerville 1996; Hancox et al 2002), where seismic shaking can be up to 50% stronger at short periods than outside the uplifted area. However, allowance must also be made for topographic effects on high ridges and cliffs, which are more susceptible to landsliding during earthquakes because of topographic amplification of ground shaking, as was shown by the landsliding and ground motions recorded during the 22 February 2011 Christchurch earthquake (Dellow et al 2011; Kaiser et al 2013).

Figure A.21 Map showing the distribution of landslides and liquefaction effects that occurred during the 1968 Inangahua earthquake in relation to the earthquake epicentre, the distribution of aftershocks, MM isoseismals, and the underlying seismogenic fault plane.

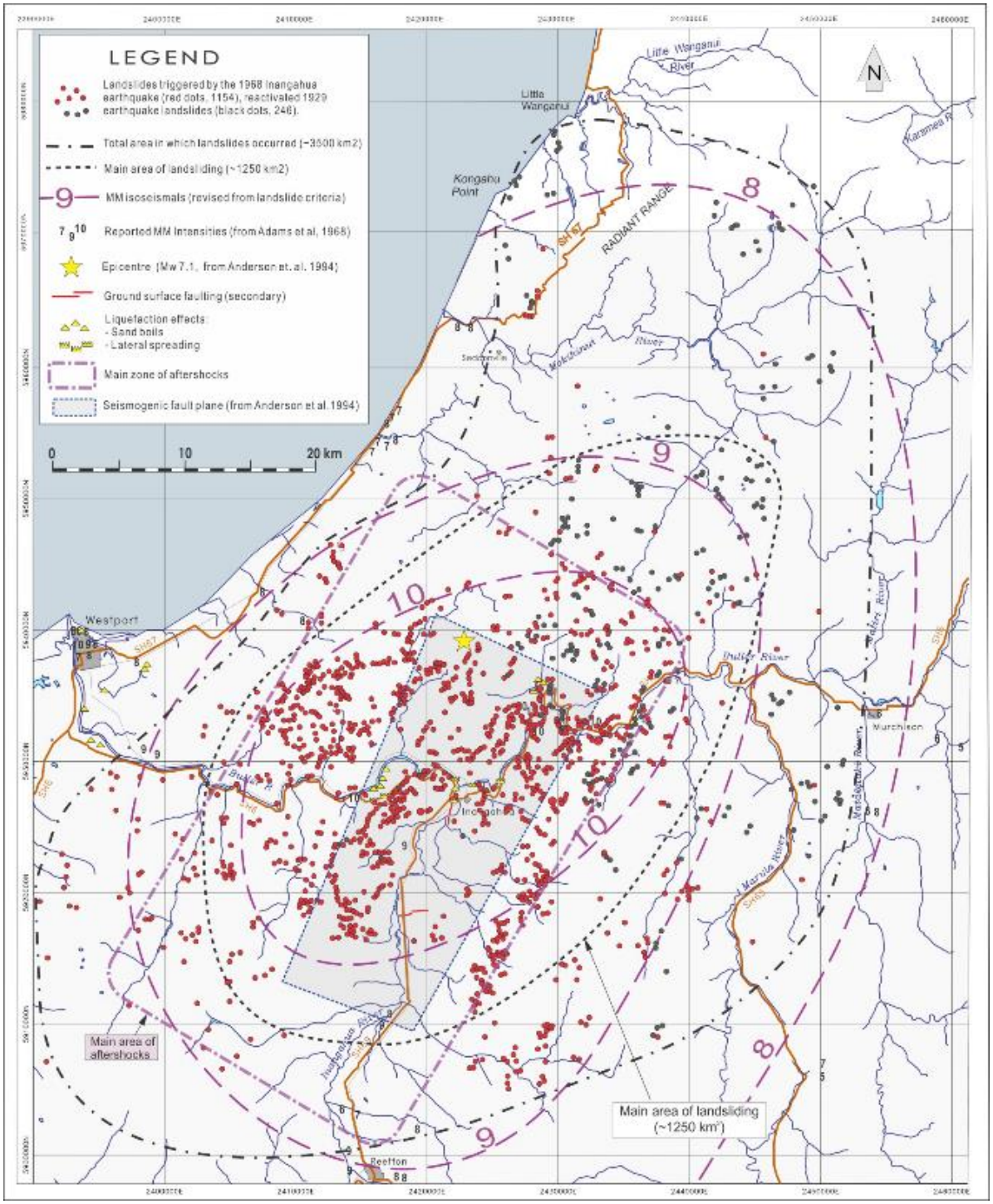

Source: Hancox et al (2014)

A3.2 Slope failure mechanisms

It is widely known that strong earthquake shaking can cause landslides in several ways (Keefer 1984; Crozier 1986, Hancox et al 1997). For example, horizontal and vertical ground accelerations (PGA) during earthquakes can temporarily increase the effective slope gradient (angle) and gravitational shear stresses within a slope; the strength of slope materials can be decreased due to a reduction in the inter-granular bonding and frictional resistance on joints, bedding planes and other rock defects; and cyclic loading during earthquakes can cause increased pore water pressures in slope materials, which results in strength loss within a rock mass, and possibly liquefaction in fine sands and silts.

Landslides are often classified into different types based on the materials involved and the mode of slope movement (Cruden and Varnes 1996; Hungr et al 2014), and typically include rock falls, rock slides, soil and debris falls, slides, and debris flows (annex A.1).

In a pioneering study of world-wide earthquakes Keefer (1984) grouped landslides into three broad categories: disrupted slides and falls, coherent slides, and lateral spread and flows:

- *Disrupted landslides* include rock and debris falls and slides, and rock avalanches, in which the slope movement is generally rapid with significant internal disruption, and often involving long run-out of debris.
- *Coherent landslides* involve rock, debris, and slumps and rotational slides, in which the movement is typically slow with little internal disruption and small displacements (< 2m), and often involving open cracking on the ground surface. Observations in New Zealand suggest that coherent landslides typically occur on slopes of fine, cohesive soils in areas of Tertiary mudstone (eg 2013 Cook Strait earthquake, 2014 Eketahuna earthquake) and also weathered volcanic tephra deposits (eg 1987 Edgecumbe earthquake). Typical slope and ridge crest cracking associated with incipient coherent landslides that occurred during the 1987 and 2013 earthquakes is illustrated in figures A.24 and A.25.
- *Lateral spreads and flows* occur in soils (earth and debris) and involve translational movements of relatively intact material along a subsurface liquefied zone. Such landslides are usually the result of soil liquefaction in saturated sands, gravels, or silts. Displacements are typically less than 2m, but can be large flow-type failures, with high levels of internal disruption.

In his study of 40 world-wide earthquakes Keefer (1984) found that disrupted landslides comprise about 86% of all the landslides reported, coherent slides comprised 8% and lateral spreads 6%. Similar results were reported by Hancox et al (1997; 2002; 2014) who found that most historical coseismic landslides in New Zealand were small (<1,000m^3) disrupted falls and slides of rock and soil. For such landslides the most common failure mechanism often involves planar (translational) sliding on the soil or regolith/bedrock interface, bedding planes, joint surfaces, crush zones, shear zones, and fault zones.

Figure A.22 shows multiple debris slides in weathered granite which occurred during the Inangahua earthquake in the upper Buller Gorge. Typical rock falls triggered by the 2011 Christchurch earthquake are shown in figures A.6 and A.7, and figure A.23 shows joint controlled rock falls of granite which occurred on many SH6 road cuts during the Inangahua earthquake. Other types of disrupted landslides are shown in figures A.6 to A.9 and A.12 to A.16.

Figure A.22 Multiple shallow debris slides occurred in weathered granite in the upper Buller Gorge during the 1968 Inangahua earthquake.

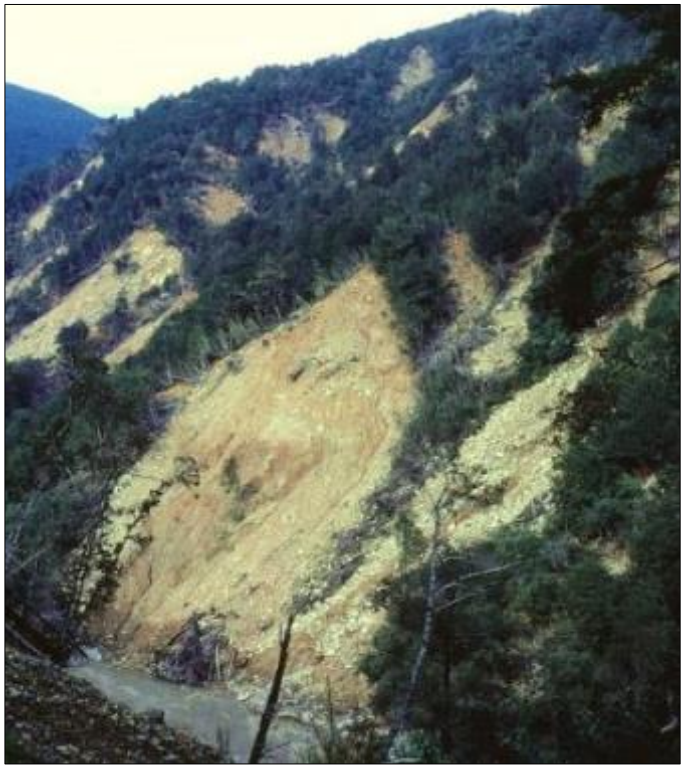

Figure A.23 Joint-controlled rock falls in weathered granite damaged many SH6 road cuts in the upper Buller Gorge during the 1968 Inangahua earthquake. In this photo most of the rock fall debris that initially blocked the road has been cleared away, but the cut slope is still highly vulnerable to further rock falls.

Fewer coherent landslides have been identified during coseismic landslide reconnaissance studies in New Zealand. This may be because open cracks on slopes are more difficult to recognise as a coherent landslide. Ridge crest cracking was noted after the 1987 Edgecumbe earthquake and similar features were mapped following the 2013 Cook Strait and Lake Grassmere earthquakes, and the 2014 Eketahuna earthquake. Figure A.24 shows ridge crest cracking associated with an incipient coherent landslide that developed on the hills west of the Tarawera River during the Edgecumbe earthquake. Figure A.25 shows similar slope cracking that occurred during the 2013 Lake Grassmere earthquake. Typical coherent landslides (partly developed rotational slides) in Tertiary mudstone are illustrated in figures A.26 and A.27.

Figure A.24 Typical ridge crest cracking (incipient coherent landslide) formed in cohesive soils (weathered tephra deposits) on hills during the 1987 Edgecumbe earthquake.

Photo: DL Homer (1987)

Figure A.25 Slope crest cracking (incipient coherent landslide) which occurred in the Ward area during the 2013 Lake Grassmere earthquake.

Photo: D Townsend (2013)

Figure A.26 Typical coherent landslide: ~100,000m³ rotational slide in mudstone which occurred on the 100m high cliffs 1km west of Cape Campbell during the 2013 Cook Strait earthquake.

Photo: GT Hancox (2013)

Figure A.27 Google Earth image (2004) of a very large (~30Mm³) partly-developed rotational (coherent) landslide in Tertiary mudstone on the ~150–250m high cliffs at Cape Turnagain on the Wairarapa coast. This landslide may have occurred in 1855 and was reactivated during the 1904 Cape Turnagain earthquake.

A3.3 Size of failures and consequences to infrastructure and buildings

A3.3.1 Size of slope failures

Previous studies of earthquake-induced landslides in New Zealand (Hancox et al 1997; 2002; Dowrick et al 2008) have shown that the size of coseismic landslides varies considerably with topography, geology and the strength of earthquake shaking. The size and nature of slope failures that occur at different shaking intensities are summarised in table A.4.

Table A.4 Landslides and environmental effects in the New Zealand (2008) MM intensity scale for intensities MM5 to MM10.

MM5	▪ Loose boulders may occasionally be dislodged from steep slopes.
MM6	▪ Trees and bushes shake, or are heard to rustle. ▪ Loose material may be dislodged from sloping ground, e.g. existing slides, talus and scree slopes. ▪ A few very small ($\leq 10^3$ m^3) soil and regolith slides and rock falls from steep banks and cuts. ▪ A few minor cases of liquefaction (sand boil) in highly susceptible alluvial and estuarine deposits.
MM7	▪ Water made turbid by stirred up mud. ▪ Small slides such as falls of sand and gravel banks, and small rock-falls from steep slopes and cuttings common. ▪ Instances of settlement of unconsolidated, or wet, or weak soils. ▪ A few instances of liquefaction (i.e. small water and sand ejections). ▪ Very small ($\leq 10^3$ m^3) disrupted soil slides and falls of sand and gravel banks, and small rock falls from steep slopes and cuttings are common. ▪ Fine cracking on some slopes and ridge crests. ▪ A few small to moderate landslides (10^3 –10^5 m^3), mainly rock falls on steeper slopes (>30˚) such as gorges, coastal cliffs, road cuts and excavations. ▪ Small discontinuous areas of minor shallow sliding and mobilisation of scree slopes in places. ▪ Minor to widespread small failures in road cuts in more susceptible materials. ▪ A few instances of non-damaging liquefaction (small water and sand ejections) in alluvium.
MM8	▪ Cracks appear on steep slopes and in wet ground. ▪ Significant landsliding likely in susceptible areas. ▪ Small to moderate (10^3-10^5 m^3) slides widespread; many rock and disrupted soil falls on steeper slopes (steep banks, terrace edges, gorges, cliffs, cuts etc.). ▪ Significant areas of shallow regolith landsliding, and some reactivation of scree slopes. ▪ A few large (10^5-$_6$ m^3) landslides from coastal cliffs, and possibly large to very large ($\geq 10^6$ m^3) rock slides and avalanches from steep mountain slopes. ▪ Larger landslides in narrow valleys may form small temporary landslide-dammed lakes. ▪ Roads damaged and blocked by small to moderate failures of cuts and slumping of road-edge fills. ▪ Evidence of soil liquefaction common, with small sand boils and water ejections in alluvium, and localised lateral spreading (fissuring, sand and water ejections) and settlements along banks of rivers, lakes, and canals etc. ▪ Increased instances of settlement of unconsolidated, or wet, or weak soils.
MM9	▪ Cracking of ground conspicuous. ▪ Landsliding widespread and damaging in susceptible terrain, particularly on slopes steeper than 20˚. ▪ Extensive areas of shallow regolith failures and many rock falls and disrupted rock and soil slides on moderate and steep slopes (20˚-35˚ or greater), cliffs, escarpments, gorges, and man-made cuts. ▪ Many small to large (10^3-10^6 m^3) failures of regolith and bedrock, and some very large landslides (10^6 m^3 or greater) on steep susceptible slopes. ▪ Very large failures on coastal cliffs and low-angle bedding planes in Tertiary rocks. Large rock/debris avalanches on steep mountain slopes in well-jointed greywacke and granitic rocks. Landslide-dammed lakes formed by large landslides in narrow valleys. Damage to road and rail infrastructure widespread with moderate to large failures of road cuts and slumping of roadedge fills. Small to large cut slope failures and rock falls in open mines and quarries ▪ Liquefaction effects widespread, with numerous sand boils and water ejections on alluvial plains, and extensive, potentially damaging lateral spreading (fissuring and sand ejections) along banks of rivers, lakes, canals etc.). Spreading and settlements of river stop-banks likely.
MM10	▪ Landsliding very widespread in susceptible terrain. ▪ Similar effects to MM9, but more intensive and severe, with very large rock masses displaced on steep mountain slopes and coastal cliffs. Landslide-dammed lakes formed. Many moderate to large failures of road and rail cuts and slumping of roadedge fills and embankments may cause great damage and closure of roads and railway lines. ▪ Liquefaction effects (as for MM9) widespread and severe. Lateral spreading and slumping may cause rents over large areas, causing extensive damage, particularly along river banks, and affecting bridges, wharfs, port facilities, and road and rail embankments on swampy, alluvial or estuarine areas.
Notes: *(1) "Some or "few" indicates that threshold for response has just been reached at that intensity. (2) Environmental damage (response criteria) occurs mainly on susceptible slopes and in certain materials, hence the effects described above may not occur in all places, but can be used to reflect the average or predominant level of damage or MM intensity in an area. (3) Environmental criteria not defined for MM11 and 12, as those intensities have not been reported in New Zealand. Earlier versions of the MM intensity scale suggest that environmental effects at MM11-12 are similar to MM9- 10, but are more widespread and severe. (4) This appendix is based on Hancox et al. 1997, 2002, and Dowrick et al., 2008*	

Source: Dowrick et al (2008)

As indicated in table A.4, landslides triggered by earthquakes in New Zealand range from individual boulders of less than 1m^3 at MM5 and MM6 to very large ($\geq 10^6$m^3 and greater) landslides at MM9 and MM10. In general, earthquake-induced landslides in New Zealand are larger, more often deeper-seated than landslides triggered by rainstorms, and they occur suddenly without warning over very large areas (Crozier et al 2008). Examples of some coseismic slope failures that have occurred in New Zealand in the

last 150 years have been discussed in section A2.1. Historical evidence suggests that most of the larger (10^5–10^6m^3) coseismic landslides occur on steep slopes, especially coastal cliffs of ~100m or more in height (figures A.5, A.17, A.26 and A.27), escarpments (figure A.3) and high mountain ridges (figures A.8 and A.9). Failures on cut slopes (figures A.13, A.14 and A.15) are generally smaller in size (~10^3–10^5m^3), although very large failures (10^6m^3 greater) have also occurred (figures A.12 and A.16).

A3.3.2 Consequences to infrastructure

Historically, the consequences of earthquake-induced landslides to infrastructure and buildings in New Zealand has been significant within ~20–30 km of the epicentre (in the 'near field'), causing substantial damage and often the closure of roads and railway lines for days and weeks, bringing down electricity transmission lines, and severely damaging or destroying a large number of buildings built within the runout or collapse zones of landslides (table A.1, section A3.1.). The most damaging earthquakes have been shallow (<~30 km deep) events of M6.3 or greater. Earthquakes that have caused the most landslide damage to the roading and rail infrastructure of New Zealand are: Murchison 1929 (M_w 7.8), Napier (Hawkes Bay) 1931 (M_w7.8), Wairarapa June 1942 (M_w 7.2), Inangahua 1968 (M_w 7.1), Edgecumbe 1987 (M_w 6.5), Arthurs Pass 1994 (M_w 6.7), and Christchurch 2011 (M_w 6.3).

No large (≥ M7) earthquakes have occurred in hilly metropolitan areas like Wellington, where high unsupported cut slopes have been constructed along infrastructure routes over the last 65 years. As a consequence, these slopes have not been subjected to severe earthquake shaking (MM8 or greater). Steep, high cut slopes such as those along SH1 in Ngauranga Gorge, Wellington (figure A.18) are likely to be vulnerable to landsliding during the next Wellington fault earthquake (M ~7.5, intensity MM9–10). The steep old coastal slope above SH1 and the North Island Main Trunk railway line and station at Paekakariki, where a landslide occurred during the 1855 Wairarapa earthquake (figure A.28), is likely to fail again during a strong earthquake. The coastal highway and railway line to the south between Paekakariki and Pukerua Bay is also thought to be highly vulnerable to closure by landslides during a future large earthquake in the Wellington region.

Other infrastructure routes that are considered to be vulnerable to future earthquake-induced landsliding during a Wellington fault earthquake are SH3 in the Manawatu Gorge (figure A.29), and the Rimutaka Hill road. This highway (SH2) was closed by rock falls during the 1855 and 1942 Wairarapa earthquakes, and is expected to be vulnerable to further slope failures during a future Wellington fault earthquake. Slope failure is possibly less likely at the recently reshaped Muldoon's Corner (Brabhaharan and Stewart 2015) where 45–55º batter angles and grouted rock anchors appear to have reduced batter failure potential (figure A.30). In the South Island, the next alpine fault earthquake (M_w 8.0+) is likely to cause severe (MM9–10) shaking within 50–70km of the fault over its rupture length, which is expected to cause widespread landsliding over more than ~30,000km^2 (Robinson and Davies 2013). Such landsliding is expected to cause significant damage to infrastructure in the region, especially on the West Coast (SH6) and the Arthur's Pass highway (SH73), transmission lines and the viaduct, which is built across the site of a prehistoric rock avalanche (figure A.31). Further significant slope failures can be expected to occur in this area during a future alpine fault earthquake and other large earthquakes in the region.

Figure A.28 Aerial view of the large (100,000m³) rock slide *(rs)* caused by the 1855 earthquake on the ~45°, ~200m high slope above the railway station *(RS)* and SH1 highway at Paekakariki.

Figure A.29 Large landslides triggered by rainstorms closed SH3 in the Manawatu Gorge for 3 months in 2004 (A), and at another site for 13 months in 2011 (B). A large earthquake could trigger similar landslides at a number of sites within the gorge where the steep marginally stable slopes have been cut back for road widening.

Figure A.30 Photos showing the major earthworks completed in May 2012 to ease bends at Muldoon's Corner on the Rimutaka Hill road (SH2). The cuts are up to 55m high with batters up to 55° and an overall slope of ~50°, which is steeper than the long-term angle for greywacke slopes (~40–45°). Grouted rock anchors *(ra)* are likely to have reduced the potential for coseismic batter failures in this area.

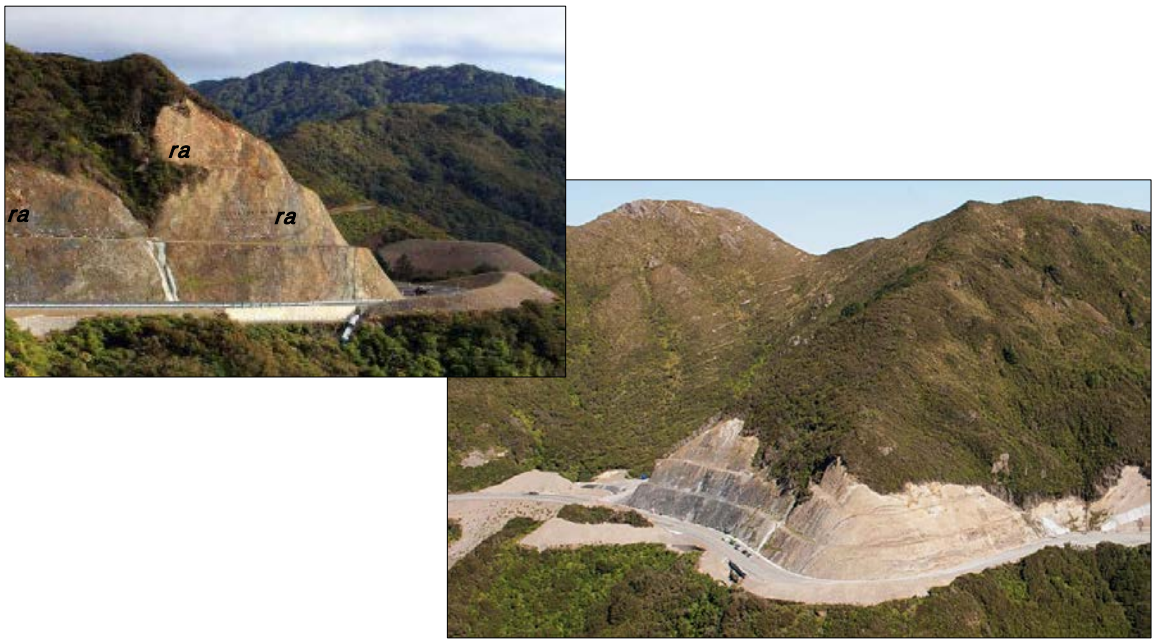

Photos: G Hancox and NZ Transport Agency

Figure A.31 Built below a prehistoric rock avalanche source area (sa) at the 'zig-zag' *(zz)* on SH73 at Arthur's Pass, the viaduct *(v)* and electricity transmission lines *(tl)* are at significant risk from another rock avalanche at this site during the next alpine fault earthquake and other large earthquakes in the region.

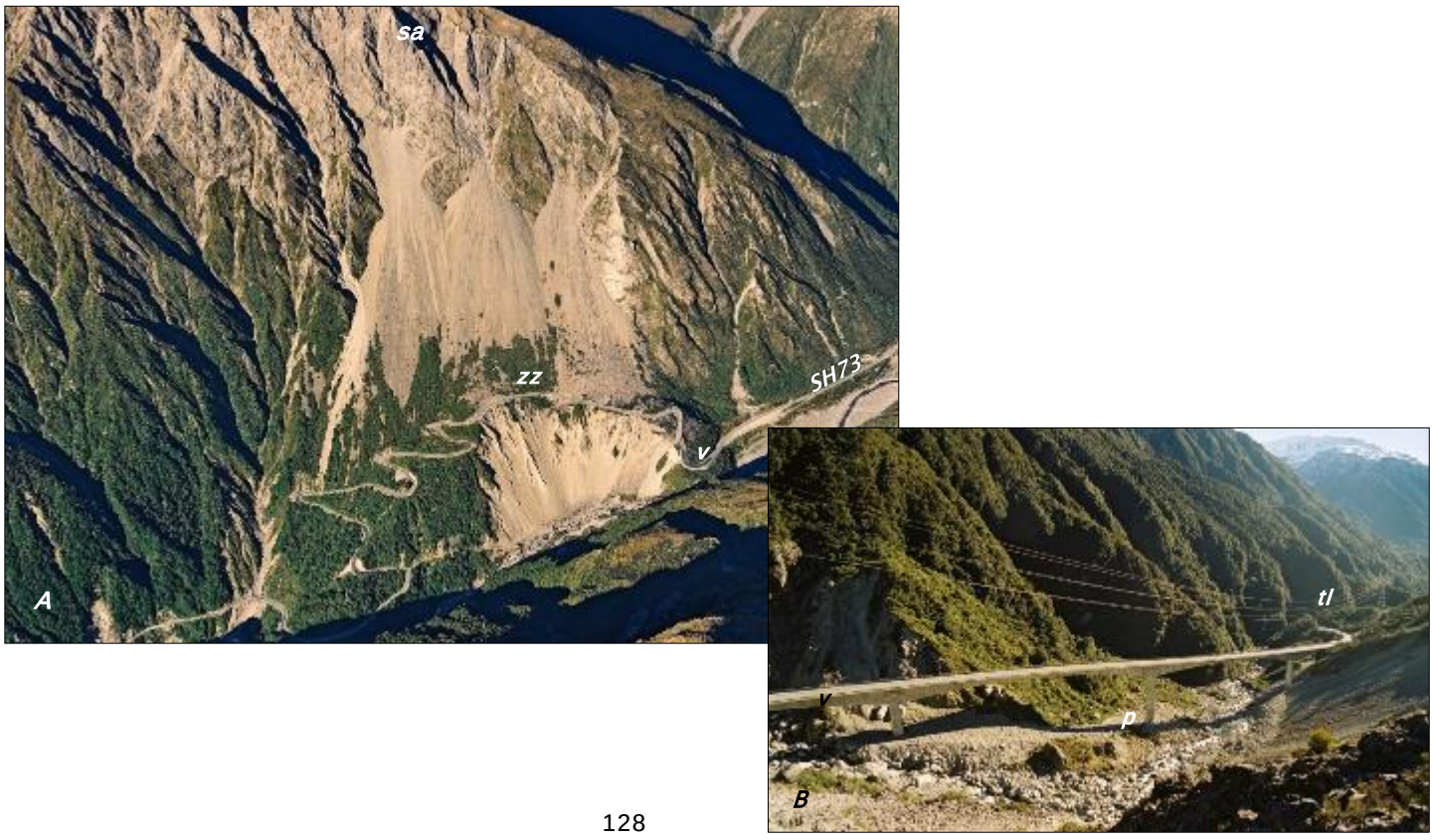

A3.3.3 Consequences to buildings

In the last 100 years, landslides triggered by three major earthquakes in New Zealand have caused considerable damage to houses in rural and urban areas and resulted in 22 known deaths:

(1) During the *1929 Murchison earthquake* landslides destroyed four farm houses and killed 14 people. The largest of these coseismic failures was the Matakitaki Landslide, a ~18 million m^3 rock-slide avalanche of Tertiary sandstone and mudstone formed on a ~35º dip-slope. The failure ran out ~1km across the Matakitaki Valley, destroying two houses and killing four people (figure A.32). One of the houses destroyed by the landslide was on the eastern side of the river, about 800m from the base of the slope that failed (figures A.32B and C).

Figure A.32 (A) Located in the Matakitaki Valley 5km south of Murchison, the Matakitaki landslide *(ML)* was triggered by the 1929 Murchison earthquake. (B) and (C) show the top story of a house *(H)* which was carried ~100m across the valley floor by the rapidly-moving slurry of rocks, mud, and water.

Photos: A) DL Homer, GNS Science, 1995; B) and C) Alexander Turnbull Library

In the Maruia Valley another farm house was destroyed and four more people died during the Murchison earthquake when ~4.5 million m^3 of Tertiary sandstone on a steep spur collapsed onto a river terrace where the house was located. The landslide mass dammed and diverted the Maruia River, which subsequently exhumed a band of hard sandstone to form the Maruia Falls. Further down valley at Ariki, another spur of Tertiary sandstone collapsed onto a terrace, destroying a house and killing two people. Both houses destroyed in the Maruia Valley were located tens of metres out from the base of the slope, but were within the runout zones of the rapidly moving mass of large sandstone blocks and trees that overwhelmed them.

Other buildings destroyed by landslides during the Murchison earthquake were at Kahurangi Point (110km north of epicentre), where a landslide destroyed the lighthouse keeper's house, and near Takaka (120km from the epicentre) a limestone cliff collapsed onto the powerhouse of the Tarakohe Cement Works. That failure destroyed the building and killed an engineer (figure A.33).

(2) *1968 Inangahua earthquake:* Another destructive and fatal rockfall occurred during the Inangahua earthquake when a rock fall from a limestone bluff destroyed a farm house and killed two of the occupants (figure A.34). These examples illustrate the high susceptibility of dip slopes, steep spurs, ridges, and high cliffs to future coseismic slope failures, and the vulnerability of houses and occupants within potential landslide runout zones below these types of slopes.

Figure A.33 The Murchison earthquake triggered a fall of large blocks (B) of Tertiary limestone on a cliff at the Tarakohe Cement Works near Takaka. The rock fall buried and destroyed the powerhouse and killed an engineer.

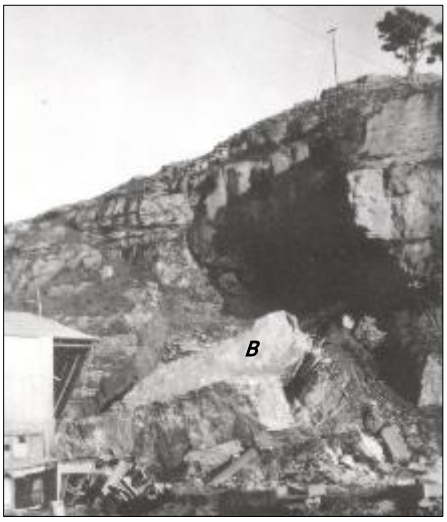

Figure A.34 (A) The 1968 Inangahua earthquake triggered a large rock fall *(RF)* from a limestone bluff, which destroyed a farm house and killed two occupants. (B) The roof of the house *(R)* was carried 50m downslope to the Buller Gorge road (SH6). (C) Shows the house that was destroyed before the earthquake.

Photos 1968: (A) DL Homer, GNS Science; (B) GC Wood Collection 5417fr20, Nelson Provincial Museum; (C) Nelson Evening Mail

RF

(3) *The 2011 Christchurch earthquake:* The shallow M_w 6.2 earthquake on 22 February 2011 located 6km southeast of Christchurch caused widespread building damage and liquefaction in Christchurch city and numerous landslides and rock falls throughout the Port Hills. Five deaths resulted from earthquake-induced rock falls, one during an aftershock four hours after the mainshock. Hundreds of houses were damaged by earthquake-induced rock falls and ground cracking, particularly in the suburbs of Sumner and Redcliffs where many coastal cliff collapses occurred (Dellow et al 2011; Hancox et al 2011). The extensive building damage caused by rock falls has been attributed to the extremely high ground shaking associated with the earthquake, with recorded peak ground accelerations (PGA) ranging from 0.3–1.4g (horizontal) and 0.4–2.2g (vertical) in the Port Hills area (Bradley and Cubrinovski 2011; Kaiser et al 2012). Rock fall damage in the worst affected areas appears to have been associated with a PGA of greater than 0.4g and MM shaking intensities of MM8 to MM9 (Hancox et al 2011; Bradley and Cubrinovski 2011). Examples of buildings that were extensively damaged by rock falls during the 2011 Christchurch earthquake are shown in figures A.35, A.36 and A.37.

Figure A.35 One house (left) was destroyed and another (centre) badly damaged by cliff collapses at Redcliffs during the 2011 Christchurch earthquake. Fatalities occurred at both of these sites.

Photo: G Hancox

The most significant rock fall damage to houses occurred where large masses (hundreds to thousands of cubic metres) of basaltic rocks collapsed onto houses built at the foot of steep former quarry faces (figure A.6) and old (Holocene) coastal cliffs (figures A.35 and A.36). However some houses in the valley bottoms, often several 100m from steep slopes and bluffs, were damaged by individual boulders ranging in size from 0.1m^3 to more than 10m^3. At one site in Raupaki a house was struck by four rocks, including a ~15m^3 boulder which smashed right through the house (figure A.37). Significant damage to houses was also caused by tension cracks and vertical ground displacements associated with incipient (coherent) landsliding along the tops of coastal cliffs and headlands, and the crests of ridges, for example in the Clifton, Heathcote and Redcliffs areas (Dellow et al 2011).

Figure A.36 The back section of this house located at the foot of the old sea cliff at Redcliffs was severely damaged by rock falls and had to be demolished.

Photo: G Hancox

Figure A.37 This house at Raupaki (A) was hit by four rocks, including a 15m³m boulder (B) which bounced and rolled ~600m downslope and smashed right through the house.

Photos: GNS: (A) G Hancox, (B) D Barrell

A3.4 Influence of ground condition, topography, and seismogenic factors

A3.4.1 Ground condition (classes)

In their studies of historical coseismic landsliding in New Zealand, Hancox et al (1997; 2002) identified five ground classes of different rock and soil types with varying landslide susceptibility. From these studies and data from significant earthquakes since 2000 (tables A.1 and A.3), the main types of ground classes (condition) based on soil and rock types and terrain characteristics (slope angle and slope types) are summarised as follows:

Class 1 Bedrock: mainly hard and strong, massive to thickly bedded, with widely spaced jointing. Includes indurated Torlesse rocks (greywacke and argillite), schist, plutonic intrusives (granite, diorite) and volcanics; unweathered to slightly weathered, with thin (< 1–2m) surficial deposits. *Relative landslide susceptibility*: low to very low.

Class 2 Bedrock: Thickly to thinly bedded, slightly to moderately weathered Tertiary rocks (sandstone, mudstone, limestone) on gentle to moderate slopes (15–30º dip slopes), and steep scarp slopes (escarpments); with variable regolith and surficial deposits. *Relative landslide susceptibility*: moderate to high.

Class 3 Bedrock: Closely jointed greywacke and argillite, plutonic and volcanic rock rocks; moderately to highly weathered, with thick (>5 m) regolith and colluvium on high, steep to very steep (~45–60º or >) slopes, especially on steep high ridges; also steep slopes and unsupported cuts in unconsolidated sand and gravel deposits. *Relative landslide susceptibility*: high to very high.

Class 4 Susceptible terrain features, including: (a) very steep (>45º) natural slopes (cliffs, escarpments, gullies) in jointed hard rocks (greywacke, granite, volcanics), weak to strong Tertiary sedimentary rocks and poorly consolidated soils (loess, pumice); (b) unsupported high (>3–6m), steep (>60º) cuts in jointed rocks, soils and regolith. *Relative landslide susceptibility*: high to very high.

Class 5 Saturated, loose and unconsolidated, fine-grained, alluvial, estuarine and marine deposits (fine sand, silt), and other soft sediments, non-engineered fills and reclamations on flat, low-lying terrain and gentle slopes (<10°). *Relative landslide susceptibility*: high to very high.

Significant aspects of the effects of these ground classes or conditions have already been discussed in sections 3.1 to 3.3.

A3.4.2 Topographic effects

Previous studies of coseismic landsliding in New Zealand (eg Hancox et al 1997; 2002) have shown that topographic factors such as slope angle, slope height, and local amplification effects significantly influenced the severity of the landsliding that occurred at different sites. The 2011 Christchurch earthquakes provided valuable additional data on the amplification of earthquake motions on steep, high slopes due to geological and topographic factors. McVerry et al (2013) noted that unusually strong ground shaking was associated with the M_w 6.2 earthquake in Christchurch on 22 February 2011. The peak ground acceleration (PGA) in central Christchurch exceeded 1.8g. The highest PGA of 2.2g recorded at Heathcote Valley Primary School was the highest PGA ever recorded in New Zealand, and one of the highest ever recorded in the world (Dellow et al 2011; Kaiser et al 2012; Bradley 2012).

During the 22 February 2011 earthquake, and again during the M_w 6.0 earthquake in June 2011, there was severe ground failure and building damage on high ridges, and extensive rock falls occurred on coastal cliffs in the Port Hills suburbs of Sumner, Redcliffs and Mount Pleasant, southeast of Christchurch. Field inspections indicated localised high levels of damage associated with landslide activity and/or topographic shape (Dellow et al 2011; Hancox et al 2011; Kaiser et al 2013). Studies carried out by Massey et al (2012a; 2012b) on the slopes that failed and those that did not fail during the 2010/2011 Canterbury earthquake sequence, reported that the height, slope angle and shape of the slopes were the controlling factors on the susceptibility of the cliffs to failure and on the nature of the failure (whether it comprised the fall of an individual boulder or many boulders, eg debris avalanches). These studies also report that slope shape, geometry and geology may have influenced the severity of the ground shaking experienced near the cliff.

To characterise the seismic site response of hill slopes in the Port Hills and assess the extent to which amplification influenced ground motions, new seismological data was collected during the aftershock sequence using small-scale temporary GeoNet arrays at four locations in the coastal suburbs southeast of Christchurch (Kaiser et al 2013). A seismometer array at Kinsey Terrace in Sumner transects an area of surface deformation where permanent coseismic ground displacements of greater than 1m were recorded.

Stations within the mapped deformation area showed preliminary pga amplification effects of 1.5 to 4 times compared to sites on undamaged land further up the slope (Anna Kaiser, pers comm April 2013).

About 3km to the northwest at Mount Pleasant an array on a ridge crest slope where there was significant shaking damage to houses located on convex breaks-in-slope showed preliminary PGA amplification factors up to two times compared with those recorded at the toe of the slope and on flatter ground above the slope crest (Anna Kaiser, pers comm April 2013). The amplification patterns suggest these effects are due to topographic shape (Kaiser et al 2013). The work by Kaiser et al (2013) therefore supports the observations made by Massey et al (2012a; 2012b) that local variations in topography and materials strongly influence ground motion in hillside areas of variable topography in the Port Hills of Christchurch.

The studies by Massey et al (2012a; 2012b), Kaiser et al (2013) and McVerry et al (2013) have confirmed there is now considerable case history evidence and instrumental data showing that topography, and boundaries between contrasting geological materials can substantially amplify seismic shaking (eg PGA) by a factor of up to 1.5 to 4 times, as shown by the 2011 earthquakes in Christchurch. Studies are now being carried out by GNS Science to determine appropriate amplification factors for use in the Wellington area.

A3.4.3 Seismogenic factors

Many studies have shown that the occurrence of earthquake-induced landsliding is strongly related to topography (particularly hillslope gradient and slope height), and the strength of earthquake shaking, with the latter controlled mainly by the magnitude, distance from the epicentre, and the focal depth of an earthquake (Keefer 1984; 2002; Hancox et al 1997; 2002). There is also evidence that other seismogenic factors are important in determining the strength of shaking (ground motions) associated with an earthquake of a given magnitude. Some of these factors include the amount and type of fault slip or focal plane mechanism (normal, strike slip, reverse), the energy that is released and the stress drop, and the location of a site in relation to the seismogenic fault plane, that is whether a site is on the downthrown (foot wall) or upthrown side (hanging wall) of the fault. Other seismogenic factors that can affect landslide occurrence are the directions of fault movement, and the propagation and directivity of seismic waves in relation to the topography (alignment of ridges and slopes) and geological features such as dip slopes and escarpments.

Earthquake mechanism: Many studies of coseismic landsliding have shown there is a clear decrease in landslide occurrence away from the earthquake source. There is also good evidence of increased landsliding on the upthrown side of faults, especially reverse faults, for which strong ground motions can be up to 50% stronger than outside uplifted areas (Abrahamson and Somerville 1996; Hancox et al 2002). The high levels of ground shaking and landsliding associated with reverse faulting is clearly shown by the 1929 Murchison and the 1968 Inangahua earthquakes discussed earlier (table A.1), and more recently by the February 2011 M_w6.3 earthquake in Christchurch. That earthquake, which had a reverse faulting mechanism, caused extremely strong ground shaking, with PGA in Christchurch city of 1.8g (up to 1.8 times the acceleration due to gravity) and up to 2.2g in Heathcote Valley, the highest PGA recorded in New Zealand (Dellow et al 2011; Kaiser et al 2012; Bradley and Cubrinovski 2011; Bradley 2012). The exceptionally strong shaking that occurred was undoubtedly the reason for the unexpected high level of slope instability and damage caused by mass movements during the 2011 Christchurch earthquake.

Energy release and stress drop: The difference that stress drop and the amount of energy released during an earthquake can make to shaking intensity and landslide generation was clearly demonstrated by the M_w7.6 Dusky Sound earthquake in July 2009. Located on the Fiordland subduction zone interface at a depth of 30km, 100km southwest of Te Anau, this event was the largest earthquake in New Zealand in the last 80 years (Fry et al 2010).

The 2009 earthquake caused small-scale shallow landsliding over ~5,600km^2 of the mountains southwest of Te Anau, which was considerably less than the ~10,000km^2 affected by the smaller magnitude (M_w7.2) Fiordland earthquake in 2003. The difference in the severity of the landsliding that occurred in 2009 compared with 2003 has been attributed by Hancox et al (2010) to a combination of factors, including:

- the southward directivity of fault rupture propagation
- low (~0.2MPa) stress release of the 2009 earthquake, compared with 0.5MPa in 2003
- lower ground shaking, with a maximum (albeit relatively low) PGA of 0.14g, compared with 0.17g in 2003 (Fry et al 2010). The low stress release of the 2009 earthquake, along with seaward directivity of the fault rupture, is thus believed to account for the relatively low recorded ground motions and the low level of damage and landsliding caused by the earthquake.

A4 Summary and conclusions

This report presents a detailed review of literature relating to coseismic landsliding and performance of slopes during historical earthquakes in New Zealand. The earthquakes considered include 31 events from 1848 to 2015 which caused significant landsliding.

The main findings and lessons learned from this review are summarised as follows:

1 Occurrence of landslides:

   a In New Zealand, very small to small (<10^3–10^4m^3) landslides occur during shallow (depth < ~30km) earthquakes of magnitude 5, but significant landsliding occurs only at magnitude 6 or greater. The minimum MM intensity threshold for landsliding is MM6, while the most common intensities for significant landsliding are MM7 and MM8, with an equivalent peak ground acceleration (pga) of approximately 0.1–0.5g.

   b The largest landslides (10^6–10^8m^3) occur mainly on steep to very steep slopes (35–60º or >) more than 50–100m high at shaking intensities of MM9–10, with PGAs of ~0.35–1.0g or greater. Escarpments, dip slopes, and cliffs of Tertiary limestone, sandstone and mudstone, cliffs of jointed volcanic rocks, and high, steep mountain ridges are frequently prone to large and very large (10^5–≥10^6m^3) rock slides and avalanches during large (M ≥ 7.0) earthquakes.

   c There is good evidence that slope angle (hillslope gradient) has a very strong influence on the likelihood of failure during earthquakes. In New Zealand about 10% of landslides occur on low angle slopes (≤ 25º), ~30% occur on moderate slopes (25–35º), ~40% on moderate to steep slopes (35–45º), and about 20% occur on steep to very steep slopes (45–60º or >). This distribution reflects slope angle frequency in landslide-affected areas, where there is generally a relatively low percentage of slopes steeper than 45º, and slopes steeper than 60º are difficult to detect with most currently available digital elevation models.

   d Small to large (10^3–10^5m^3) rock and debris falls and slides often occur on ridges and spurs, and on the steep sides and heads of streams and rivers, especially where slopes have been undercut by fluvial or glacial erosion. Unsupported man-made cuts for roads, railway lines, and open excavations for buildings and quarries are particularly prone to coseismic landsliding. Shaking of MM6 or greater causes small to large failures on steep (≥~50°) unsupported road and railway cuts more than 3 m high, resulting in road closures and disruption of transport.

   e Studies of coseismic landsliding in New Zealand have shown that there is a strong correlation between landslide occurrence and the underlying fault rupture zone as indicated by the zone of

aftershocks. This association suggests that for some earthquakes landslide distribution may provide a general indication of the earthquake epicentre and the extent of the fault rupture zone.

f There is also convincing evidence that during reverse fault earthquakes, the landslides that occur are concentrated more on the hanging (upthrown) wall of the fault, where seismic shaking can be up to 50% stronger at short periods than outside the uplifted area, although topographic and geological factors must also be taken into account.

2 Landslide types and failure mechanisms:

a Landslides are often classified into different types using the Varnes classification, which is based on the slope materials involved and the mode of slope movement. On this basis landslide types typically include rock falls, rock slides, soil and debris falls, slides, avalanches, and debris flows. Earthquake-induced landslides can also be grouped, based on the amount of movement and the degree of material disruption, into three categories: disrupted slides and falls, coherent slides, and lateral spread and flows.

b Coseismic landslides in New Zealand are commonly mostly (≥ ~85%) small to large (~10^3–$10^5$$m^3$) disrupted falls, slides, and avalanches of rock, debris, and soil. The most common failure mechanisms appear to involve translational sliding on the soil/regolith and bedrock interface, or sliding and release on rock defects such as bedding planes, joint surfaces, crush zones, shears, and fault zones.

All these failure mechanisms are typically seen in road cut failures.

c Coherent landslides mainly involve partial slumps and rotational slides in soft rocks and soils. Slope movements typically involve small displacements (< 2m) with little internal disruption, and often involve open cracking on the ground surface. Observations in New Zealand suggest that coherent landslides typically occur on ridge crests and slopes in cohesive soils, regolith, Tertiary mudstone, and volcanic tephra. Fewer (≤ ~10%) coherent landslides are recognised after earthquakes, probably because slope cracking is less obvious in the terrain.

3 Size of failures and consequences to infrastructure and buildings:

a During New Zealand earthquakes landslides typically range in size from boulders of less than 1m^3 at MM5 and MM6, to very large (≥$10^6$$m^3$ and greater) landslides at MM9 and MM10. In general, coseismic landslides in New Zealand are larger, more often deeper-seated than landslides triggered by rainstorms, and they occur suddenly without warning over very large areas. Many very large to giant landslides (10^6–$10^8$$m^3$) have occurred during historical earthquakes over the last 150 years, but very few failures of this size have occurred during rainstorms.

b Historically, the consequences of coseismic landslides to infrastructure and buildings in New Zealand have been significant within ~30km of the epicentre (near field) of shallow moderate to large earthquakes (M6–7 or >) where shaking intensities ranged from MM8–10. Landslides have caused significant damage to roads and railway lines resulting in their closure and disruption of transport. Extensive landslides closed the Buller Gorge road between Murchison and Westport for 22 months after the M_w7.8 Murchison earthquake in 1929, and 10 weeks after the M_w7.1 Inangahua earthquake in 1968. The resulting landslide damage during those events to roads, especially cut batters and road platforms, was more severe than has occurred during other New Zealand earthquakes.

c Landsliding or associated ground damage has also brought down electricity transmission lines and severely damaged or destroyed a large number of buildings within the runout or collapse

zones of landslides. In the last 100 years landslides triggered by earthquakes have caused considerable damage to houses and similar buildings in rural and urban areas, and resulted in 22 known deaths.

d At least six buildings were destroyed and 14 people were killed by very large landslides during the 1929 Murchison earthquake. Another two people died in a house that was destroyed by a rock fall and during the 1968 Inangahua earthquake. More recently the February 2011 Christchurch earthquake caused widespread landslides and rock falls throughout the Port Hills. Hundreds of houses were damaged and five deaths resulted from earthquake-induced rock-falls and ground cracking on coastal cliffs and ridges. The extensive rock fall damage has been attributed to the extremely high ground shaking associated with the earthquake (PGA 0.3–1.4g horizontal, and 0.4–2.2g vertical).

4 Influence of ground condition, topography, and seismogenic factors:

a Landslide susceptibility and effects during earthquakes have been shown to vary considerably with ground conditions (classes), especially the soil and rock types and the terrain characteristics (slope angle and slope types). Areas of strong, less weathered bedrock with few joints, thin soils, and lower hill slope gradients have low to moderate relative landslide susceptibility. Very steep (>45º) slopes (high ridges, cliffs, escarpments) in well jointed rocks (greywacke, granite, and volcanics), weak to strong Tertiary sedimentary rocks, and poorly consolidated soils, and steep (>50º) cuts in weak, jointed rocks, soils and regolith tend to have high to very high relative landslide susceptibility.

b There is now considerable case history evidence and instrumental data showing that topography, and the boundaries between geological units can significantly amplify seismic ground shaking (eg PGA) by a factor of up to 1.5 to 4 times, as demonstrated by studies following the 2011 Christchurch earthquake. The potential for increased shaking intensity at the tops of cliffs and steep slopes needs to be taken into account for the siting of buildings and the design of cut slopes.

c Seismogenic factors that have been shown to influence the size and frequency of landslides during earthquakes and the areas over which they occur include: earthquake magnitude, depth, focal mechanism (normal, strike slip, reverse), the energy released and stress drop, and the site location relative to the fault plane.

d There is good evidence of the increased size and frequency of landslides on the upthrown side of reverse faults, as shown by size and high density of landslides triggered by the 1929 Murchison and 1968 Inangahua earthquakes, and more recently by rock falls triggered by the February 2011 Christchurch earthquake. The 2.2g PGA recorded in Heathcote Valley during the latter event was the highest recorded in New Zealand. The exceptionally strong shaking that occurred during the Christchurch earthquake was undoubtedly the reason for the high level of slope instability and damage caused by mass movements.

e The influence that stress drop and the direction and amount of energy released during an earthquake can have on shaking intensity and landslide generation was clearly demonstrated by the M_w7.6 Fiordland earthquake in July 2009. That earthquake caused only minor, superficial landsliding compared to the M_w7.2 earthquake in 2003 due to the southward directivity of fault rupture, and the lower stress release (~0.2MPa) compared to the 2003 earthquake (0.5MPa).

A5 References

Abrahamson, NA and PG Somerville (1996) Effects of the hanging wall and footwall on ground motions recorded during the Northridge earthquake. *Bulletin of the Seismological Society of America 86*, no.1B: S93–S99.

Adams, JE (1978) Late Cenozoic erosion in New Zealand. Unpublished PhD thesis (Geology), Victoria University of Wellington, New Zealand (March 1978).

Adams, RD, GA Eiby and MA Lowry (1968) Preliminary reports on the Inangahua earthquake, New Zealand, May 1968: Preliminary seismological report. *New Zealand DSIR Bulletin 193*: 7–16.

Anderson, H, S Beanland, G Blick, D Darby, G Downes, J Haines, J Jackson, R Robinson and T Webb (1994) The 1968 May 23 Inangahua, New Zealand, earthquake: an integrated geological, geodetic, and seismological source model. *New Zealand Journal of Geology and Geophysics 37:* 59–86.

Baird, HF (1931) The Hawkes Bay earthquake of 3 February, 1931. Unpublished report of the Christchurch Magnetic Observatory (now at Seismological Observatory, Wellington).

Brabhaharan, P and DL Stewart (2015) Rock engineering of cut slopes to provide resilience, Muldoon's Corner realignment, Rimutaka Hill Road, Wellington. *Proceedings of 12th ANZ Geomechanics Conference.* Wellington, February 2015.

Brabhaharan, P, GT Hancox, ND Perrin and GD Dellow (1994) *Earthquake-induced slope failure hazard study, Wellington region: reports and maps covering six study areas (Wellington City, Hutt Valley, Porirua and Kapiti).* Prepared for Wellington Regional Council by Works Consultancy Services Ltd and Institute of Geological & Nuclear Sciences.

Bradley, BA (2012) Observed ground motions in the 4 September 2010 Darfield and 22 February 2011 Christchurch Earthquakes. *NZSEE Conference, 2012, paper 037.*

Bradley, BA and M Cubrinovski (2011) Near-source strong ground motions observed in the 22 February 2011 Christchurch earthquake. *Bulletin of the NZ Society for Earthquake Engineering 44,* no.4: 181–194.

Bullen, KE (1938) On the epicentre of the 1934 Pahiatua earthquake. *New Zealand Journal of Science and Technology 20:* 62–66.

Carey, J and B Rosser (2015) Reconnaissance report on landslides triggered by the M_L 6.0 Wilberforce earthquake of 6 January 2015. *GNS Science Report 2015/34.*

Cowan, HA (1991) The North Canterbury earthquake of September 1, 1888. *Journal of the Royal Society of New Zealand 21,* no.1: 1–12.

Crozier, MJ (1986) Landslides: causes, consequences & environment. New Hampshire USA: Croom Helm. 252pp.

Crozier, MJ, GT Hancox, GD Dellow and ND Perrin (2009) Slip sliding away: landsliding in New Zealand. Chapter 8 in *A continent on the move – New Zealand geoscience into the 21st century*. IJ Graham (Chief Ed). Wellington: Geological Society of NZ in association with GNS Science.

Cruden, DM and DJ Varnes (1996) Landslide types and processes. Chapter 3, pp36-75 in Landslides – investigation and mitigation. AK Turner and RL Schuster (Eds). *Special report 247, Transportation Research Board.* Washington DC: National Research Council.

Dai, FC and CF Lee (2002) Landslide characteristics and slope instability modelling using GIS, Lantau Island, Hong Kong. *Geomorphology 42*: 213–228.

Dai, FC, C Xu, X Yao, L Xu, XB Tu and QM Gong (2011) Spatial distribution of landslides triggered by the 2008 Ms 8.0 Wenchuan earthquake, China. *Journal of Asian Earth Sciences 40*: 883–895.

Dellow, GD and GT Hancox (2006) The influence of rainfall on earthquake-induced landslides in New Zealand. *Earthquakes and Urban Development: New Zealand Geotechnical Society Conference*, Nelson, 2006.

Dellow, G, M Yetton, C Massey, G Archibald, DJA Barrell, D Bell, Z Bruce, A Campbell, T Davies, G De Pascale, M Easton, PJ Forsyth, C Gibbons, P Glassey, H Grant, R Green, G Hancox, R Jongens, P Kingsbury, J Kupec, D Macfarlane, B McDowell, B McKelvey, I McCahon, I McPherson, J Molloy, J Muirson, M O'Halloran, N Perrin, C Price, S Read, N Traylen, R Van Dissen, M Villeneuve and I Walsh (2011) Landslides caused by the 22 February 2011 Christchurch earthquake and management of landslide risk in the immediate aftermath, *Bulletin of the New Zealand Society for Earthquake Engineering 44*: 227–238.

Douglas, JS (1969) Inangahua Earthquake 1968: damage to state highways. *Bulletin of the New Zealand National Society for Earthquake Engineering 2,* no.1: 47–58.

Duckworth, WJH (1969) Inangahua Earthquake 1968: damage to railway track. *Bulletin of the New Zealand National Society for Earthquake Engineering 2,* no.1: 59–63.

Downes, GL (1995) Atlas of isoseismal maps of New Zealand earthquakes. *Institute of Geological and Nuclear Sciences monograph 11,* 304pp.

Downes, GL (2004) Procedures and tools used in the investigation of New Zealand's historical earthquakes. *Annals of Geophysics 47,* no.2/3: 339–419.

Downes GL (2006) Analysis of the M_s6.8, M_w7.0–7.2 Cape Turnagain, New Zealand, earthquake. *Bulletin of the New Zealand Society for Earthquake Engineering 39*, no.4: 183–207.

Downes, GL, D Dowrick, E Smith and K Berryman (1999) The 1934 Pahiatua earthquake sequence: analysis of observational and instrumental data. *Bulletin of the NZ Society for Earthquake Engineering 32:* 221–245.

Downes, GL, DJ Dowrick, RJ Van Dissen, JJ Taber, GT Hancox and EGC Smith (2001) The 1942 Wairarapa, New Zealand, earthquakes: analysis of observational and instrumental data. *Bulletin of the New Zealand Society for Earthquake Engineering 34:* 125–157.

Dowrick, DJ (1994) Damage and intensities in the magnitude 7.8 1929 Murchison, New Zealand, Earthquake. *Bulletin of the New Zealand National Society for Earthquake Engineering 27,* no.3: 190–204.

Dowrick, DJ (1998) Damage and intensities in the magnitude 7.8 Hawke's Bay earthquake, New Zealand. *Bulletin of the New Zealand National Society for Earthquake Engineering 31,* no.3: 139–163.

Dowrick, DJ and S Sritharan (1993) Peak ground accelerations recorded in the 1968 Inangahua earthquake and some implications. *Bulletin New Zealand National Society for Earthquake Engineering 26,* no.6: 349–355.

Dowrick, DJ, GT Hancox, ND Perrin and GD Dellow (2008) The modified Mercalli intensity scale – revisions arising from New Zealand experience. *Bulletin of the New Zealand Society for Earthquake Engineering 41,* no.3: 193–205.

Eiby, GA (1968) An annotated list of New Zealand earthquakes, 1460–1965. *New Zealand Journal of Geology and Geophysics 11*: 630–647.

Eiby, GA (1990) The Lake Coleridge earthquakes of 1946. *Bulletin of the New Zealand National Society for Earthquake Engineering 23:* 150–158.

Franks, CAM, RD Beetham and G Salt (1989) Ground response and seismic response resulting from the 1987 Edgecumbe earthquake, New Zealand. *New Zealand Journal of Geology and Geophysics 32:* 135–144.

Fry, B, S Bannister, J Beavan, L Bland, B Bradley, S Cox, J Cousins, G Hancox, C Holden, R Jongens, W Power, G Prasetya, M Reyners, J Ristau, R Robinson, S Samsonov, N Welch, K Wilson and the GeoNet team (2010) The M_w7.6 Dusky Sound earthquake of 2009: preliminary report. *Bulletin of the New Zealand Society for Earthquake Engineering 43,* no.1: 24–40.

GeoNet (nd) Earthquake data reported on the GeoNet website. www.geonet.org.nz/.

Grapes, RH and G Downes (1997) The 1855 Wairarapa earthquake: analysis of historic data. *Bulletin of the N.Z. National Society for Earthquake Engineering 30,* no.4: 271–368.

Grapes, RH, T Little and G Downes (1998) The Awatere Fault rupture of 1848, New Zealand: historic and present day evidence. *New Zealand Journal of Geology and Geophysics 41*: 387–399.

Guerrieri, L and E Vittori (2007) Intensity scale ESI (Environmental Seismic Intensity Scale) 2007. *Memorie Descrittive della Carta Geologica d'Italia 74.* Rome: Servizio Geologico d'Italia – Dipartimento Difesa del Suolo, APAT.

Guthrie-Smith, H1 (1969) *Tutira – the story of a New Zealand sheep station*. Reed.

Hancox, GT and ND Perrin (2009) Green Lake landslide and other giant and very large post-glacial landslides in Fiordland, New Zealand. *Quaternary Science Reviews: Special issue 'Natural hazards, extreme events, and mountain topography 28*, nos11–12: 1020–1036.

Hancox, GT, CI Massey and ND Perrin (2011) Landslides and related ground damage caused by the Mw 6.3 Christchurch earthquake of 22 February 2011. *New Zealand Geomechanics News 81:* 53–67.

Hancox, GT, ND Perrin and GD Dellow (1997) Earthquake-induced landsliding in New Zealand and implications for MM intensity and seismic hazard assessment. *GNS Science client report 43601B*. 85pp.

Hancox, GT, ND Perrin and GD Dellow (2002) Recent studies of earthquake-induced landsliding, ground damage, and MM intensity in New Zealand. *Bulletin of the New Zealand Society for Earthquake Engineering 35,* no.2: 59–95.

Hancox, GT, SC Cox and R Jongens (2010) The nature and significance of landslides caused by the Mw 7.6 earthquake in Fiordland, New Zealand. *Proceedings of 11th IAEG Congress.* Auckland, September 2010, pp219–228.

Hancox, GT, WF Ries and B Rosser (2015) (in prep). Landslides caused by the M_s 7.8 Murchison earthquake of 17 June 1929 in northwest South Island, New Zealand. *GNS Science report* 2015/xx.

Hancox, GT, SC Cox, IM Turnbull and MJ Crozier (2003) Reconnaissance studies of land-slides and other ground damage caused by the M_w 7.2 Fiordland earthquake of 22 August 2003. *GNS Science report SR2003/30.* 32pp.

Hancox, GT, SC Cox, IM Turnbull and MJ Crozier (2004) Landslides and other ground damage caused by the MW7.2 Fiordland earthquake of 22 August 2003. *Proceedings of the 9th Australia New Zealand Conference on Geomechanics.* Auckland, February 2004. 7pp.

Hancox, GT, WF Ries, B Lukovic and RN Parker (2014) Landslides and ground damage caused by the M_w 7.1 Inangahua earthquake of 24 May 1968 in northwest South Island, New Zealand. *GNS Science report* 2014/06. 93pp.

Hancox, GT, D Dellow, M McSaveney, B Scott and P Villamor (2004) Reconnaissance studies of landslides caused by the ML 5.4. Lake Rotoehu earthquake and swarm of July 2004. *Institute of Geological & Nuclear Sciences science report 2004/24.* 21pp.

Hancox, GT, RM Langridge, ND Perrin, M Vandergoes and G Archibald (2013) Recent mapping and radiocarbon dating of three giant landslides in northern Fiordland, New Zealand. *GNS Science report 2012/45.* 50pp.

Henderson, J (1933) The geological aspects of the Hawke's Bay earthquakes. *New Zealand Journal of Science and Technology XV,* no.1: *38–75.*

Henderson, J (1937) The west Nelson earthquakes of 1929 (with notes on the geological structure of West Nelson). *The New Zealand Journal of Science and Technology XIX,* no.2: 66–144.

Hungr, O, S Leroueil and L Picarelli (2014) The Varnes classification of landslide types, an update. *Landslides 11*: 167–194.

Jibson, RW, EL Harp and JA Michael (2000). A method for producing digital probabilistic seismic landslide hazard maps. *Engineering Geology 58,* 271–289.

Kaiser, A, A Holden and C Massey (2013) Determination of site amplification, polarization and topographic effects in the seismic response of the Port Hills following the 2011 Christchurch earthquake. *New Zealand Society for Earthquake Engineering Conference,* Wellington, April 2013.

Kaiser, A, C Holden, J Beavan, D Beetham, R Benites, A Celentano, D Collett, J Cousins, M Cubrinovski, G Dellow, P Denys, E Fielding, B Fry, M Gerstenberger, R Langridge, C Massey, M Motagh, N Pondard, G McVerry, J Ristau, M Stirling, J Thomas, SR Uma and J Zhao (2012) The M_w 6.2 Christchurch earthquake of February 2011: preliminary report. *New Zealand Journal of Geology and Geophysics 55*: 67–90.

Keefer, DK (1984) Landslides caused by earthquakes. *Geological Society of America Bulletin 95:* 406–421.

Keefer, DK (2002) Investigating landslides caused by earthquakes – a historical review. *Surveys in Geophysics 23*: 473–510.

Kingsbury, PA and WJ Hastie (1995) *Seismic hazard map series: earthquake induced slope failure.* Map sheets and notes for Wellington City, Porirua, Hutt Valley and Kapiti, Greater Wellington Regional Council.

Lin, G-W, H Chen, N Hovius, M-J Horng, D Dadson, P Meunier and M Lines (2008) Effects of earthquake and cyclone sequencing on landsliding and fluvial sediment transfer in a mountain catchment. *Earth Surf. Process. Landforms 33:* 1354–1373.

Lensen, GJ and RP Suggate (1968) Inangahua earthquake—preliminary account of the geology. Pp 17–36 in Preliminary reports on the Inangahua earthquake, New Zealand, May 1968. RD Adams, GA Eiby, MA Lowry, GJ Lensen, RP Suggate and WR Stephenson (Eds). *New Zealand Department of Scientific and Industrial Research bulletin 193*.

Lowry, MA, SS Ede and JS Harris (1989) Assessment of seismic intensities resulting from the 1987 Edgecumbe earthquake, New Zealand, and implications for modernising the intensity scale. *New Zealand Journal of Geology and Geophysics 1989 32:* 145–153.

McKay, A (1902) *Report on the recent seismic disturbances within Cheviot County in North Canterbury and the Amuri district of Nelson, New Zealand (November and December 1901).* Wellington, Government Printer. 88pp.

McVerry, GH, GT Hancox and CJ Massey (2013) Update of peak ground accelerations for the Transmission Gully Project, *GNS Science consultancy report 2013/106*. 22pp.

Marshall, P (1933) Effects of earthquake on coast-line near Napier. *New Zealand Journal of Science and Technology XV,* no.1: 79–92.

Massey, CI, MJ McSaveney and D Heron (2012b) Canterbury earthquakes 2010/11 Port Hills slope stability: life-safety risk from cliff collapse in the Port Hills. *GNS Science consultancy report 2012/124.*

Massey, CI, MJ McSaveney, MD Yetton, D Heron, B Lukovic and ZRV Bruce (2012a) Canterbury earthquakes 2010/11 Port Hills slope stability: pilot study for assessing life-safety risk from cliff collapse. *GNS Science consultancy report 2012/57.*

Morgan, PG (1920) Earthquakes in the Gisborne-East Cape district. 1914. *N.Z. Geological Survey Bulletin 21 (new series):* 81–83.

Ongley, M (1937) The Wairoa earthquake of 16 September 1932. 1. Field observations. *New Zealand Journal of Science and Technology 18:* 845–851.

Ongley, M (1943) Wairarapa earthquake of 24th June, 1942, together with a map showing surface traces of faults recently active. *New Zealand Journal of Science and Technology B25:* 67–78.

Parker, RN (2013) *Hillslope memory and spatial and temporal distributions of earthquake-induced landslides.* Durham theses, Durham University. Available at Durham E-Theses Online: http://etheses.dur.ac.uk/7761/

Parker, R, G Hancox, D Petley, C Massey, A Densmore and N Rosser (2015) Spatial distributions of earthquake-induced landslides and hillslope preconditioning in northwest South Island, New Zealand. *Paper submitted to Earth Surface Processes,* January 2015.

Paterson, BR and JB Berrill (1995) Damage to State Highway 73 from the 29 May 1995 Arthur's Pass earthquake. *Bulletin of New Zealand National Society for Earthquake Engineering 28, no.4:* 300–310.

Paterson, BR and PJ Bourne-Webb (1994) Reconnaissance report on highway damage from the 18 June 1994, Arthur's Pass earthquake. *Bulletin of the New Zealand National Society for the Earthquake Engineering 27,* no.3: 222–226.

Pattle, A and JH Wood (1995) Ground shaking intensity and damage at Lake Coleridge Power Station in the 18 June 1994 Avoca River earthquake. *Bulletin of New Zealand National Society for Earthquake Engineering 27,* no.3: 227–230.

Pearce, AJ and CL O'Loughlin (1985) Landsliding during a M7.7 earthquake. Influence of geology and topography. *Geology 13:* 855–858.

Pender, MJ and TW Robertson (Eds) (1987) Edgecumbe earthquake: reconnaissance report. *Bulletin of New Zealand National Society for Earthquake Engineering 20,* no.3: 201–249.

Perrin, ND (1990) Field inspection report on the Dannevirke (Weber) earthquake of 13 May 1990. *N.Z. Geological Survey immediate report W51947, project 541.400.*

Power, W, G Downes, M McSaveney, J Beavan and G Hancox (2005) The Fiordland earthquake and tsunami, New Zealand, 21 August 2003. Tsunamis: *Advances in Natural and Technological Hazards Research, Vol. 23, p.31–42, DOI:10.1007/1001-4020-3331-1001_1002.*

Qi, S, Q Xu, H Lan, B Zhang and J Liu (2010) Spatial distribution analysis of landslides triggered by 2008.5.12 Wenchuan Earthquake, China. *Engineering Geology 116:* 95–108.

Quigley, M, R Van Dissen, P Villamor, N Litchfield, D Barrell, K Furlong, T Stahl, B Duffy, E Bilderback, D Noble, D Townsend, J Begg, R Jongens, W Ries, J Claridge, A Klahn, H Mackenzie, A Smith, S Hornblow, R Nicol, S Cox, R Langridge and K Pedley (2010) Surface rupture of the Greendale Fault during the Mw 7.1 Darfield (Canterbury) earthquake, New Zealand: initial findings. *Bulletin of the New Zealand Society for Earthquake Engineering 43,* no.4: 236–242.

Read, SAL and S Sritharan (1993) Reconnaissance report on the Ormond Earthquake of 10 August 1993. *Bulletin of the New Zealand National Society for Earthquake Engineering 26,* no.3: 292–308.

Read, SAL and WJ Cousins (1993) The Ormond earthquake of 10 August 1993: an overview of ground damage effects and strong-motions. PP166–175 in *Proceedings of Technical Conference and Annual Meeting, New Zealand National Society of Earthquake Engineering.* Wairakei. 18–20 March 1994.

Reyners, M, P McGinty and K Gledhill (1998) Ormond New Zealand earthquake of 10 August 1993: rupture in the mantle of the subducting Pacific plate. *New Zealand Journal of Geology and Geophysics 41*: 179–185.

Robinson, TR and TRH Davies (2013) Potential geomorphic consequences of a future great (M_w = 8.0+) alpine fault earthquake, South Island, New Zealand. *Natural Hazards and Earth System Sciences 13:* 2279–2299.

Rosser, BJ, D Townsend, E McSaveney and W Reis (2014) Landslides and ground damage associated with the M_w6.2 Eketahuna earthquake, 20 January 2014. *GNS Science report 2014/51.* 34 p.

Smith, EGC, BJ Scott and JH Latter (1984) The Waiotapu earthquake of 1983 December 14. *Bulletin of the New Zealand National Society for Earthquake Engineering 17:* 272 –279.

Speight, R (1933) The Arthur's Pass earthquake of 9th March 1929. *New Zealand Journal of Science and Technology 15:* 173–182.

Stephenson, WR (1968) Inangahua earthquake-engineering seismology, in Preliminary reports on the Inangahua earthquake, New Zealand, May 1968. *N.Z. Department of Scientific and Industrial Research bulletin 193.*

Van Dissen, R, J Cousins, R Robinson and M Reyners (1994) The Fiordland earthquake of 10 August 1993: a reconnaissance report covering tectonic setting, peak ground acceleration, and landslide damage. *Bulletin of the New Zealand National Society for Earthquake Engineering 27,* no.3: 147–154.

Yang, JS (1989) Seismotectonic study of the central Alpine Fault region, South Island, New Zealand. Unpublished PhD Thesis. Victoria University of Wellington, New Zealand.

Acknowledgement

The author of this appendix wishes to thank GNS Science colleagues Sally Dellow and Jon Carey, and Pathmanathan Brabhaharan of Opus Consultants for their helpful reviews.

Annex A.1: Classification and types of landslides

Landslide is a general term for gravitational movements of rock or soil down a slope. Landslides are classified on the mode and speed of the slope movement, and the type of materials involved, such as rock, soil, debris, earth, and mud (Cruden and Varnes 1996).

Rock is a hard or firm intact mass and in its natural place before movement occurs. *Soil* includes silt, clay, sand, gravel and boulders. In a recent update of the Varnes landslide classification (Hungr et al 2014), *mud* is described as an unsorted mixture of soil materials with sufficient silt and clay content to produce plasticity (cohesiveness), and with high moisture content, while *debris* is defined as a mixture of sand, gravel, cobbles and boulders, often with varying proportions of silt and clay, both with varying organic content. The word *debris* is often used to describe any material displaced by a mass movement, but this wider (informal) meaning of the term is not part of the Varnes landslide classification. The term *earth* is not recognised in geological and geotechnical practise, but is widely used as part of the term *earth flow* (a cohesive, plastic, clayey soil, often mixed and remoulded).

Landslides are usually classified or described in terms of: (a) the type of material involved (rock, earth, debris, or sand, mud etc) and (b) the type of movement – fall, topple, slide, flow, spread, which are kinematically distinct modes of movement. Combining these two parameters produces a range of different landslide types such as: *rock fall, rock slide, rock topple, debris slide, debris flow,* and *earth flow*.

The main types of landslides based on Varnes classification are illustrated in figure A1.1 (after Cruden and Varnes 1996) and summarised in table A.1.2 (after Hungr et al 2014).

Table A.1.1 Characteristics of the main types of landslides *(after Cruden and Varnes 1996)*.

Landslide type (based on movement)	**General characteristics**
Landslides (generic term)	Downslope gravitational movements of rocks and 'soils' (top soil, colluvium etc) by falling, sliding, or flowing. Slope failures occur when the destabilising forces (slope steepness, weight and ground water) exceed the resisting forces (shear strength of rock and soil materials).
Falls	**Falls** are masses of rock, soil, or debris that move rapidly down very steep slopes (>40º) by free fall, bounding or rolling. Disrupted soil and debris falls most common.
Slides	**Slides** are masses of rock, soil, or debris that slide down planes of weakness (bedding, joints, and faults) and other surfaces. Rotational slides (or slumps) in soft rocks and soils move on curved failure surfaces. Disrupted soil and debris slides are most common. Landslides are also referred to (non-specifically) as slips, landslips, or slippages.
Avalanches	**Rock and debris avalanches** are very rapid, long run-out failures on steep slopes (>35–40º) more than 150–200m high. They may start as falls or slides, and transform into flows (wet or dry) as they travel downslope. Such landslides occur mainly in hill country and on high mountain slopes.
Debris flows and debris floods	**Debris flows** are a type of landslide: they have much higher sediment concentrations (like wet concrete) than debris floods, and are potentially much more hazardous and destructive. Objects impacted by debris floods are surrounded or buried by gravel, but are often largely undamaged. **Debris floods** are rapid hyper-concentrated flows of water loaded with sediment, often mainly coarse gravel and sand. Debris flows and debris floods are mainly responsible for building alluvial (debris) fans. The revised Varnes classification of landslides (Hungr et al 2014) classes these as a type of flow landslide.

Figure A.1.1 Examples of landslide types (after Cruden and Varnes 1996)

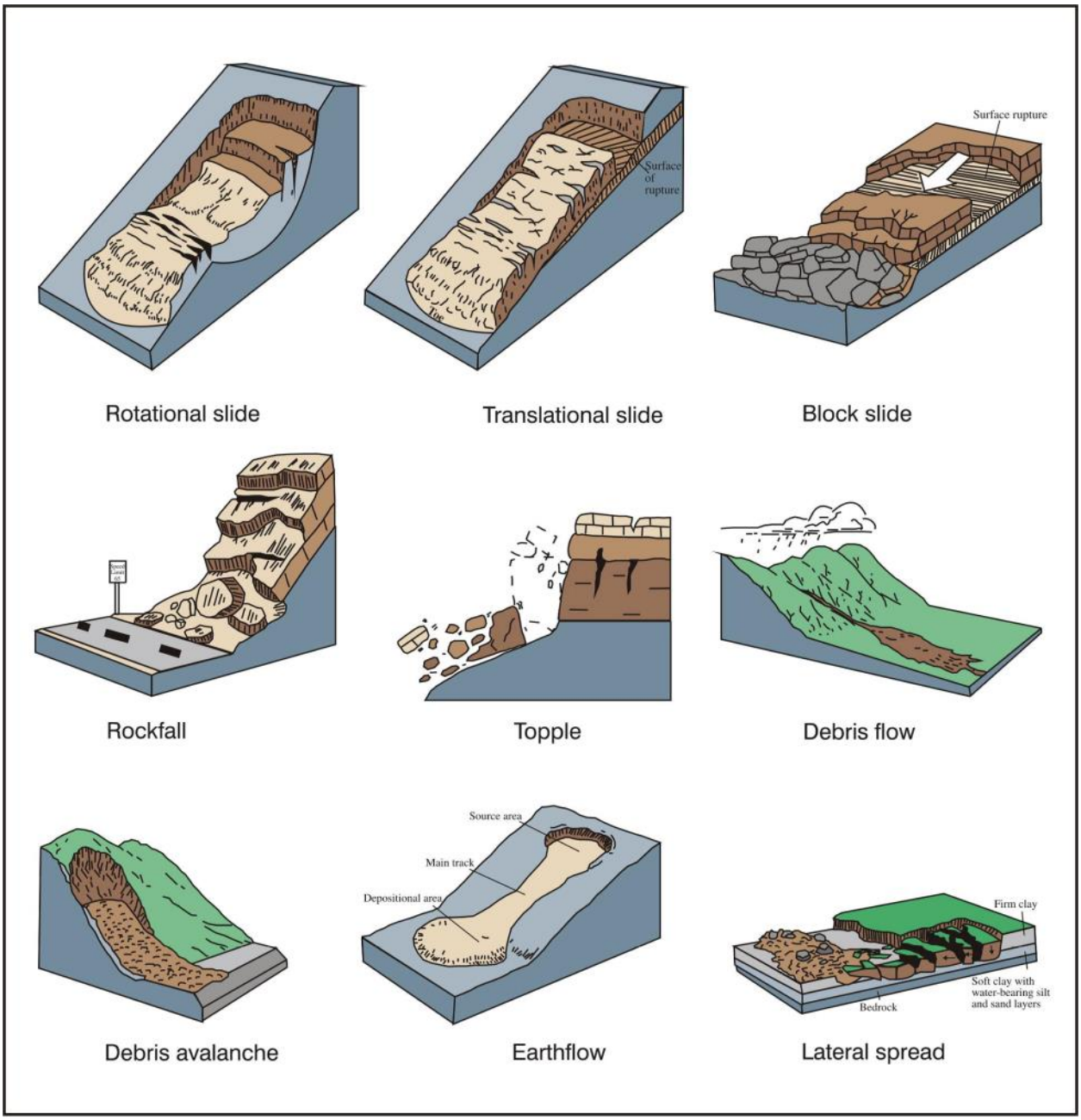

Landslides can occur without an obvious trigger or they can be triggered by toe undercutting (natural or man-made), but are most often initiated by heavy rainfall (eg ~100mm or > in 24 hours), or strong earthquake shaking. Shaking of MM intensity MM7 can cause small failures ($\leq 10^3$–$10^4 m^3$), but MM8 or greater is generally required for larger (10^4–$10^6 m^3$ or >) landslides (Hancox et al 1997; 2002; Dowrick et al 2008), annex B.1.

Table A.1.2 Summary of the proposed new version of the Varnes classification system (after Hungr et al 2014)

Type of movement	Rock	Soil	
Fall	1 *Rock/ice* fall[a]	2 *Boulder/debris/silt* fall[a]	*3*
Topple	4 Rock block topple[a]	5 Gravel/sand/silt topple[a]	
	4 Rock flexural topple		
Slide	6 Rock rotational slide	11 *Clay/silt* rotational slide	
	7 Rock planar slide[a]	12 Clay/silt planar slide	
	8 Rock wedge slide[a]	13 *Gravel/sand/debris* slide[a]	
	9 Rock compound slide	14 Clay/silt compound slide	
	10 Rock irregular slide[a]		
Spread	15 Rock slope spread	16 Sand/silt liquefaction spread[a]	
		17 Sensitive clay spread[a]	
Flow	18 Rock/ice avalanche[a]	19 Sand/silt/debris dry flow	
		20 Sand/silt/debris flowslide[a]	
		21 Sensitive clay flowslide[a]	
		22 Debris flow[a]	
		23 Mud flow[a]	
		24 Debris flood	
		25 Debris avalanche[a]	
		26 Earthflow	
		27 Peat flow	
Slope deformation	28 Mountain slope deformation	30 Soil slope deformation	
	29 Rock slope deformation	31 Soil creep	
		32 Solifluction	

Notes: The words in italics are placeholders (use one only, or combinations if appropriate).

[(a)] Movement types that usually reach extremely rapid velocities as defined by Cruden and Varnes (1996). The other landslide types are most often (but not always) extremely slow to very rapid.

Annex B.1: Modified Mercalli intensity scale

B.1.1 Landslide criteria in the modified Mercalli (MM) intensity scale

Figure B.1.1 Landslide and environmental effects (MM5 to (MM10) – New Zealand 2008

MM5	▪ Loose boulders may occasionally be dislodged from steep slopes.
MM6	▪ Trees and bushes shake, or are heard to rustle. ▪ Loose material may be dislodged from sloping ground, e.g. existing slides, talus and scree slopes. ▪ A few very small ($\leq 10^3$ m^3) soil and regolith slides and rock falls from steep banks and cuts. ▪ A few minor cases of liquefaction (sand boil) in highly susceptible alluvial and estuarine deposits.
MM7	▪ Water made turbid by stirred up mud. ▪ Small slides such as falls of sand and gravel banks, and small rock-falls from steep slopes and cuttings common. ▪ Instances of settlement of unconsolidated, or wet, or weak soils. ▪ A few instances of liquefaction (i.e. small water and sand ejections). ▪ Very small ($\leq 10^3$ m^3) disrupted soil slides and falls of sand and gravel banks, and small rock falls from steep slopes and cuttings are common. ▪ Fine cracking on some slopes and ridge crests. ▪ A few small to moderate landslides (10^3 –10^5 m^3), mainly rock falls on steeper slopes (>30˚) such as gorges, coastal cliffs, road cuts and excavations. ▪ Small discontinuous areas of minor shallow sliding and mobilisation of scree slopes in places. ▪ Minor to widespread small failures in road cuts in more susceptible materials. ▪ A few instances of non-damaging liquefaction (small water and sand ejections) in alluvium.
MM8	▪ Cracks appear on steep slopes and in wet ground. ▪ Significant landsliding likely in susceptible areas. ▪ Small to moderate (10^3-10^5 m^3) slides widespread; many rock and disrupted soil falls on steeper slopes (steep banks, terrace edges, gorges, cliffs, cuts etc.). ▪ Significant areas of shallow regolith landsliding, and some reactivation of scree slopes. ▪ A few large (10^{5-6} m^3) landslides from coastal cliffs, and possibly large to very large ($\geq 10^6$ m^3) rock slides and avalanches from steep mountain slopes. ▪ Larger landslides in narrow valleys may form small temporary landslide-dammed lakes. ▪ Roads damaged and blocked by small to moderate failures of cuts and slumping of road-edge fills. ▪ Evidence of soil liquefaction common, with small sand boils and water ejections in alluvium, and localised lateral spreading (fissuring, sand and water ejections) and settlements along banks of rivers, lakes, and canals etc. ▪ Increased instances of settlement of unconsolidated, or wet, or weak soils.
MM9	▪ Cracking of ground conspicuous. ▪ Landsliding widespread and damaging in susceptible terrain, particularly on slopes steeper than 20˚. ▪ Extensive areas of shallow regolith failures and many rock falls and disrupted rock and soil slides on moderate and steep slopes (20˚-35˚ or greater), cliffs, escarpments, gorges, and man-made cuts. ▪ Many small to large (10^3-10^6 m^3) failures of regolith and bedrock, and some very large landslides (10^6 m^3 or greater) on steep susceptible slopes. ▪ Very large failures on coastal cliffs and low-angle bedding planes in Tertiary rocks. Large rock/debris avalanches on steep mountain slopes in well-jointed greywacke and granitic rocks. Landslide-dammed lakes formed by large landslides in narrow valleys. Damage to road and rail infrastructure widespread with moderate to large failures of road cuts and slumping of roadedge fills. Small to large cut slope failures and rock falls in open mines and quarries ▪ Liquefaction effects widespread, with numerous sand boils and water ejections on alluvial plains, and extensive, potentially damaging lateral spreading (fissuring and sand ejections) along banks of rivers, lakes, canals etc.). Spreading and settlements of river stop-banks likely.
MM10	▪ Landsliding very widespread in susceptible terrain. ▪ Similar effects to MM9, but more intensive and severe, with very large rock masses displaced on steep mountain slopes and coastal cliffs. Landslide-dammed lakes formed. Many moderate to large failures of road and rail cuts and slumping of roadedge fills and embankments may cause great damage and closure of roads and railway lines. ▪ Liquefaction effects (as for MM9) widespread and severe. Lateral spreading and slumping may cause rents over large areas, causing extensive damage, particularly along river banks, and affecting bridges, wharfs, port facilities, and road and rail embankments on swampy, alluvial or estuarine areas.
Notes: *(1) "Some or " few" indicates that threshold for response has just been reached at that intensity. (2) Environmental damage (response criteria) occurs mainly on susceptible slopes and in certain materials, hence the effects described above may not occur in all places, butcan be used to reflect the average or predominant level of damage or MM intensity in an area. (3) Environmental criteria not defined for MM11 and 12, as those intensities have not been reported in New Zealand. Earlier versions of the MM intensity scale suggest that environmental effects at MM11-12 are similar to MM9- 10, but are more widespread and severe. (4) This appendix is based on Hancox et al. 1997, 2002, and Dowrick et al., 2008*	

Figure B.1.2 Relationship of MM intensity to peak ground acceleration (PGA) and earthquake-induced landslide opportunity

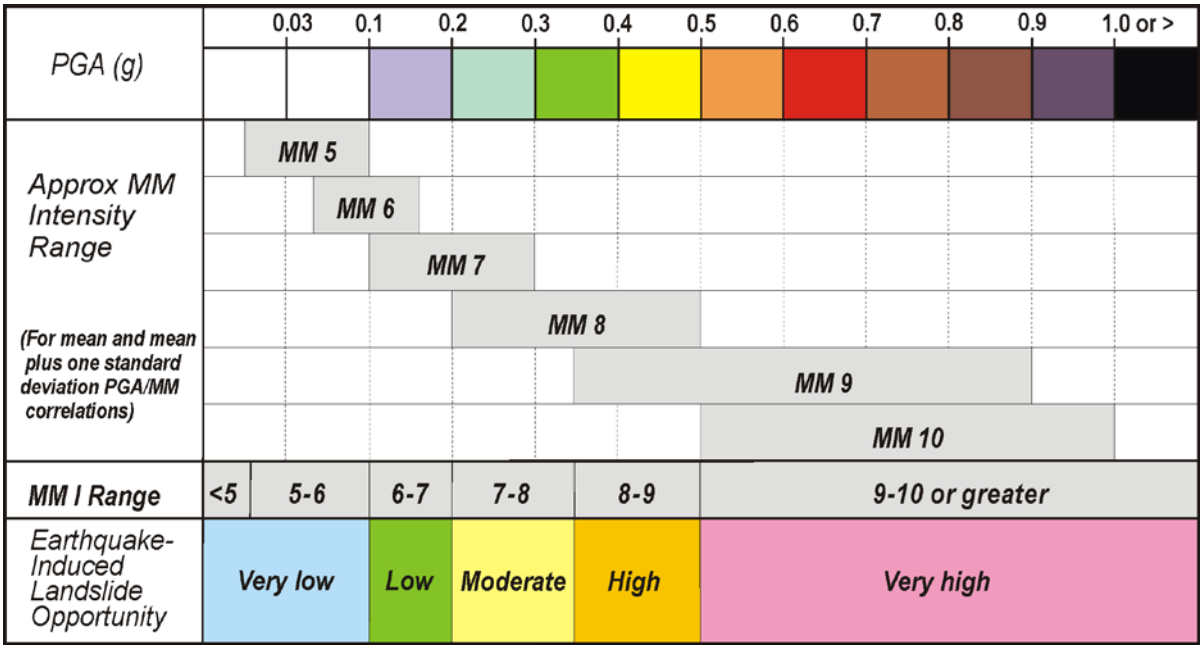

Source: Hancox et al (2002)

The graph above shows the relationship of MM intensity to PGA range based on the mean and mean plus one standard deviation correlations of Murphy and O'Brien (1977) landslide opportunity on New Zealand (from Hancox et al 2002). The overlap in the PGA values for different MM intensities reflects the scatter in PGA/MM data.

The earthquake-induced landsliding opportunity classes define the relative likelihood of earthquake-induced landslides occurring in areas of different shaking (PGA/MM Intensity) based on ground damage effects established for New Zealand. Five classes of relative earthquake-induced landsliding opportunity are recognised, as follows:

Very low	*(≤ MM5–6):*	*Very small rock and soil falls on the most susceptible slopes.*
Low	*(MM6–7):*	*Small landslides, soil and rock falls may occur on more susceptible slopes (particularly road cuts and other excavations), along with minor liquefaction effects (sand boils) in susceptible soils.*
Moderate	*(MM7–8):*	*Significant small to moderate landslides are likely, and liquefaction effects (sand boils) expected in susceptible areas. Noticeable damage to roads.*
High	*(MM8–9):*	*Widespread small-scale landsliding expected, with a few moderate to very large slides, and some small landslide-dammed lakes; many sand boils and localised lateral spreads likely. Severe damage to roads, with many failures of steep high cuts and road-edge fills.*
Very high	*(≥MM9):*	*Widespread landslide damage expected. Many large to extremely large landslides; sand boils are widespread on alluvium, and lateral spreading common along river banks; landslide-dammed lakes are often formed in susceptible terrain. Extensive very severe damage to roads – failures of steep high cuts and road-edge fills.*

B.1.3 Landslide size

The terms used in this annex and throughout the report to describe landslide size in terms of landslide volume (m^3) are as follows:

- Very small ($<10^3 m^3$)
- Small (10^3–$10^4 m^3$)
- Moderate (10^4–$10^5 m^3$)
- Large (10^5–$10^6 m^3$)
- Very large (10^6–$10^8 m^3$)
- Giant ($\geq 10^8 m^3$)

The terms very small to very large were first introduced by Hancox et al (1997; 2002) in their studies of earthquake-induced landslides in New Zealand, and have since been adopted internationally (Guerrieri and Vittori 2007).

More recently the term 'giant landslide' was introduced for less common, extremely large landslides with volumes of 100 million m^3 or greater of which there are two historical examples in New Zealand, both of which occurred during 1929 Murchison earthquake (Hancox et al 2002), and at least 20 prehistoric examples in Fiordland and south Westland (Hancox and Perrin 2009; Hancox et al 2013).